Distribution Agreement

In presenting this thesis or dissertation as a partial fulfillment of the requirements for an advanced degree from Emory University, I hereby grant to Emory University and its agents the non-exclusive license to archive, make accessible, and display my thesis or dissertation in whole or in part in all forms of media, now or hereafter known, including display on the world wide web. I understand that I may select some access restrictions as part of the online submission of this thesis or dissertation. I retain all ownership rights to the copyright of the thesis or dissertation. I also retain the right to use in future works (such as articles or books) all or part of this thesis or dissertation.

Signature:

_____ _____

Megan Katherine Murphy Date

Maturation of Autologous and Heterologous Neutralization Breadth
in Subtypes A and B HIV-1 Infection

By

Megan Katherine Murphy

Doctor of Philosophy
Graduate Division of Biological and Biomedical Sciences
Immunology and Molecular Pathogenesis

_____
Cynthia A. Derdeyn, Ph.D.
Advisor

_____
S. Gnanakaran, Ph.D.
Committee Member

_____
Eric Hunter, Ph.D.
Committee Member

_____
David A. Steinhauer, Ph.D.
Committee Member

_____
Ifor R. Williams, M.D., Ph.D.
Committee Member

Accepted:

_____
Lisa A. Tedesco, Ph.D.
Dean of the James T. Laney School of Graduate Studies

_____
Date

Maturation of Autologous and Heterologous Neutralization Breadth in Subtypes A and B HIV-1 Infection

By

Megan Katherine Murphy
B.S., University of Central Florida, 2007

Advisor: Cynthia A. Derdeyn, Ph.D.

An abstract of
a dissertation submitted to the faculty of the
James T. Laney School of Graduate Studies of Emory University
in partial fulfillment of the requirements for the degree of
Doctor of Philosophy

Graduate Division of Biological and Biomedical Sciences
Immunology and Molecular Pathogenesis
2013

Abstract

Maturation of Autologous and Heterologous Neutralization Breadth
in Subtypes A and B HIV-1 Infection

By Megan Katherine Murphy

Precise routes of viral escape from autologous neutralizing antibodies have been inadequately deciphered in human immunodeficiency virus (HIV-1) infection, especially as they extend from their points of origin along lineages that may influence or direct the expansion of heterologous neutralization potential. Only one quarter of HIV-1 infected people will generate neutralizing antibodies with potent, cross-clade recognition profiles, but we do not understand what distinguishes these individuals or their infections from others.

What follows is an investigation into the roots of humoral neutralization breadth. We first determined, in a cohort of sixteen subtype B-infected viremic patients in the United States, the status of the B cell compartment during chronic infection and subsequent effects on neutralization potential. Then, in one Rwandan subtype A-infected seroconverter (R880F), we pinpointed the primary neutralizing antibody target and the successive pathways of immune evasion using envelope glycoproteins from the transmitted/founder virus and longitudinal escape variants.

In the chronically infected subjects, plasma from three of sixteen (19%) individuals showcased broad heterologous neutralization, which partnered with high levels of total IgG production. Measures of immune activation, dysregulation, CD4 T cell count, and plasma viral load, however, did not differentiate them from the thirteen patients with lower humoral neutralizing activity. In subject R880F, a single mutation at one of three clustered residues proximal to gp120's third hypervariable loop conferred early viral escape. This putative epitope subsequently elicited at least two somatically related monoclonal antibodies, which bound and neutralized viral envelopes containing a subset of the established escape mutations. Resistance to this secondary wave of immune pressure then arose in later viral envelopes through introduction of two N-linked glycosylation motifs that presumably obscured this consistently targeted space. At 16-months post-infection, what had been a narrow, regional response evolved to force recognition/neutralization of distinct envelope portions, which resulted in moderate cross-clade neutralization breadth.

Our data suggest that B cell dysregulation does not directly forestall the observed scope of neutralization. Instead, unveiling a certain chain of envelope mutations could drive B cells toward the production of broadly neutralizing antibodies. Appreciating this knowledge during immunogen construction could positively impact HIV-1 vaccine design.

Maturation of Autologous and Heterologous Neutralization Breadth in Subtypes A and B HIV-1 Infection

By

Megan Katherine Murphy
B.S., University of Central Florida, 2007

Advisor: Cynthia A. Derdeyn, Ph.D.

A dissertation submitted to the faculty of the
James T. Laney School of Graduate Studies of Emory University
in partial fulfillment of the requirements for the degree of
Doctor of Philosophy

Graduate Division of Biological and Biomedical Sciences
Immunology and Molecular Pathogenesis
2013

Dedication

For my parents,
Darlene and James Murphy

Acknowledgements

I would like to thank:

- Cindy for Paris, Santa Fe, Whistler, Galway, Bangkok, Keystone, Boston, Honolulu, and the dual opportunities to learn and teach.
- Susan, Projet San Francisco, and the Zambia-Emory HIV Research Project.
- My mother and father for the carbon monoxide detector, cable TV, and beginning in the mid-1980s to raise alongside me the idea that I could achieve anything.
- Erin for all of those trips to my mailbox that yielded greeting cards from Florida.
- Tara for Elphaba Watch, the Sally Hansen clinic, and “Call Me Maybe” recordings.
- Erica for beginning and ending graduate school with me inside of Woodruff Health Sciences Center Library study rooms (and letting me go first at all of those joint RIPs in between).
- Rachel, Vanessa, and Zephyr for being my longest and best friends.
- Amanda, Elizabeth, Eugene, Jane, Kathryn, Nick, Robin, and Travis for bar trivia.
- Cari, Crystal, Devon, Hiro, Jarad, Josh, Kate H., Kate S., Mimi, Oliver, and Ryan for being my first family in Atlanta.
- Alfred, Dan, Debby, Jessica, Lara, Laura, Martin, Neil, and Zach for making the lab a fun place to be again.
- Brian, Dave, Effie, Eric, Gnana, Ifor, Jane, Jon, Lauren, Linda, and Paul for invaluable technical and intellectual support.
- Every last human volunteer and animal involved in biomedical research. You are so important. We will never be able to repay you.

Table of Contents

Introduction

The Etiology of AIDS

Clinical recognition of acquired immune deficiency syndrome (AIDS) surfaced in the United States around 1981, but this ailment's etiologic agent would not be formally isolated and described until 1983 [1]. Human immunodeficiency virus or HIV, by its textbook definition, is a single-stranded, positive-sense, enveloped RNA virus, of the genus *Lentivirus* and the family *Retroviridae*. Its RNA-dependent DNA polymerase known as reverse transcriptase, an enzyme dually discovered in 1970 by Howard Temin and David Baltimore, breaks molecular biology's central dogma and converts the virus's genomic RNA anatomy (*gag, pol, env, tat, rev, nef, vif, vpr,* and *vpu*) into DNA [2,3]. The first three listed genes underpin essential viral functions, mediating virion architecture, enzymatic activity, and host cell entry ability/phenotype. The latter six listed genes encode regulatory/accessory proteins that enhance viral infectivity and engender minor immune escape strategies. Primary modes of HIV transmission include unprotected sex acts, injection drug use, and from an HIV^+ mother to her child.

The complete RNA genome of HIV spans roughly ten kilobases, and two copies are incorporated into each virion that buds from the plasma membrane of an infected cell. Such susceptible target cells in a host, namely a subset of lymphocytes, express the cellular molecule CD4. Viral envelope binding of this receptor, in conjunction with binding of either co-receptor CCR5 or CXCR4, promotes productive human infection with HIV and, eventually, an accompanying selective depletion of $CD4^+$ T cells [4-7]. In the majority of patients, a subsequent loss of immune function allows for opportunistic infections to arise if viral suppression interventions such as antiretroviral therapy (ART) are not undertaken and maintained.

Classification, Genesis, Prevalence, and Diversity of HIV-1

In its broadest organization, HIV can be separated into two distinct types. From there, groups and subtypes (or clades) emerge as the virus is characterized more narrowly through phylogenetics, and these classifications adopt predictable geographic patterns. HIV type 1 (HIV-1) groups M-P and HIV type 2 (HIV-2) groups A-H exist because of distinct episodes in viral species jumps from nonhuman primates to humans [8]. HIV-1 group M, which likely arose via transferral of SIV_{cpz} from the chimpanzee *Pan troglodytes troglodytes*, autonomously constitutes the contemporary global pandemic [9]. This zoonotic transmission is estimated to have occurred in the interval between the mid-nineteenth century and the beginning of the twentieth century [10-12].

Within just group M, nine pure subtypes have been identified (A, B, C, D, F, G, H, J, and K) with A and F sometimes further partitioned into sub-subtypes (A1-A4, F1, F2) [13]. The two subtypes actively studied herein, A and B, together account for one quarter of contemporary global HIV-1 infections [14]. Data collected by the Joint United Nations Programme on HIV/AIDS and the World Health Organization from 186 countries gauges that, in total, 34.0 million people are infected with HIV-1 (as of November 2011); furthermore, 2.5 million people became newly infected, and 1.7 million people died because of AIDS in 2011 [15].

Calculations place inter-subtype genetic divergence between 25 and 35% while intra-subtype variance fluctuates from 15 to 20% [13,16,17]. These measures ultimately depend on the subtypes and genetic regions examined. Rational vaccine design suggests that viral commonalities should be exploited to achieve maximal efficacy, but such viral elasticity underscores the challenges that obstruct scientific success. Among the reasons for HIV-1's burgeoning variability are the inherent imprecision of reverse transcriptase, the

sheer number of viral particles produced daily (millions), and the continuous opportunity for genetic recombination [7,18-23]. This latter phenomenon, for instance, has given rise to just over 50 described circulating recombinant forms (CRFs) [8]. These viruses fall outside of classical subtypic categorization, as they are composed piecemeal from the genetic material of at least two distinct HIV-1 viruses. To assume the CRF nomenclature, a virus must also have been isolated from at least three disparate individuals without epidemiologic relatedness [24]. If this criterion is not met, the virus is instead assigned the unique recombinant form (URF) designation. Thus, the global framework for HIV-1 consists of viral variants that are functionally and structurally similar, yet genetically quite diverse.

HIV-1 Envelope: gp120 and gp41

Much of the observed viral diversity in this contemporary pandemic originates in the viral envelope. The essential retroviral gene *env*, which typically measures between 2.5 and 3 kilobases, encodes the gp120 and gp41 HIV-1 envelope glycoproteins. These two disparate subunits are cleaved from a common protein precursor known as gp160 (named for its approximate molecular weight, 160 kilodaltons). The surface subunit, gp120, is responsible for binding to the CD4 receptor and CCR5/CXCR4 co-receptors and therefore determines tropism, whilst the transmembrane subunit, gp41, docks the envelope glycoproteins to the viral surface and facilitates fusion of viral and target cell membranes. Heterodimers of heavily glycosylated, non-covalently associated gp120 and gp41 trimerize and decorate the viral surface at a rate of approximately 5-10 trimeric spikes per virion [25].

Examination of gp120's linear sequence reveals five "conserved" domains, named C1 through C5, interspersed with five "hypervariable" domains, named V1 through V5 [26]. Solved crystal structures (HIV-1, SIV) and cryo-electron microscopy data yield important

information regarding the orientation and proximity of these regions in the three-dimensional conformation of envelope [27-34]. Structurally, a gp120 monomer can be divided into three spatial groups: the inner domain, the bridging sheet, and the outer domain. As its name suggests, gp120's inner domain is largely tucked into the core or interior of an envelope trimer; likewise, the outer domain occupies the exterior or circumference of the protein, away from a central axis of formation. The C1 and C5 regions majorly constitute the inner domain, which lacks obvious glycosylation, is thought to form contacts with gp41, and undergoes significant rearrangement upon CD4 binding [35]. This rearrangement prepares envelope for co-receptor binding by bringing together two disparate portions of the unliganded protein to form the bridging sheet, a structure composed of four strands in a compact anti-parallel beta-sheet that links the inner domain to the outer domain. Elements of all three spatial groups contribute to a CD4 binding site (CD4bs). V3, a component of the outer domain, mainly determines co-receptor usage, though CCR5/CXCR4 preference can be influenced by V1V2 and gp41 [36-40].

Autologous Neutralization

Because the HIV-1 envelope glycoproteins are surface-exposed, gp120 (and gp41 to a lesser extent) becomes the primary focus of an infected host's neutralizing antibody response. Observed envelope diversity is then due, in part, to this pressure exerted from the humoral immune system. Identified hypervariable loops undergo significant mutation and can, subsequently, facilitate escape from neutralizing antibodies [41]. Awareness of the specific autologous targets in envelope has developed significantly in the last decade. Multiple, distinct escape pathways are operative in each patient during HIV-1 infection [42-45]. Besides simple mutational variation, other proposed mechanisms of humoral immune

evasion include alteration of the amount and orientation of carbohydrate moieties, insertions and deletions in the viral envelope, and conformational masking of immunogenic targets [46-49]. Efforts to characterize the HIV-1 envelope landscape have pinpointed the following regions of common vulnerability: V1V2, V3, the alpha2 helix in C3, certain carbohydrate epitopes, and the membrane-proximal external region (MPER) in gp41. Antibodies specific for these and other undefined regions of envelope begin to arise after one to two months of infection [42,50-55].

V1V2

Because of their combined length and flexible accommodation of insertions/deletions, the first and second hypervariable loops of HIV-1 envelope effectively maneuver to cover and shield epitopes [46,56-58]. As studies have continued over time, however, this region has also been appreciated as an early and direct target of neutralizing antibodies.

In a 2006 study, early (1- to 6-months post-infection) and chronic (24- to 47-months post-infection) V1V2 sequences from nine subtype A HIV-1 infected subjects were engineered into a common, intra-clade but heterologous backbone [46]. Chimeric envelopes containing early V1V2 regions tested sensitive to neutralization by autologous plasmas collected throughout the duration of infection; later time point V1V2 regions, however, typically tested resistant. The study authors consequently hypothesized that mutations occurring within V1V2 in these patients likely mediated the phenotypic switch and allowed chronic viruses to escape from immune recognition. Defined alterations lengthened the hypervariable loops and augmented glycosylation. Hypervariable loop extension as a common escape mechanism for V1V2 was later corroborated [59].

Several investigations in our laboratory also confirmed the direct immunogenicity of V1V2 in subtype C-infected subjects. In four heterosexual epidemiologically-linked transmission pairs, each composed of a chronically infected donor partner and a newly infected recipient partner, V1V2 domains from neutralization-sensitive recipient envelopes were swapped for homologous regions from their respective donors [59]. Transfer of V1V2 simultaneously transferred the neutralization-resistant phenotype. The extended lengths and augmented numbers of glycosylation sites in donor envelope hypervariable domains were hypothesized to mediate this phenomenon. A later set of experiments in Zambian subject Z205F separated out exactly which envelope mutations conferred neutralizing antibody escape [42,45]. Out to 26-months post-infection, V1V2 was the major determinant of neutralization resistance in tested envelopes [42]. Five somatically related, autologous monoclonal antibodies from this patient pinned down the sites of immune evasion to position 134 in V1 and 189 in V2 [45].

V3

The third hypervariable region, despite its name, faces mutational and structural constraints, no doubt because of its functional role in co-receptor binding [60,61]. A disulfide bond pins together the two ends of this loop that traditionally occupies 30-35 amino acids and often assumes an overall positive charge [62]. Chronologically, one of the first waves of antibody specificity to be measured during HIV-1 infection is anti-V3. Though present and exhibiting potent activity against laboratory-adapted isolates in *in vitro* neutralization assays, these anti-V3 antibodies often do not participate in autologous neutralization [63-65].

C3/The Alpha2 Helix

A common secondary structure in proteins, the alpha helix is often mentioned in conjunction with the beta-pleated sheet. Intra-molecular hydrogen bonding that occurs between the carbonyl oxygen (C=O) of every i^{th} residue and the amide hydrogen (N-H) of every $(i+4)^{th}$ residue stabilizes this protein framework [66]. Alpha2, one such helix that stretches eighteen amino acids, appears in the third constant or C3 region of the HIV-1 envelope. This region, which follows V3 in gp120's linear sequence, is structurally situated in the outer domain, providing some rigidity or stability during receptor binding and likely forming contacts with V4 [29,67,68]. What we appreciate about the alpha2 helix comes predominantly from studies of subtype C infection.

Investigators first recognized the potential for this structure to exact different roles in different HIV-1 subtypes in 2002. That year, the structure was described as a region under strong diversifying pressure in subtype C but not in subtype B. Indeed, if sequences from acute subtype C HIV-1 infection are tracked longitudinally from the origin of seroconversion, one of gp120's first and most concentrated mutational hotbeds is the alpha2 helix. Computing codon-specific ratios of nonsynonymous to synonymous substitutions (dN/dS) to measure the residue-specific variability of the HIV-1 envelope demonstrated that these amino acid alterations conferred an unknown viral advantage [69]. A second study paralleled the subtype C-specific finding five years later when alpha2 helix entropy was studied in 582 subtype C and 634 subtype B envelope sequences and revealed that positional variation soared only in the subtype C alpha2 helix [67].

Our laboratory performed a mutual information analysis with greater than seventy donor/recipient envelopes from five subtype C transmission pairs to identify residues in gp120 that could predict the neutralization-resistant phenotype. Nine positions fell out of

the study, five of which were located within the alpha2 helix. These five, helical residues coincided with the positions found previously to be under strong positive selection in subtype C (dN/dS>3) [47]. Overlap between these two independent studies offered evidence that the subtype C alpha2 helix could contribute to neutralization escape. Though important, these heretofore analytical studies offered no mechanistic data regarding functional contribution of the alpha2 helix. Chimeric envelope studies undertaken to determine the function of the mutational patterns in the alpha2 helix have yielded limited information. In all of the subtype C patients examined in our laboratory, the alpha2 helix alone was insufficient in conferring resistance, suggesting that the exact connection between this helix and humoral immunity is not straightforward [42,47]. One exception is South African patient CAP88 [64]. An autologous monoclonal antibody directly targeting the alpha2 helix was isolated from this individual and characterized in 2011 [70].

The Glycan Shield

Each potential N-linked glycosylation site (PNGS) within a protein is defined by the N-X-(S/T) sequence motif where asparagine (N) is followed first by X (any of the 20 amino acids except proline) and then by serine (S) or threonine (T) [71-73]. The presence of a glycan sequon does not guarantee the presence of a carbohydrate, as glycosylation may not occur if the PNGS involves certain N-X-S combinations or is adjacent to specific amino acids [74-76]. Previous studies determined the median number of potential N-linked glycosylation sites in gp120 to be 25, with the range extending from 18 to 33 sites [77]. In general, a conserved PNGS (one that can be readily aligned among diverse HIV-1 envelopes) is occupied by a high-mannose glycan. By contrast, a PNGS located in an area of length and sequence variation, such as a surface-exposed hypervariable domain, is

usually occupied by a complex carbohydrate and may be added, deleted, or shifted in response to selective pressure. Despite the variability in PNGS pattern across viral variants, the median number and range of sites in gp120 remains constant over time and across subtypes.

What is currently understood about the effect of glycosylation on HIV-1 immune escape comes a decade after the 'glycan shield' was first formally postulated in 2003. At that time, it was hypothesized that changes in viral envelope residues could affect glycan packing; the proposed mechanism would build a glycan cage around the envelope proteins that disallowed recognition by neutralizing antibodies without any overt detrimental influence on CD4 binding [48]. The report centered on two of three acute, ART-naïve patients whose envelopes gained neutralization resistance through modification of PNGS, either alone or in combination with other non-glycan mutations. In essence, investigators concluded that viruses wrapped in fluctuating glycan coats mutated to outcompete autologous B cell recognition. Sites of glycosylation in the viral envelope are now also appreciated as direct autologous neutralization targets [45].

MPER/gp41

Titers of anti-gp41 antibodies often arise first, near the onset of infection and preceding any anti-V3 specificity, but few of these antibodies are believed to be truly neutralizing. The transmembrane and cytoplasmic portions of gp41 are initially out of reach for human immune recognition, at least in their native conformations on a virion. Similarly camouflaged, the piece of gp41 that attaches the gp120/gp41 heterodimer to the viral surface and contains the MPER epitope experiences limited exposure. When iterations of the core MPER epitope were engineered into antigens from *E. coli*, hepatitis B, or influenza

during immunogen fabrication, MPER-specific antibodies with activity against primary HIV-1 isolates did not arise [78-80]. This region of gp41, therefore, might be inadequately immunogenic unless presented in a native envelope context. Even then, gp41 in total may not be the best candidate for elicitation of protective neutralizing antibody responses.

Heterologous Neutralization

As many as a quarter of global HIV-1 patients mount broadly neutralizing antibody responses [81]. This means that, in addition to recognizing the autologous viral quasispecies, humoral effectors resident in these subjects can contest cross-clade envelope diversity--the elemental intention of many infectious disease vaccination programs. Paralleling known viral targets of autologous neutralizing antibodies, the reactivities of all anti-HIV broadly neutralizing antibodies described to date converge at the suspected envelope sites: the CD4bs (b12, VRC01, VRC-PG04, 3BNC117, 3BNC60, NIH-45-46), V1V2 and V3 (PG9, PG16, CH01-04, PGT141-145), glycan-specific moieties (2G12, PGT121-123/125-128/130-131/135-137), and gp41's MPER (Z13, 4E10, 2F5, CAP206-CH12) [82-93].

Unfortunately, these responses appear temporally far into infection, typically requiring two to four years to accumulate, and as a result do not stem the progression of disease [94-96]. What differentiates these individuals immunologically and otherwise from the majority of those who fail to mount heterologous responses is currently unknown and under investigation.

Default human adaptive immune responses deploy several strategies to diversify the neutralizing antibody repertoire. Stochastic combinations of variable (V), diversity (D), and joining (J) gene segments are fused together at non-templated seams during the

recombination of antibody heavy and light chains [97]. After this formation, circulating antibodies that have encountered their cognate antigens undergo a process of affinity maturation whereby somatic hypermutation of the complementarity-determining regions (CDRs) tailors the antibody contact surface to augment antigenic recognition [97]. Sequencing and structural inspection of broadly neutralizing antibodies against HIV-1 reveal that one of two characteristics customarily enables their activity: massive somatic hypermutation or elongated CDRs.

Influenza, an enveloped virus of significant health impact like HIV-1, seasonally rounds on the human population, leaving in its wake the stimulation and production of monoclonal viral neutralizers. Heavy and light chain pairing in these antibodies yields a modest amount of somatic hypermutation that fails to tip over even a 10% threshold [98,99]. Any of the typical, isolated anti-HIV broadly neutralizing antibodies, by contrast, usually exhibit elevated levels of somatic hypermutation sometimes exceeding even 30%. Extended CDR H2 and CDR H3 domains have been described in HIV-1 infection [92,100,101]. The structural protrusion that a long CDR affords allows penetration, for example, of the HIV-1 glycan shield. Why these specializations arise and the means to accelerate their development are not understood.

Summary

To clarify the maturation of autologous neutralizing antibodies in subtype A HIV-1 infection, this dissertation delineates in great detail the course of a humoral immune response in one Rwandan seroconverter, R880F. Plasma sampling performed during the first six months of infection illuminates a call and response dynamic between host and pathogen that centers at the base of the V3 loop in gp120. Neutralization titers spike in

temporal waves where epitopes metamorphose subtly to avoid recognition. Autologous monoclonal antibodies evolve in response, and minimal light chain alteration incrementally tackles more viral variants.

To unravel what influences the evolution of heterologous neutralization breadth, this body of work also examines later time point R880F plasmas against a cross-clade panel of viral pseudotypes. Epitopes consistently targeted during acute infection push subsequent neutralizing antibody responses away from the V3-proximal space. The moderate heterologous neutralization capacity that arises does not share epitopic space with early targets. Furthermore, evaluation of sixteen subtype B chronically infected patients in the United States tells us that immune dysregulation itself does not inevitably constrain recognition of heterologous viral envelopes. In this subset of individuals, even those with significant perturbation of B cells could potently neutralize inter-subtype HIV-1 species. These studies together suggest that early viral and immune events could program the emergence of breadth later in infection.

Chapter 1

Viral Escape From Neutralizing Antibodies in Early Subtype A HIV-1 Infection Drives An Increase in Autologous Neutralization Breadth

Published in *PLoS Pathogens*, 9(2):e1003173, 2013

Megan K. Murphy performed all of the experiments in this study, except as follows:

Initial mutational studies- Ling Yue (Figure 3, partial)

Monoclonal antibody crystallization- Xiang-Peng Kong, Ruimin Pan (Figure 7)

Monoclonal antibody isolation- James E. Robinson, Saikat Boliar (Figure 5A-B)

Structural modeling- S. Gnanakaran, Anurag Sethi, Jianhui Tian (Figures 4 and 8D)

Megan K. Murphy and Cynthia A. Derdeyn wrote the manuscript.

Abstract

Antibodies that neutralize (nAbs) genetically diverse HIV-1 strains have been recovered from a subset of HIV-1 infected subjects during chronic infection. Exact mechanisms that expand the otherwise narrow neutralization capacity observed during early infection are, however, currently undefined. Here we characterized the earliest nAb responses in a subtype A HIV-1 infected Rwandan seroconverter who later developed moderate cross-clade nAb breadth, using (i) envelope (Env) glycoproteins from the transmitted/founder virus and twenty longitudinal nAb escape variants, (ii) longitudinal autologous plasma, and (iii) autologous monoclonal antibodies (mAbs). Initially, nAbs targeted a single region of gp120, which flanked the V3 domain and involved the alpha2 helix. A single amino acid change at one of three positions in this region conferred early escape. One immunoglobulin heavy chain and two light chains recovered from autologous B cells comprised two mAbs, 19.3H-L1 and 19.3H-L3, which neutralized the founder Env along with one or three of the early escape variants carrying these mutations, respectively. Neither mAb neutralized later nAb escape or heterologous Envs. Crystal structures of the antigen-binding fragments (Fabs) revealed flat epitope contact surfaces, where minimal light chain mutation in 19.3H-L3 allowed for additional antigenic interactions. Resistance to mAb neutralization arose in later Envs through alteration of two glycans spatially adjacent to the initial escape signatures. The cross-neutralizing nAbs that ultimately developed failed to target any of the defined V3-proximal changes generated during the first year of infection in this subject. Our data demonstrate that this subject's first recognized nAb epitope elicited strain-specific mAbs, which incrementally acquired autologous breadth, and directed later B cell responses to target distinct portions of Env. This immune re-focusing could have triggered the evolution of cross-clade antibodies and suggests that exposure to a specific

sequence of immune escape variants might promote broad humoral responses during HIV-1 infection.

Introduction

Protective vaccines against viral infections generally elicit nAb responses that are comparable to those in natural infections [1]. It is, therefore, widely accepted that an optimal vaccine against HIV-1 will need to produce nAbs, but features such as the high genetic diversity and mutability of HIV-1 Env pose unique obstacles. While broad neutralization of HIV-1 will likely be difficult to achieve through immunization, renewed optimism exists because of breakthroughs in the HIV-1 vaccine and nAb research fields. In the recently concluded RV144 vaccine trial, modest protection from acquisition of infection was observed and correlated with high levels of antibodies that recognized the V1V2 hypervariable domain of Env gp120 [2]. To date, these anti-V1V2 antibodies are the only immune correlate of vaccine-mediated protection against HIV-1 in humans. In nonhuman primate models, Barouch *et al*. reported that strong vaccine-induced protection against a diverse simian immunodeficiency virus (SIV) challenge in rhesus macaques correlated with V2-binding antibody titer along with nAb titers against two neutralization-sensitive heterologous SIV Envs [3]. Taken together, these results support the concept that antibodies are important for protection against HIV-1 infection and lead to the hypothesis that even higher vaccine efficacy could be achieved if broad nAbs can be induced [4].

The latest intensified efforts to recover and characterize potent and broad mAbs from chronically infected subjects with exceptional neutralization breadth have yielded important clues regarding how these mAbs overcome Env diversity. Such cross-clade neutralizing mAbs have been shown to target conserved elements in the CD4 binding site (CD4bs) (e.g. VRC01, PGV04), V1V2-dependent and trimer-enhanced (quaternary) epitopes (e.g. PG9, PG16), the gp41 membrane proximal external region (MPER) (e.g. 4E10, CAP206, 10E8), and glycan/V3-dependent epitopes (e.g. PGT128) [5-11]. For each

class of ‘super’ mAb, characterization of the variable domains of the immunoglobulin heavy and light chains (VH and VL, respectively), in terms of their structure, germline gene utilization, level of somatic hypermutation, and the features of their heavy chain third complementarity-determining regions (CDR H3s), has unveiled specific characteristics that facilitate extraordinary neutralizing capacity [8,12-15]. Importantly, substantial nAb breadth usually requires two to three years of infection to develop and occurs in only about 20-30% of infected subjects [16,17]. Furthermore, individuals with 'elite' neutralizing activity constitute only about 1% of chronically infected subjects [18]. The reasons why nAb breadth does not develop earlier or more frequently are not known but could include autoreactivity leading to clonal deletion of B cells [19], impaired affinity maturation [20], or induction of a particular Ig germline family [10,13,15,21,22]. It is also possible that early viral escape contributes to the process of increasing nAb breadth [23,24].

A paradox of neutralization breadth is that targets known to mediate this phenomenon, such as HXB2 residue N160 in V2 (targeted by PG9, PG16) or N332 near V3 (targeted by PGT128), are well conserved and present in many transmitted/founder Envs, but broad cross-clade activity only develops in a subset of individuals. The mere presence of these targets is not, then, sufficient to elicit broadly neutralizing antibodies in early infection. Here we describe the initial nAbs in a subtype A HIV-1 infection that target the N332-proximal region of gp120 that has been previously associated with broad neutralization by mAbs recovered from a chronic subtype CRF02_AG infection [6,8] and strain-specific nAb responses in early subtype B infection [25]. Early escape involved a single amino acid substitution in this region, which appeared to drive a modest increase in the autologous neutralization breadth of somatically related mAbs. Later escape entailed the addition and/or shifting of glycans recognized by several previously described broadly

neutralizing mAbs, but these changes were not targeted by the cross-neutralizing nAbs that developed later in this subject. The combinatorial interplay among early nAb targets, viral escape pathways, and antibody somatic hypermutation could, therefore, shape the ultimate development of heterologous nAb breadth across subjects.

Materials and Methods

Ethics statement

Both the Emory University Institutional Review Board and the Rwanda Ethics Committee approved informed consent and human subjects protocols, and subject R880F provided written informed consent for study participation.

Study subject R880F (IAVI 00C175038)

Longitudinal plasma and PBMC samples were obtained from ART-naïve subject R880F during enrollment in International AIDS Vaccine Initiative (IAVI) Protocol C at Projet San Francisco (PSF) in Kigali, Rwanda, as part of a multi-site study of early HIV-1 infection in adult Africans. The PSF cohort, which provides voluntary HIV-1 testing, counseling, and condom provision to cohabiting heterosexual couples, is discussed in more comprehensive detail in [47,48]. Plasma viral load determination (reported in Table 1) was underwritten by IAVI and performed at Contract Lab Services (CLS) in South Africa using an Abbott m2000 system where typical detection ranged between 160 and $4x10^7$ copies/ml.

Amplification, cloning, and function screening of HIV-1 env genes from R880F

Conditions for plasma viral RNA extraction and purification, cDNA synthesis, and nested single-genome PCR amplification have been described previously [49]. Subsequent full-length Env gp160 coding regions (plus Rev, Vpu, and partial Nef) were TA cloned into the CMV promoter-driven expression plasmid pcDNA3.1/V5-His-TOPO (Invitrogen) and screened for biological function as pseudoviruses following co-transfection with an Env-deficient subtype B proviral plasmid (pSG3Δ*env*) in 293T cells using FuGENE HD (Roche or Promega). Forty-eight hours later, supernatant was collected, clarified at 3,000 rpm for 20

min, and used to infect Tzm-bl cells. Following another 48-hour incubation, β-galactosidase staining was performed, and wells were scored positive or negative for blue foci.

Envelopes used for heterologous breadth screen

Fourteen subtype A, B, and C envelopes were used to evaluate the heterologous neutralization breadth of R880F mAbs 19.3H-L1 and 19.3H-L3 along with autologous 16-month and 3-year plasmas. One A/C recombinant and three subtype C early transmitted variants were previously cloned in our laboratory, as described in [49]: A/C-R66M is R66M 7Mar06 3A9env2; C-Z205F is Z205F 27Mar03 ("0-month") EnvPL6.3 [29,31]; C-Z1792M is Z1792M 18Dec07 3G7env2; and C-Z185F is Z185F 24Aug02 ("0-month") EnvPB3.1 [29]. Ten envelopes were obtained through the AIDS Research and Reference Reagent Program, Division of AIDS, NIAID, NIH: from Dr. Julie Overbaugh, A-Q769-b9 is $Q769_{ENVb9}$ (Cat#11545), A-Q769-d22 is $Q769_{ENVd22}$ (Cat#10458), A-Q461 is $Q461_{ENVd1}$ (Cat#11544), and A-Q23 is $Q23_{ENV17}$ (Cat#10455) [50-52]; from Drs. David C. Montefiori, Feng Gao, and Ming Li, B-SS1196 is SS1196.1 (Cat#11020), and B-TRO is TRO, clone 11 (Cat#11023) [53]; from Drs. Beatrice H. Hahn, Yingying Li, and Jesus F. Salazar-Gonzalez, B-gp160opt is pConBgp160-opt (Cat#11402), C-gp160opt is pConCgp160-opt (Cat#11407), and C-Z214M is ZM214M.PL15 (Cat#11310) [54-56]; and from Drs. Cynthia A. Derdeyn and Eric Hunter, C-Z109F is ZM109F.PB4 (Cat#11314) [57].

PCR-based site-directed mutagenesis

Mutations were created through PCR using two overlapping primers that contained the mutated sequence per Env, in a strategy similar to that described previously [29,31,58,59]. Briefly, the plasmids containing 0-A6, 0-B24, 2-A3, 2-B12, 5-B52, A-Q461, C-Z205F, C-

Z109F, or C-Z214M *env* genes were amplified with the following sets of forward (F) and reverse (R) primer sequences, where the mutated nucleotides are underlined:

For mutants 0-A6 I295N and 2-B12 I295N

F 5'-cagcctgtgaatattacgtgtattagaactggc-3' & R 5'-gccagttctaatacacgtaatattcacaggctg-3'

For mutant 0-B24 I295R

F 5'-gcccagcctgtgagaattacgtg-3' & R 5'-cacgtaattctcacaggctgggc-3'

For mutant 0-B24 I295T

F 5'-cttgcccagcctgtgacaattacgtgtattag-3' & R 5'-ctaatacacgtaattgtcacaggctgggcaag-3'

For mutants 0-A6 S335N and 2-B12 S335N

F 5'-gcatattgtaatgtcaatagaacagaatgg-3' & R 5'-ccattctgttctattgacattacaatatgc-3'

For mutant 5-B52 S335N

F 5'-gcatattgtaatgtcaatagaacaggatgg-3' & R 5'-ccatcctgttctattgacattacaatatgc-3'

For mutant 2-B12 S335Q

F 5'-gcatattgtaatgtccaaagaacagaatgg-3' & R 5'-ccattctgttctttggacattacaatatgc-3'

For mutant 2-A3 K338D

F 5'-gtcagtagaacagactggaatgacactttac-3' & R 5'-gtaaagtgtcattccagtctgttctactgac-3'

For mutant 2-A3 K338G

F 5'-gtcagtagaacaggatggaatgacactttac-3' & R 5'-gtaaagtgtcattccatcctgttctactgac-3'

For mutant 2-A3 K338G D341N

F 5'-gtcagtagaacaggatggaatgacactttac-3' & R 5'-gtaaagtgtcattccatcctgttctactgac-3'

Followed by

F 5'-gtagaacaggatggaataacactttacaacaggtag-3' & R 5'-ctacctgttgtaaagtgttattccatcctgttctac-3'

For mutant 2-A3 K338I

F 5'-gtcagtagaacaatatggaatgacactttac-3' & R 5'-gtaaagtgtcattccatattgttctactgac-3'

For mutant 2-A3 K338Q

F 5'-gtcagtagaacacaatggaatgacactttac-3' & R 5'-gtaaagtgtcattccattgtgttctactgac-3'

For mutant 2-A3 K338R

F 5'-gtcagtagaacaagatggaatgacactttac-3' & R 5'-gtaaagtgtcattccatcttgttctactgac-3'

For mutant 0-B24 D341N

F 5'-cagaatggaataacactttacaacagg-3' & R 5'-cctgttgtaaagtgttattccattctg-3'

For mutant 0-B24 E456K

F 5'-gagatggtggtaaggatattaacag-3' & R 5'-ctgttaatatccttaccaccatctc-3'

For mutant A-Q461 N295I

F 5'-ccaagcctgtgataattacttgtatcagacctggc-3' & R 5'-gccaggtctgatacaagtaattatcacaggcttgg-3'

For mutant A-Q461 N335S

F 5'-gcacattgtgttgtcagtagaacagagtggaataac-3' & R 5'-gttattccactctgttctactgacaacacaatgtgc-3'

For mutant A-Q461 N295I N335S

F 5'-ccaagcctgtgataattacttgtatcagacctggc-3' & R 5'-gccaggtctgatacaagtaattatcacaggcttgg-3'

Followed by

F 5'-gcacattgtgttgtcagtagaacagagtggaataac-3' & R 5'-gttattccactctgttctactgacaacacaatgtgc-3'

For mutant C-Z205F N335S

F 5'-caagcatattgtagcattagtaaaagtaaatggaatgac-3' & R 5'-gtcattccatttacttttactaatgctacaatatgcttg-3'

For mutant C-Z109F N335S

F 5'-gaaaggcatattgtaaaattagtggaagtgagtggaatg-3' & R 5'-cattccactcacttccactaattttacaatatgcctttc-3'

For mutant C-Z214M N295I

F 5'-caacttacagaagctgtaataattacgtgtatgaggccc-3' & R 5'-gggcctcatacacgtaattattacagcttctgtaagttg-3'

The PCR cycling parameters were 1 cycle of 95°C for 2 min; 30 cycles of 95°C for 20 sec, 50°C to 60°C for 20 sec (the optimal annealing temperature was determined for each primer set), and 72°C for 2 min; and 1 cycle of 72°C for 3 min. The samples were then stored at 4°C. The 25-ml PCR mixtures contained 62.5-250 ng of each primer, 5-30 ng of the plasmid template, 0.4 mM dNTPs, and 1X reaction buffer. PfuUltra II Fusion HS DNA Polymerase (Stratagene) was used to generate the PCR amplicons, which were digested with 20U *DpnI* (NEB) for 1 hr to remove contaminating template DNA and then transformed into maximum-efficiency XL10-Gold ultracompetent cells (Stratagene) so that the DNA volume did not exceed 5% of the cell volume. Transformed cells were plated onto LB-ampicillin agar plates, which generally resulted in 50 to 100 colonies. Isolated colonies were

inoculated into LB-ampicillin broth for overnight shaking (225 rpm at 37°C), and plasmids were purified using a QIAprep spin miniprep kit (Qiagen). All *env* mutations were confirmed by nucleotide sequencing.

DNA sequencing and analysis

Sanger DNA sequencing of wild-type and mutant envelope genes and immunoglobulin genes was executed with an ABI 3730xl DNA Analyzer and BigDye Terminator v3.1 chemistry at one of two facilities: the University of Alabama at Birmingham Center for AIDS Research (P30-A127767) DNA Sequencing Shared Facility or GenScript. Nucleotide sequences were edited and assembled using Sequencher v5.0 and deposited into GenBank under accession numbers JX096639-JX096660 for wild-type *env* clones and JX124277-JX124282 for immunoglobulin genes. Amino acid sequences were translated and aligned using Geneious v5.0.3.

Neutralization assay

Five-fold serial dilutions of heat-inactivated R880F plasma samples, antibody-containing 293T supernatants, or purified R880F monoclonal antibodies were assayed for neutralization potential against viral pseudotypes in the Tzm-bl indicator cell line, with luciferase as the ultimate readout, as described previously [29,37,57,58,60]. In short, Tzm-bl cells were plated and cultured overnight in flat-bottomed 96-well plates. Pseudovirus (2,000 IU) in DMEM with ~3.5% FBS (HyClone), 40 mg/ml DEAE-dextran was incubated with serial dilutions of plasma, supernatant, or antibody, and subsequently, 100 ml was added to the plated Tzm-bls for a 48 hr infection before being lysed and evaluated for luciferase activity. Data was retrieved from a BioTek Synergy HT multi-mode microplate

reader with Gen 5, v1.11 software, the average background luminescence from a series of uninfected wells was subtracted from each experimental well, infectivity curves were generated using GraphPad Prism v4.0c where values from experimental wells were compared against a well containing virus only with no test reagent, and IC_{50} values were determined using linear regression in Microsoft Excel for Mac 2011, v14.0.2.

Homology modeling of Env V3-proximal residues 295, 338, and 341

The subject R880F 0-B24 Env gp120 sequence was modeled using the MODELLER program [61]. The template for the homology model was a subtype A gp120 obtained by longtime all-atom molecular dynamics simulation using the CHARMM27 potential in the NAMD program [62]. This simulated gp120 was modeled using all known CD4-bound gp120 structures (Protein Data Bank [PDB] accession numbers 1G9M [63],1RZK [22], 2B4C [64], 2NY7 [65], 3JWD and 3JWO [66], and 3LMJ [43]) as templates. In all of these structures, the core of gp120 was highly similar; however, it should be noted that none of these structures is subtype A. Multiple templates were used because it has been shown that this creates high quality homology models. In addition, each template has slightly different regions of gp120 resolved. Before modeling, the templates were arranged in the trimeric state, which has been resolved using cryo-electron microscopy (PDB accession number 3DNO [67]), to ensure that the hypervariable loops did not sterically clash with the neighboring monomers. During modeling, disulfide constraints were added for the conserved cysteines present in all gp120 sequences. All sequence alignments used for modeling templates were based on sequences in the HIV-1 database (www.hiv.lanl.gov).

Modeling of Env V3-proximal glycans at residues 295 and 335

The subject R880F 0-B24 Env gp120 sequence mutated with N295 and N335 was modeled using the protocol described in [31]. Xleap in AmberTools kit 1.4 was used to add two glycans at residues N295 and N335. A five-mannose glycan was used in this simulation because it was found to be the most abundant glycan form in the immunodeficiency virions [68]. Amber99SB force field [69] was used for the gp120 protein, and GLYCAM06 force field [70] was used for the five-mannose glycan. All the systems were minimized using a 3-step protocol in which the protein was gradually allowed to move. These steps were: heavy atoms fixed (5,000 steps), protein backbone atoms fixed (5,000 steps), and all atoms free to move (20,000 steps). The system was gradually heated in a four-step process. The initial temperature was set to 100 K, and only hydrogen atoms were allowed to move for 25,000 fs. In the second step, the temperature was set at 300 K, and heavy atoms in the protein were harmonically constrained for the next 25,000 fs. Then the temperature was raised to 500 K, and backbone atoms were harmonically constrained for 25,000 fs. Force constants for all harmonic constraints were set to 1 kcal $mol^{-1}Å^{-2}$. Finally, the temperature was raised to 700 K, and the backbone atoms in the core of gp120 were constrained for the next 4.925 ns. The coordinates were saved once every ps, in these 5 ns. The MD simulation was performed using NAMD 2.8 [62]. The conformation at the end of the 5 ns MD simulation was used in this study.

Cloning of immunoglobulin VH and VL genes from R880F B cells

A viably frozen PBMC sample from subject R880F was collected at 16-months post-infection and was used to recover autologous mAbs 19.3H-L1 and 19.3H-L3. The first phase of recovery was performed in the Robinson laboratory. Non-B cells were depleted

using immunomagnetic beads (Miltenyi). Approximately 100,000 B cells were recovered, and for memory B cell stimulation, the cultures were incubated for 3 days in RPMI medium containing 10% FCS, Epstein-Barr virus, 2 μg/ml R848 (InVivogen), and 100 U/ml IL-2 (Dr. Maurice Gately, Hoffmann - La Roche Inc. [71]). The cells were then plated into 3,840 wells in the same medium at low cell densities (30 to 50 cells/well) in forty 96-well tissue culture plates containing irradiated macrophage or human placental fibroblast feeder cells. Starting at 12 days of culture, B cell culture supernatants were screened every 3 to 4 days for antibodies that neutralized the autologous founder pseudovirus containing Env 0-B24, or that showed ELISA reactivity with 0-B24 Env glycoproteins in previously described assays [31,38]. Supernatant from 63 wells screened positive for inhibitory activity in the Tzm-bl assay, and 35 of these were also positive for gp120 binding activity in ELISA. The positive cultures were placed in RNAlater between days 17 to 21 after stimulation. RNA was purified from 12 lysates of these B cell cultures that had been found to be antibody positive. RNA from each well was reversed transcribed into cDNA encoding VH and lambda/kappa VL genes, which were then amplified in a nested PCR as described by Liao *et al*. [72]. VH and VL gene products were assembled by overlapping PCR into pairs of linear expression vectors encoding full-length human Ig heavy and light chain genes [72]. These vectors were co-transfected into wells containing 80–90% confluent 293T cells. Two days later, supernatants of transfected cultures were tested for antibody activity in the same assays used to screen B cell cultures. One well of 293T cells transfected with VH and VL genes originating from a single B cell culture designated 19.3H (plate 19, well 3H) was found to be antibody positive. The antibody (or antibodies) produced was thus named 19.3H. 293T cells expressing antibody 19.3H were serially passaged at limiting cell densities under blasticidin selection (for maintenance of the Ig vector) to obtain multiple

clones. Selected 19.3H-derived clones were expanded into stable antibody producing cell lines to facilitate purification of the antibody by Protein A affinity chromatography.

To obtain VH and VL sequences that corresponded to the 19.3H antibody activity, VH and VL genes were isolated from the selected 19.3H-derived 293T cell clones using two different methods in the second phase of recovery. The first method was used in the Robinson laboratory. VH and VL genes were re-amplified from the selected 293T cell clones and inserted into expression plasmids obtained from InVivoGen: pFUSE-CHIg-hG1, containing the constant region of the human IgG1 heavy chain, and pFUSE2-CLIg-hl2 containing the constant region of human Ig lambda 2 light chain, respectively. First, the pFuse vectors were linearized by digestion with *EcoRI* and then subjected to PCR with primers to generate annealing sites of 15 nucleotides that were homologous with ends of the inserts [73].

IgVH FWD 5'-CGAACCGGTGACGGTGTCGTGGAAC-3' and
REV 5'-ACCGGTGATCTCAGGTAGGCGCC-3',
IgVLambda FWD 5'-CCAACAAGGCCACACTGGTGTGTCTC-3' and
REV 5'-ACCGGTGATCTCAGGTAGGCGCC-3',
IgVKappa FWD 5'-GAACTGCCTCTGTTGTGTGCCTGCTG-3' and
REV 5'-ACCGGTGATCTCAGGTAGGCGCC-3')

Second, the SuperScript III One-Step RT-PCR System (Invitrogen) was used to amplify the Ig variable regions from 293T-cell-derived mRNA using primers designed to synthesize inserts for use with the ligation-independent In-Fusion cloning system (Clontech). The forward primer was used for heavy/light chain inserts and contained a non-annealing tag with 15 nucleotides of homology to the upstream insertion site on the plasmid.

IgVH,IgVLambda,IgVKappa
FWD 5'-CCTGAGATCACCGGTGCTAGCACCATGGAGACAGACACACTCC-3'

Reverse primers for each heavy and light chain contained 15-20 nucleotides that overlapped with the 5' end of the constant regions in linearized pFuse vectors.

IgVH REV 5'-CACCGTCACCGGTTCGGGGAAGTAG-3'

IgVLambda REV 5'GTGTGGCCTTGTTGGCTTGAAGCTCCTC-3'

IgVKappa REV 5'-CACAACAGAGGCAGTTCCAGATTTCAACTGCTC -3'

The In-Fusion reaction was performed according to manufacturer's instructions. Plasmids containing inserts were grown in JM109 competent cells, and at least five colonies were picked for subsequent nucleotide sequencing.

A second approach was performed in the Derdeyn laboratory to recover the VH and VL genes from the 19.3H-derived 293T cell clones, and from In-Fusion plasmids generated in the Robinson lab, such that all VH and VL genes would be expressed from the same plasmid vector for the neutralization studies. PCR of VH and lambda/kappa VL genes was performed essentially as described by [74,75]. Briefly, nested PCR was performed using PfuUltra II Fusion HS DNA Polymerase (Stratagene) using the primers described. The first round amplified the leader to constant regions of the VH and VL genes, using cDNA from a 19.3H-derived 293T clonal cell line or In-Fusion plasmid DNA as a template. The second round PCR was performed to amplify the variable regions. PCR products were gel purified, digested with appropriate enzymes (*AgeI* and *SalI* for VH, *AgeI* and *XhoI* for VL, all enzymes from NEB), and cloned into the plasmid expression vectors kindly provided by Dr. Patrick Wilson (heavy - accession number FJ475055, lambda - accession number FJ517647). Plasmids were grown in One Shot TOP10 chemically competent *E. coli* cells (Invitrogen) and purified with a QIAprep spin miniprep kit (Qiagen). At least three separate colonies were picked and sequenced. In the end, one VH and two somatically related lambda VL genes were recovered from five 19.3H-derived 293T clonal cell lines. The VH combined

with either of the VLs (but not randomly with VLs from other R880F B cell cultures) produced robust neutralizing activity against the R880F founder Envs 0-A6 and 0-B24. Further characterization of the mAbs against the larger panel of R880F Envs revealed that the VLs had distinct neutralizing capacities when combined with the 19.3H VH, but no neutralizing activity when combined randomly with R880F VHs from other B cell wells. The mAbs containing the different VLs were then designated 19.3H-L1 and 19.3H-L3.

Production of monoclonal antibodies

293T cells were cultured in T-75 flasks in DMEM with 10% FBS until 80% confluency was reached. Equal amounts (6µg) of VH- and VL-containing plasmids were mixed with FuGENE HD (Roche) at a 1:3 ratio and used for transfection. After 24 hr, media was removed, cells were washed twice with PBS, and the media was replaced with basal media (DMEM, 1% PSG, 1% Nutridoma SP). Cells were incubated for four days at 37°C, after which the supernatant was harvested. Cell debris was removed by centrifugation at 1,500 rpm for 5 min. Approximately 50 ml culture supernatant was used for antibody purification using a Protein A/G Spin column (Pierce) according to manufacturer's instructions. Purified antibodies were concentrated using Vivaspin concentrators (GE), and protein concentrations were determined using a Nanodrop spectrophotometer (BioTek).

Biotinylation of monoclonal antibodies

Four monoclonal antibodies were biotinylated with the EZ-Link Sulfo-NHS-LC-Biotinylation Kit (Thermo Scientific) for use in ELISA protocols: 19.3H-L1 and 19.3H-L3 isolated here from R880F, 6.4C isolated from Z205F [31], and PGT128 obtained through the IAVI Neutralizing Antibody Consortium (NAC) Protocol G mAb Reagent Program [6,76]. For

each mAb, 50 µg were diluted in 500 µl 1X PBS (0.1M sodium phosphate, 0.15M NaCl, pH 7.2) for a final protein concentration of 100 µg/ml. A 50-fold molar excess of biotin was incubated with each mAb for 1 hour at room temperature. Excess biotin was removed via Zeba Desalt Spin Column, per the manufacturer's instructions.

gp120 binding and competition ELISAs

Reacti-Bind polystyrene 96-well plates (Thermo Scientific) were coated overnight at 4°C with 100 µl/well of 2 µg/ml R880F 0-A6/B24, R880F 0-A6/B24 I295R, or R880F 0-A6/B24 E338K purified gp120 protein (Life Technologies, GeneArt) in PBS. Note that blank control wells were coated with gp120 protein but were never subjected to mAb incubation to determine background absorbance, which averaged at 0.055, and assays were performed in duplicate. Plates were subsequently washed six times with 1X PBS-T (Thermo Scientific; 10 mM sodium phosphate, 0.15M NaCl, 0.05% Tween-20) and blocked with 200 µl/well of 1X B3T buffer (150 mM NaCl, 50 mM Tris-HCl, 1 mM EDTA, 3.3% FBS, 2% BSA, 0.07% Tween-20) for 1 hour at 37°C in a CO_2-free incubator. During this incubation step, a two-fold dilution series that spanned 11 wells was prepared in 1X B3T for each biotinylated mAb (19.3H-L1, 19.3H-L3, PGT128, or the negative control, 6.4C) to be tested for binding, beginning at a concentration of 10 µg/ml. Plates were washed six times with 1X PBS-T a second time, and 100 µl/well of serially-diluted mAb was incubated for 1 hour at 37°C. Plates were washed six times with 1X PBS-T a third time, and 100 µl/well of a 1:10,000 dilution of high sensitivity streptavidin horseradish peroxidase (HRP) conjugate (Thermo Scientific) in 1X B3T was incubated for 1 hour at 37°C. After a final six-time wash with 1X PBS-T, 100 µl of room temperature SureBlue 3,3',5,5' tetramethylbenzidine (TMB) microwell peroxidase substrate solution (KPL) was added to each well and incubated for 5

minutes at room temperature. To cease colorimetric development, 100 µl/well of 2M H_2SO_4 was added, and absorbance values at 450 nm were read with a BioTek Synergy HT multi-mode microplate reader. Data was retrieved with KC4 v3.4 software, and binding curves were generated using GraphPad Prism v5.0d.

The gp120 binding ELISA protocol was minimally modified to measure the competitive binding of multiple mAbs, via the following alterations: Only R880F 0-A6/B24 gp120 protein was used, and PGT128 was excluded from the competitions. The first of two 100 µl/well mAb incubation steps was performed via a three-fold dilution series that spanned 7 wells; here, each mAb to be tested for competition (19.3H-L1, 19.3H-L3, or the negative control, 6.4C) was prepared in 1X B3T, beginning at a concentration of 10 µg/ml. The second of two 100 µl/well mAb incubation steps involved addition of a constant 1 µg/ml biotinylated competitor (either 19.3H-L1 or 19.3H-L3) across all wells. Wells were washed six times with 1X PBS-T between these two 1 hour, 37°C incubations. To determine 100% binding for 1 µg/ml biotinylated 19.3H-L1, 19.3H-L3, and 6.4C, duplicate wells were incubated with 1X B3T only during the first mAb incubation step and the appropriate biotinylated competitor during the second. The average absorbance for biotinylated 6.4C alone was 0.056. Background absorbance averaged at 0.048.

Determination of Fab crystal structures

Fab fragments of monoclonal antibodies 19.3H-L1 and 19.3H-L3 were crystallized using previously described methods [41,77-79]. In short, Fab fragments were generated by papain digestion, purified using affinity and size exclusion chromatography, concentrated, and crystallized with the hanging drop method. Fab 19.3H-L1 was crystallized with a well

solution containing 0.17 M $(NH4)_2SO_4$, 0.085 M cacodylate pH 6.5, 25.5% (w/v) polyethylene glycol (PEG) 8000, and 15% (v/v) glycerol. Fab 19.3H-L3 was crystallized with a well solution containing 28% PEG 4K, 0.17 M Li_2SO_4, 0.085 M Tris pH 8.5, and 15% glycerol. X-ray diffraction data were collected at beamline 23-ID-D GM/CA-CAT at the Advanced Photon Source of Argonne National Laboratory, and the data sets were processed using HKL2000 [80]. Crystal structures were solved by the molecular replacement method using MOLREP in CCP4 [81,82]. A homologous Fab (PDB code 3NH7) was used as the starting model. The structures were refined using COOT [83] and PHENIX [84], and analyzed using ICM [85]. The Protein Data Bank (http://www.rcsb.org/pdb) accession numbers for the coordinates of the structures of Fabs 19.3H-L1 and 19.3H-L3 are 4F57 and 4F58, respectively.

Results

Subtype A HIV-1 undergoes alternating cycles of antibody neutralization and viral escape during the first year of infection.

To examine the course and magnitude of autologous HIV-specific humoral activity in a Rwandan seroconverter, R880F, establishment and evolution of the earliest detectable nAb responses were evaluated. This subject was identified as antigen positive, antibody negative on 5Jan07 and then as antibody positive on 12Jan07. This latter date of seroconversion was designated as the 0-month time point for our analyses. Subsequent samples were chronologically coded from this originating time point forward, and each Env was given an arbitrary letter (A, B, or C) and number (1-61) designation that was preceded by the time point of isolation in months post-seroconversion. For example, Envs 0-A6 and 0-B24 were singly isolated from 0-month plasma, 2-A9 and 2-A13 from 2-month plasma, 5-A5 and 5-B52 from 5-month plasma, etc. (Table 1). These viral Envs were single-genome amplified and cloned into expression plasmids for the evaluation of Env pseudotypes. The two 0-month Envs, 0-A6 and 0-B24, had identical sequences and represented the transmitted/founder virus (Figure S1). In sum, ten envelopes from plasma at 2-months post-seroconversion, three from 5-months, five from 7-months, and two from 10-months were evaluated (Table 1).

Each Env-pseudotyped virus was assayed against autologous plasma contemporaneous to its date of isolation in the Tzm-bl neutralization assay. Plasma samples from 2-, 5-, 7-, and 10-months, but not 0-months, potently neutralized the founder Envs 0-A6 and 0-B24 (Figure 1). All longitudinal Envs were at least one log less sensitive to neutralization by contemporaneous plasma than the founder Envs and were, therefore, considered humoral escape variants (Figure 1B-E). These 0-, 2-, 5-, 7-, and 10-

month Envs all succumbed to neutralization by plasma collected at 16-months post-seroconversion (Figure 1F). Hence, the induction of de novo nAbs against contemporaneous escape variants, which we and others have previously described [26-30], also occurred during the first year and a half of infection in R880F. In this subtype A HIV-1 infected subject, a potent nAb response was detected by 2-months following the first antibody positive time point and initiated repeated rounds of neutralization and viral escape.

Residues responsible for early nAb escape coalesce to a potential V3-proximal epitope with alpha2 helix participation.

To localize the earliest nAb target and elucidate consequent mechanisms of viral escape, full-length amino acid Env sequences for all 2-month nAb escape variants shown in Figure 1B were aligned and inspected for the presence of mutational hot spots. Amino acid changes concentrated in three regions of gp120 at 2-months: in C2 immediately preceding the beginning of V3, in the alpha2 helix in C3, and in V5. Figure 2 specifically diagrams these segments of gp120; Figure S1 includes the full gp160 alignment of all 22 R880F Envs. The isoleucine at position 295 (I295; HXB2 residue 293) in C2 mutated to arginine (I295R) in two Envs or threonine (I295T) in one Env (Figure 2). Additionally, glutamic acid E338 in the alpha2 helix (HXB2 residue 337) became three different residues including aspartic acid (E338D), glycine (E338G), and lysine (E338K) in six Envs (Figure 2). Of note, compared to the founder Env sequence, E338K was the sole mutation in the entire 2-A3 Env sequence (Figure S1). We concluded, then, that this single mutation directly mediated nAb escape. The aspartic acid at position 341 (D341; HXB2 residue 340), also in the alpha2 helix, changed to asparagine (D341N) in one Env (Figure 2). Finally, the glutamic

acid at position 456 (E456; HXB2 residue 460) in V5 switched to lysine (E456K) in four Envs (Figure 2).

The potential escape mutations at I295, D341, and E456 were introduced into the founder Env 0-B24 by site-directed mutagenesis to determine if these alterations could individually switch the founder Env phenotype from sensitive to resistant when assayed for neutralization by 2-month plasma. In addition, amino acid changes were introduced into escape Env 2-A3 at K338 to determine whether these mutants maintained nAb resistance. The I295R and I295T substitutions in C2 independently conferred nAb escape, with I295R producing a slightly higher level of resistance that was most evident at the 1:100 dilution of plasma (Figure 3A). For position 338, two naturally occurring substitutions (E338D from 2-A23/2-A24 and E338G from 2-B18, see Figure 2) and three artificially introduced mutations (K338I, K338Q, and K338R) independently reproduced escape Env 2-A3's wild-type level of resistance, arguing that any change at this position could provide full escape from neutralization (Figure 3B). Thus, the degree of neutralization resistance conferred by changes at I295, but not at E338, varied by the amino acid substitution. Introduction of D341N into the alpha2 helix of the founder Env 0-B24 also recapitulated the wild-type resistance level of 2-B12 (Figure 3C). Because the I295, E338, and D341 escape mutations occurred independently in the 2-month Envs, each represents a distinct lineage for escape (Figure 2). In addition, the potency of resistance was substitution-specific; I295R/T and E338D/G/K produced the highest levels of resistance, while D341N lagged somewhat behind and provided partial resistance. In contrast, the E456K mutation in V5 exerted no overt influence on neutralization phenotype when introduced into the founder Env 0-B24, despite being carried in nearly half of the 2-month escape Envs (Figure 3D). Overall, at 2-

months, the viral population utilized a common amino acid substitution mechanism that diverged down three discrete escape pathways, each of which conferred nAb resistance.

Though positions 295, 338, and 341 appear disparate in the linear gp120 sequence, these residues cluster when plotted onto a 3-dimensional representation of the R880F founder Env sequence, which was modeled using all existing structures for CD4-bound HIV-1 gp120 (Figure 4). This proposed epitope emerges near the base of the V3 domain, which is well exposed on the native trimer and is also targeted by the broadly neutralizing, glycan-dependent mAb PGT128 [8]. The spatial proximity of these three residues provides evidence for a single nAb epitope during early subtype A HIV-1 infection and an explanation for why a substitution at any one of the three positions independently caused nAb resistance.

Autologous mAbs neutralize initial escape variants and typify a subsequent wave of humoral pressure.

During HIV-1 infection, the antibodies circulating in patient plasma could ostensibly represent a heterogeneous pool with varying epitope specificities. Although we were able to identify a single, early nAb target in subject R880F using autologous plasma and 3-dimensional modeling, this epitope could be recognized by a polyclonal nAb response mediated by more than one B cell [31]. To illuminate the characteristics of individual monoclonal effectors, we PCR amplified and cloned antibody VH and VL genes from memory B cells present in a cryopreserved R880F peripheral blood mononuclear cell (PBMC) sample collected at 16-months post-seroconversion (Table 1). Multiple VHs and VLs were obtained, but only one VH, named 19.3H-HC, neutralized the founder Env when combined with either of two highly related VLs. Sequence analysis revealed that the R880F

VH utilized IGHV3-30*02, IGHD1-7*01, and IGHJ4*02 gene segments based on matching within the SoDA database [32] and demonstrated 23.2% mutation across its framework (FWR) and complementarity-determining regions (CDR), as compared with germline at the amino acid level (Figure 5A). The VLs, named 19.3H-L1 and 19.3H-L3, were clonal relatives, both using IGLV2-14*01 and IGLJ2*01 gene segments based on matching within the SoDA database [32] and exhibiting mutation rates of 13.6% and 14.5% from the putative germline, respectively (Figure 5B). Five total amino acid differences between the 19.3H-L1 and 19.3H-L3 VLs congregated in and around CDR1: 19.3H-L3 contained two threonines (T) and one phenylalanine (F) in CDR1 that were not present in 19.3H-L1, while arginine (R) and glutamic acid (E) residues arose just downstream of CDR1 in the FWR2 region of 19.3H-L1 that were not present in 19.3H-L3 (Figure 5B). The VL CDR3 domains of 19.3H-L1 and 19.3H-L3 were identical and contained five amino acid differences from the putative germline. The two R880F mAbs produced by combination of 19.3H-HC and 19.3H-L1 or 19.3H-L3 are hereafter referenced solely by their VL designations.

Figure 5 demonstrates that both 19.3H-L1 (C) and 19.3H-L3 (D) neutralized the founder Envs 0-A6 and 0-B24, although 19.3H-L3 did so with approximately one log greater potency. In addition to neutralizing the founder Env, both mAbs neutralized the 2-month plasma escape Env 2-B12 with similar potencies. 19.3H-L3 also neutralized plasma escape variants 5-B52 and 2-B31 potently, and 2-A9 and 2-A13 to a much lesser extent. The remaining 2- and 5-month escape variants, and all 7- and 10-month escape variants were resistant to both mAbs. This result suggests that the mAbs are representative of those that circulated within the first few (2-5) months of infection; because they were isolated from memory B cells, 19.3H-L1 and 19.3H-L3 do not reflect the ability of the 16-month plasma nAbs to neutralize all longitudinal R880F Envs (Figure 1F, Table 2). To

provide evidence for the specificity and authenticity of 19.3H-L1 and 19.3H-L3, the common VH, 19.3H-HC, was co-transfected with other autologous VL genes from two randomly selected R880F B cell wells. One VL utilized the same IGLV2-14*01 gene segment as 19.3H-L1 and 19.3H-L3 (Figure S2A,E); one did not (Figure S2B,E). Conversely, the 19.3H-L3 VL was paired with an autologous VH from a different R880F B cell well (Figure S2C,E). All three chimeric antibody supernatants were assayed for activity against a smaller panel of ten longitudinal R880F Envs, and no neutralizing activity was observed (Figure S2A-C), suggesting that stochastic pairing of R880F VHs and VLs does not confer neutralizing activity.

To map the specificity of mAbs 19.3H-L1 and 19.3H-L3 in finer detail, we utilized the point mutants from Figure 3, with the addition of double mutant 2-A3 K338G D341N, which was representative of escape Env 5-B52. As previously mentioned, 19.3H-L1 neutralized Env 2-B12 in addition to the founder Envs; Env 2-B12 was the only Env in the panel that shared with the founder Env all three unmutated residues at positions I295, S335, and E338 (Figure 2, Table 2). A change at any one of these positions resulted in resistance to 19.3H-L1 neutralization (Figure 5C, Table 2). 19.3H-L1 neutralized 2-B12 more potently than the founder Envs; this was directly attributed to D341N, as this single substitution introduced into Env 0-B24 (0-B24 D341N) increased the founder Env's sensitivity to that of 2-B12 (Figure 5C, Table 2). Despite sharing a common VH with 19.3H-L1, 19.3H-L3 demonstrated a distinct pattern of specificity. In contrast to 19.3H-L1, 19.3H-L3 neutralized the founder and 2-B12 Envs equivalently. In this case, then, the D341N mutation (0-B24 D341N) had very little effect on the neutralization phenotype (Figure 5D). 19.3H-L3 also neutralized Envs carrying the I295T substitution (0-B24 I295T and 2-B31) but displayed a much weaker level of neutralization capacity against Envs

containing the I295R substitution (0-B24 I295R, 2-A9, and 2-A13). 19.3H-L3 neutralized Envs containing the E338G substitution when it occurred in the presence of D341N (5-B52 and 2-A3 K338G D341N) but not when E338G (or any other E338 substitution) occurred in isolation (Figure 5D, Table 2). R880F mAb 19.3H-L3, therefore, had potent neutralizing activity against two Envs (5-B52 and 2-B31) and modest activity against two Envs (2-A9 and 2-A13) that were resistant to contemporaneous plasma and to mAb 19.3H-L1. Hence, the mutational program at positions 295, 338, and 341, first witnessed at 2-months post-seroconversion to facilitate immune evasion (Figure 3), likely fueled subsequent rounds of nAb recognition, and mutations that originally evolved the virus toward an escaped phenotype here conferred sensitivity to somatically related autologous mAbs (Figure 5, Table 2).

To ascertain if 19.3H-L1 and 19.3H-L3 would compete for Env binding, three R880F gp120 monomeric proteins (the 0-A6/B24 founder Env gp120, and mutants containing I295R or E338K) were synthesized, purified, and employed in a competition ELISA assay. To first establish a baseline level of binding, the R880F mAbs were biotinylated and incubated with wild-type 0-A6/B24 gp120 protein. 19.3H-L3 demonstrated more robust binding, as compared to 19.3H-L1; the negative control mAb 6.4C (directed against a highly specific epitope in V1V2 [31]), and the broadly neutralizing mAb PGT128 [8], which shares epitope space with the R880F mAbs, both failed to bind (Figure 6A). Consistent with the neutralization data in Figure 5, neither R880F mAb could bind detectably to the I295R or E338K mutant gp120 proteins (Figure 6B-C). Wild-type 0-A6/B24 gp120 protein was then pre-incubated with 19.3H-L1, 19.3H-L3, or the negative control antibody 6.4C, washed, and incubated with either biotinylated 19.3H-L1 (Figure 6D) or 19.3H-L3 (Figure 6E) to discern if initial pre-incubation could block secondary binding.

19.3H-L1 modestly competed with itself (Figure 6D) but could not effectively compete for binding with 19.3H-L3 (Figure 6E). Conversely, 19.3H-L3 strongly competed with both itself (Figure 6E) and 19.3H-L1 (Figure 6D). Thus, 19.3H-L3 neutralizes a greater number of R880F Envs than 19.3H-L1, binds more strongly to the founder 0-A6/B24 gp120, and neutralizes the Env 0-A6/B24 pseudovirus more potently, underscoring the significance of VL alterations where antigen recognition and neutralization efficacy are concerned.

Crystal structures reveal the neutral, planar epitope contact surfaces and explain the antigen-binding properties of mAbs 19.3H-L1 and 19.3H-L3.

To interrogate the antigen-binding site characteristics of R880F mAbs that influenced their distinct neutralization profiles, crystal structures of the 19.3H-L1 and 19.3H-L3 Fabs were determined to the resolutions of 1.7 Å (Figure 7A) and 2.7 Å, respectively (Table S1). Although the two Fabs were crystallized in different space groups, the resultant structures were highly similar, with root mean square deviations less than 1 Å when all of the Ca atoms were superimposed (data not shown). Several structural analyses were employed, including calculations of Optical Docking Area (ODA, shown in Figure 7B, which predicted the antigen-binding sites by calculating the desolvation free energy of the surfaces), surface pockets, and electrostatic surface potentials. ODA analyses indicated that the antigen-binding sites of 19.3H-L1 and 19.3H-L3 were very flat, forming roughly rectangular shapes approximately 15 Å wide and 30 Å long on top of the six CDR loops (Figure 7C). No pockets existed in these binding surfaces, and the shared CDR H3, although it was 18 amino acids long (Kabat numbering scheme [33]), did not protrude. Such flat antigen-binding sites likely interact with epitopes formed by residues also on planar surfaces (i.e. flat-surface antigen-antibody contacts). Electrostatic surface potential

analyses showed that the 19.3H-L1 and 19.3H-L3 antigen-binding sites were essentially neutral; a couple of slightly positive regions along one side of the rectangular contact area counterbalanced a slightly negative opposite region (Figure 7C, blue and red patches, respectively).

Three CDR1 residues that differed between 19.3H-L1 and 19.3H-L3 (Ser/Thr at residue 27, Gly/Thr at residue 29, and Tyr/Phe at residue 32; Kabat numbering scheme [33]; Figure 7D) did not create any substantial structural differences between the two antigen-binding sites. These changes did, however, have the potential to influence antigen-antibody interactions. The Tyr in 19.3H-L1 to Phe in 19.3H-L3 change at residue 32 likely increased the hydrophobicity at the center of the antigen-binding site, which may have augmented hydrophobic interactions with the antigen. The Gly to Thr mutation at residue 29 added a polar side chain with additional hydrogen binding possibilities. Finally, the Ser to Thr substitution at residue 27 provided a more stable side chain. As a group, these VL alterations probably enhanced the antigen-binding affinity of 19.3H-L3, explaining its increased autologous neutralization breadth.

Addition and/or shifting of potential N-linked glycosylation sites mediate escape from mAbs 19.3H-L1 and 19.3H-L3.

As demonstrated in Figure 5, D341N appeared to be detrimental to the preservation of a neutralization-resistant phenotype, in the context of mAbs 19.3H-L1 and 19.3H-L3 during early infection. This mutation was, nonetheless, retained in later escape Envs. Inspection of the 7- and 10-month Env sequences containing D341N revealed that they had acquired additional substitutions, I295N (HXB2 residue 293) and/or S335N (HXB2 residue 334), absent from earlier Envs (Figure 2); each of these mutations affected a

potential N-linked glycosylation site (PNGS). Accordingly, we hypothesized that these co-traveling mutations compensated for the vulnerability associated with D341N in a PNGS-dependent manner. To explore this, the I295N substitution, which created a PNGS, was introduced into two mAb-sensitive Envs: 0-A6 and 2-B12. The I295N versions of these two Envs displayed high-level resistance against mAbs 19.3H-L1 and 19.3H-L3 (Figure 8A-B, Table 2). Similarly, the S335N substitution, which also incorporated a PNGS, was inserted in three mAb-sensitive Envs: 0-A6, 2-B12, and 5-B52. The S335N versions of these three Envs also became highly resistant to 19.3H-L1 and 19.3H-L3 (Figure 8A-B, Table 2). The S335N substitution shifted a well-conserved PNGS sequon at position 333 (HXB2 residue 332; Figure 8C) that is targeted by broadly neutralizing mAbs PGT128 and 2G12 [8,34,35]. To determine if the observed mAb resistance was glycan-dependent, an S335Q substitution was created in Env 2-B12. Unlike S335N, which shifted the N333 sequon down two positions, S335Q destroyed the N333 sequon altogether (Figure 8C). The resulting mutant, 2-B12 S335Q, was two logs less sensitive to neutralization by mAb 19.3H-L1 than the parental Env 2-B12, but did not reach the high level of resistance achieved by 2-B12 S335N; in contrast, S335Q had only a slight effect on neutralization by mAb 19.3H-L3 (Figure 8A-B, Table 2). High-level resistance against mAbs 19.3H-L1 and 19.3H-L3, therefore, required the addition and/or shifting of PNGS sequons, but amino acid substitution S335Q also provided partial resistance that was much more effective against mAb 19.3H-L1. Together, the data strongly support a mechanism of mAb escape that was PNGS-dependent and may have introduced glycans capable of obscuring the V3-proximal space recognized by 19.3H-L1 and 19.3H-L3 (Figure 8D). Nevertheless, the two mAbs--common heavy chain notwithstanding--appear to recognize subtly distinct epitopes.

R880F exhibits modest heterologous neutralization breadth by 16-months post-infection.

The VH, in particular the CDR H3, has generally been considered a major determinant of epitope recognition and nAb breadth. In our study, VL differences appreciably expanded the neutralization capacity of mAb 19.3H-L3 against autologous Envs. To probe whether this increase in breadth carried over to neutralization of heterologous Envs, mAbs 19.3H-L1 and 19.3H-L3 were tested against a panel of fourteen heterologous Env pseudotypes that included one A/C recombinant, four subtype A, three subtype B, and six subtype C Envs. The mAbs were unable to neutralize any of the heterologous Envs (Figure 9A-B). Thus, while mAb 19.3H-L3 possessed increased breadth against autologous Envs as compared to 19.3H-L1, this did not extend to genetically diverse Envs. Regardless of this restricted mAb cross-clade neutralization, R880F plasma collected at 16-months or 3-years post-infection did have similarly moderate breadth against heterologous Envs, which increased in potency over time (Figure 9C-D). An amino acid alignment of Envs from the heterologous breadth panel demonstrated that Envs neutralized with the greatest potency at 3-years post-seroconversion, A-Q461 and C-Z205F (IC_{50} values of approximately 1:1000), contained the N335 (HXB2 residue 334) shifted glycan associated with viral escape from mAbs 19.3H-L1 and 19.3H-L3 (Figure 9E). Furthermore, Env A-Q461 also incorporated the N295 (HXB2 residue 293) substitution indicative of mAb escape. To investigate if the N295 glycan addition and/or the shifted N335 glycan in R880F Envs could have been partially responsible for the heterologous neutralization capacity that developed in this subject, several glycan knock-out mutants were created and tested with 3-year R880F plasma (Figure 10A). Within A-Q461, the N295 PNGS was eliminated either alone or in conjunction with the N335 PNGS; the N335 PNGS was also individually knocked out (Figure 10B). The positions of interest were reverted back

to the amino acid present in the transmitted/founder Env 0-A6/B24. For C-Z205F, the N335 PNGS was similarly abolished (Figure 10B). Additionally, two heterologous Envs that were only modestly neutralized but that contained the highlighted glycans, C-Z109F and C-Z214M, were mutated as well. All six of the glycan knock-out mutants exactly mirrored their parental equivalents, suggesting that the particular glycans at positions 295 and 335 did not directly contribute to the breadth observed at 3-years post-infection. These data do suggest, however, that early viral escape events likely influenced how breadth developed in this subject, by expanding what was originally a narrow, regional response at the base of the V3 loop to recognize and neutralize distinct portions of Env across genetically diverse variants.

Discussion

Initial R880F nAbs target a novel conformational epitope at the base of the V3 domain.

Several recent studies detail the nAb responses in early subtype B and C HIV-1 infection [24,25,27,29,31,36]. Here we present the first such study of a subtype A infected individual, R880F, where the initial autologous nAb target was defined, along with the consequent routes of viral escape, and two mAbs from early infection were recovered. The kinetics of autologous nAb induction in R880F generally mimicked those described previously for early HIV-1 infection with subtypes A, B, and C [25-27,30,36,37]. Reduced neutralizing activity against contemporaneous Envs at each time point indicated a well-established repeating pattern of de novo neutralization and viral escape in subject R880F. The early escape Env 2-A3 that differed by only one amino acid residue from the founder Envs, 0-A6 and 0-B24, when combined with a comprehensive panel of mutants, supports the hypothesis that the initial site of nAb recognition was a conformational target at the base of the V3 domain. Specifically, individual mutations at I295, E338, or D341 in R880F conferred escape from 2-month plasma antibodies. The region that encompasses these mutations is close to the gp120 surface area targeted by the broadly neutralizing mAb PGT128 (recovered from a CRF02_AG elite neutralizer) [6,8], by early plasma nAbs and two mAbs recovered from a subtype B infected seroconverter [25] and by multiple autologous mAbs recovered from two subtype B infected individuals after cessation of antiretroviral treatment [38]. Thus, early nAbs across subtypes commonly target an immunogenic gp120 structure topographically situated near V3, which is well exposed on the Env trimer.

V3-adjacent regions of Env do, nevertheless, elicit strain-specific responses that are easily escaped by multiple pathways. In the study by Bar *et al*., nAbs in one of three subjects (CH40) targeted a putative conformational epitope composed of the same regions

bordering V3 that we describe here for R880F. CH40 immune evasion in the V3 flanks was, however, preceded by escape mutations in V1; this suggests that this latter region, also immunogenic in early infection, may have been targeted first [25]. Moore *et al.* recently characterized 2 of 79 subtype C infected subjects who were selected because they developed heterologous plasma neutralization breadth mediated by glycan recognition at HXB2 residue N332, another V3-proximal position. In each of these individuals, the glycan motif at HXB2 residue N334 was present in the founder Env; N332 evolved later as an escape mutation and was subsequently targeted by nAbs [24]. Interestingly, in R880F, the opposite occurred: N332 (R880F residue N333) was present in the founder Env and shifted to N334 (R880F residue N335) as an escape mutation in some Envs. Furthermore, the development of heterologous breadth in R880F was not facilitated by specific recognition of N334 and, therefore, involved additional determinants and complexity. When juxtaposed, these and our studies underscore how identical mutations, when ordered differently during infection, can sometimes drive divergent phenotypic outcomes. Thus, exposure of B cells to a specific sequence of changes in Env can program the course of nAb breadth.

Select immunoglobulin germline usage emerges in the analysis of HIV-1 nAbs.

In our previous study of autologous nAb responses during early subtype C HIV-1 infection in subject Z205F, we reported that multiple mAbs targeted the V1V2 domain [31]. These three Z205F mAbs used somatically related IGHV3-15*01 and IGLV2-14*01 germline gene segments and recognized a series of overlapping conformational epitopes centered on residues N134 in V1 and R189 in V2. Each mAb demonstrated a distinct neutralization profile against early autologous Envs, with variable sensitivity to specific glycans. R880F mAbs similarly utilized a restricted set of IGHV3-30*02 and IGLV2-14*01

germline gene segments, but, in this case, only a single isolated VH exhibited neutralization capacity when paired with the two clonally related VLs named 19.3H-L1 and 19.3H-L3 (Figure S2). In a recent study, a single VH was recovered through phage display and conferred neutralization when paired with four somatically related variants of the same kappa VL [39]. Such VL shuffling produced mAbs with varying neutralizing activities, the most potent of which was dependent on one residue in FWR2 and one residue in CDR3. Moreover, precedent sets of clonally related mAbs that show distinct neutralization potency and/or breadth have been catalogued in HIV-1 infection [6,7,15,38-40]. Within the context of our study, it is conceivable that only one R880F VL is authentic, while the other was generated by mutation during short-term in vitro stimulation of B cells. This caveat notwithstanding, variation between the neutralizing activities of mAbs 19.3H-L1 and 19.3H-L3 highlights a feasible mechanism for gradual acquisition of autologous breadth against highly related escape variants that was directly attributable to VL changes. Furthermore, in future studies it would be advantageous to recover a greater number of distinct antibodies, as our ability to understand breadth fully here was limited with only two highly related mAbs.

Notably, the mAbs from Z205F and R880F were predicted to utilize the same VL germline, IGLV2-14*01. This germline gene segment is also employed by the broadly neutralizing mAbs PG9 and PG16 that target a quaternary epitope involving V1V2 and V3 and is again paired with a VH3 family gene segment, IGHV3-33*05. These data suggest that VH3 and VL2 pairing is not uncommon for HIV-1 nAbs. Several instances of VH bias for anti-HIV mAbs have been demonstrated based on the epitope: anti-V3 mAbs preferentially use VH5-51 [41,42]; anti-CD4i mAbs preferentially use VH1-69 [22]; anti-MPER mAbs in more than one instance also utilize VH1-69 [10]; and anti-CD4bs mAbs

preferentially use VH1-46 and VH1-2 [13,15]. These pairings may simply reflect common rearrangement of these germline gene segments in the human immunoglobulin repertoire or the structural features that they bind.

Structural analysis of mAbs 19.3H-L1 and 19.3H-L3 elucidates antigen-antibody interactions in early HIV-1 infection.

Defining the structural characteristics of broadly neutralizing mAbs isolated from elite neutralizers in chronic infection has been a major focus in the HIV-1 nAb field. Unlike the Bar *et al.* study [25], our data here supply structural information regarding HIV-specific mAbs at the opposite end of the neutralization spectrum. Indeed, we are among the first to report high-resolution crystal Fab structures from early HIV-1 infection, and to show that these mAbs likely mediate planar interactions with antigen that can be subtly altered by VL changes. Structural analyses of the 19.3H-L1 and 19.3H-L3 antigen-binding sites are consistent with the neutralization data that place their epitopes at the base of the V3 domain. As this region of gp120 lies flat, any one of the three single amino acid changes that conferred escape at 2-months could potentially disrupt the planar interactions between the 19.3H-L1 and 19.3H-L3 antigen-binding sites and their epitopes, as discussed below.

Introducing a positively charged residue with a long side chain (I295R) or a glycan (I295N) at position 295 is not compatible with the flat hydrophobic surface of the 19.3H-L1/19.3H-L3 antigen-binding site. In fact, neither mAb could bind to monomeric R880F gp120 containing the I295R mutation. In this model, the I295T substitution would be less effective at conferring neutralization escape. The long, negatively charged E338 side chain is predicted to interact with one of the positively charged surface patches (Figure 7C, blue) at the edge of the 19.3H-L1/19.3H-L3 antigen-binding site, potentially forming a salt bridge

with the side chain of a positively charged residue there. The E338K mutation probably destroys this interaction and creates an electrostatic repulsion, which is also consistent with the lack of mAb binding to monomeric R880F gp120 containing the E338K mutation. Interestingly, E338D at this position does not allow 19.3H-L1 and 19.3H-L3 to neutralize the viruses, suggesting that the length of the Asp side chain is not sufficiently long to restore the possible salt bridge. These results suggest that both length and negative charge of the side chain at E338 are important for antibody binding.

The highly conserved N333 (HXB2 residue 332) PNGS at the base of V3 is located at the edge of the proposed epitope and potentially interacts with 19.3H-L1 and 19.3H-L3, as removal of this glycan (S335Q) weakens the neutralization capacities of these two antibodies, most dramatically in the case of 19.3H-L1. Moreover, the glycan shift from position 333 to 335 (S335N), toward the center of the epitope, also prevents the flat-surface antigen-antibody interaction. In combination, the structural, neutralization, and ELISA binding data indicate that mAbs 19.3H-L1 and 19.3H-L3 likely recognize overlapping epitopes that are centered on I295 and E338; however, 19.3H-L1 is more dependent on D341N and the N333 glycan motif for neutralization than 19.3H-L3. Wholly, these analyses suggest that planar motifs that lie across a flat antigen surface could mediate antibody-antigen recognition in early HIV-1 infection, prior to multiple rounds of viral escape and perhaps more extensive affinity maturation. Additionally, the specific determinants for optimal antigen recognition by each mAb, and the strengths of R880F founder Env gp120 binding, differ slightly as a result of VL variation.

Sequential exposure to certain patterns of Env escape could program humoral immunity for the development of nAb breadth.

In most cases, neutralization breadth in chronic infection has been attributed to the VH, with particular emphasis on the CDR H3 [8,22,43-45]. Few studies have, however, investigated the roots of neutralization breadth, as was done here. We found, somewhat unexpectedly, that in R880F, VL sequence variation influenced mAb 19.3H-L3's ability to neutralize two autologous escape variants that were not neutralized by mAb 19.3H-L1 during early infection. Significant augmentation of autologous neutralization via minor VL variation (instead of extensive CDR H3 lengthening) supports a potential mechanism for how escape variants that differ by only a few amino acids and/or glycans are neutralized. Based on this, we contend that the maintenance of VH-determined epitope specificity while light chain antigen contacts are varied could represent an important breadth-augmenting mechanism for B cells responding to highly related Env escape variants. More dramatic nAb structural adaptations such as the elongation of CDR H3 may require time for development, as longitudinal viral variants establish more complex ploys to escape.

Collectively, several factors appeared to shape the antibody maturation pathways in R880F: (i) the initial site of nAb recognition, (ii) VH and VL rearrangement, pairing, and somatic hypermutation, and (iii) repeated exposure to highly related Env escape variants. Our data are consequently consistent with the idea that neutralization breadth arises through the sequential exposure of somatically related B cells to a cascade of viral escape variants presenting altered versions of the same epitope. Additionally, and in contrast to the Moore *et al.* report [24], our findings demonstrate that glycans, which arose in response to the initial waves of neutralization, do not always become subsequent targets for later nAbs or promote the potential to develop heterologous breadth. Moving forward, better

understanding of how initial immunoglobulin targeting affects downstream neutralization potential could positively impact HIV-1 vaccine design. Our studies suggest that the mere presence of a PNGS does not ensure its recognition by an antibody. Sequential exposure to glycans and other Env variations may be required to drive the type of specialized antibody response associated with elite neutralization. In fact, support for this type of immunization approach has been demonstrated [46]. It is, however, currently unknown exactly how to accelerate somatic hypermutation, lengthening of the CDR H3, or the acquisition of other adaptations that lead to increased breadth. We propose that a viable vaccination strategy may involve immunizing with a carefully selected series of Env immunogens that mimic defined amino acid and/or PNGS changes that occurred during the natural viral escape process and led to increased neutralization breadth, such as those described here.

Acknowledgements

We recognize and appreciate the PSF participants, management, staff, and interns. We also acknowledge the technical support of Dr. Alfred Bere. This work was made possible, in part, by the generous support of the American people through the United States Agency for International Development (USAID). The contents are the responsibility of the study authors and do not necessarily reflect the views of USAID or the United States Government.

References

1. Plotkin SA (2010) Correlates of protection induced by vaccination. Clin Vaccine Immunol 17: 1055-1065.

2. Haynes BF, Gilbert PB, McElrath MJ, Zolla-Pazner S, Tomaras GD, et al. (2012) Immune-correlates analysis of an HIV-1 vaccine efficacy trial. N Engl J Med 366: 1275-1286.

3. Barouch DH, Liu J, Li H, Maxfield LF, Abbink P, et al. (2012) Vaccine protection against acquisition of neutralization-resistant SIV challenges in rhesus monkeys. Nature.

4. Nabel GJ, Kwong PD, Mascola JR (2011) Progress in the rational design of an AIDS vaccine. Philos Trans R Soc Lond B Biol Sci 366: 2759-2765.

5. Falkowska E, Ramos A, Feng Y, Zhou T, Moquin S, et al. (2012) PGV04, an HIV-1 gp120 CD4 Binding Site Antibody, Is Broad and Potent in Neutralization but Does Not Induce Conformational Changes Characteristic of CD4. J Virol 86: 4394-4403.

6. Walker LM, Huber M, Doores KJ, Falkowska E, Pejchal R, et al. (2011) Broad neutralization coverage of HIV by multiple highly potent antibodies. Nature 477: 466-470.

7. Zhou T, Georgiev I, Wu X, Yang ZY, Dai K, et al. (2010) Structural basis for broad and potent neutralization of HIV-1 by antibody VRC01. Science 329: 811-817.

8. Pejchal R, Doores KJ, Walker LM, Khayat R, Huang PS, et al. (2011) A potent and broad neutralizing antibody recognizes and penetrates the HIV glycan shield. Science 334: 1097-1103.

9. Zwick MB, Labrijn AF, Wang M, Spenlehauer C, Saphire EO, et al. (2001) Broadly neutralizing antibodies targeted to the membrane-proximal external region of human immunodeficiency virus type 1 glycoprotein gp41. J Virol 75: 10892-10905.

10. Morris L, Chen X, Alam M, Tomaras G, Zhang R, et al. (2011) Isolation of a human anti-HIV gp41 membrane proximal region neutralizing antibody by antigen-specific single B cell sorting. PLoS One 6: e23532.

11. Huang J, Ofek G, Laub L, Louder MK, Doria-Rose NA, et al. (2012) Broad and potent neutralization of HIV-1 by a gp41-specific human antibody. Nature 491: 406-412.

12. McLellan JS, Pancera M, Carrico C, Gorman J, Julien JP, et al. (2011) Structure of HIV-1 gp120 V1/V2 domain with broadly neutralizing antibody PG9. Nature 480: 336-343.

13. Wu X, Zhou T, Zhu J, Zhang B, Georgiev I, et al. (2011) Focused evolution of HIV-1 neutralizing antibodies revealed by structures and deep sequencing. Science 333: 1593-1602.

14. Song L, Sun ZY, Coleman KE, Zwick MB, Gach JS, et al. (2009) Broadly neutralizing anti-HIV-1 antibodies disrupt a hinge-related function of gp41 at the membrane interface. Proc Natl Acad Sci U S A 106: 9057-9062.

15. Scheid JF, Mouquet H, Ueberheide B, Diskin R, Klein F, et al. (2011) Sequence and structural convergence of broad and potent HIV antibodies that mimic CD4 binding. Science 333: 1633-1637.

16. Mikell I, Sather DN, Kalams SA, Altfeld M, Alter G, et al. (2011) Characteristics of the earliest cross-neutralizing antibody response to HIV-1. PLoS Pathog 7: e1001251.

17. Gray ES, Madiga MC, Hermanus T, Moore PL, Wibmer CK, et al. (2011) The neutralization breadth of HIV-1 develops incrementally over four years and is associated with CD4+ T cell decline and high viral load during acute infection. J Virol 85: 4828-4840.

18. Simek MD, Rida W, Priddy FH, Pung P, Carrow E, et al. (2009) Human immunodeficiency virus type 1 elite neutralizers: individuals with broad and potent neutralizing activity identified by using a high-throughput neutralization assay together with an analytical selection algorithm. J Virol 83: 7337-7348.

19. Verkoczy L, Diaz M, Holl TM, Ouyang YB, Bouton-Verville H, et al. (2010) Autoreactivity in an HIV-1 broadly reactive neutralizing antibody variable region heavy chain induces immunologic tolerance. Proc Natl Acad Sci U S A 107: 181-186.

20. Sather DN, Armann J, Ching LK, Mavrantoni A, Sellhorn G, et al. (2009) Factors associated with the development of cross-reactive neutralizing antibodies during human immunodeficiency virus type 1 infection. J Virol 83: 757-769.

21. Racanelli V, Brunetti C, De Re V, Caggiari L, De Zorzi M, et al. (2011) Antibody V(h) repertoire differences between resolving and chronically evolving hepatitis C virus infections. PLoS One 6: e25606.

22. Huang CC, Venturi M, Majeed S, Moore MJ, Phogat S, et al. (2004) Structural basis of tyrosine sulfation and VH-gene usage in antibodies that recognize the HIV type 1 coreceptor-binding site on gp120. Proc Natl Acad Sci U S A 101: 2706-2711.

23. Moore PL, Gray ES, Hermanus T, Sheward D, Tumba N, et al. (2011) Evolution of HIV-1 Transmitted/Founder Viruses Results in the Formation of Epitopes for Later Broadly Cross-Neutralizing Antibodies. In: Retroviruses ARaH, editor. AIDS Vaccine 2011. Bangkok, Thailand: Mary Ann Liebert, Inc.

24. Moore PL, Gray ES, Wibmer CK, Bhiman JN, Nonyane M, et al. (2012) Evolution of an HIV glycan-dependent broadly neutralizing antibody epitope through immune escape. Nat Med 18: 1688-1692.

25. Bar KJ, Tsao CY, Iyer SS, Decker JM, Yang Y, et al. (2012) Early Low-Titer Neutralizing Antibodies Impede HIV-1 Replication and Select for Virus Escape. PLoS Pathog 8: e1002721.

26. Richman DD, Wrin T, Little SJ, Petropoulos CJ (2003) Rapid evolution of the neutralizing antibody response to HIV type 1 infection. Proc Natl Acad Sci U S A 100: 4144-4149.

27. Wei X, J.M. Decker, S. Wang, H. Hui, J.C. Kappes, X. Wu, J.F. Salazar, M.G. Salazar, J.M. Kilby, M.S. Saag, N.L. Komarova, M.A. Nowak, B.H. Hahn, P.D. Kwong, G.M. Shaw (2003) Antibody Neutralization and Escape by HIV-1. Nature 422: 307-312.

28. Moore PL, Ranchobe N, Lambson BE, Gray ES, Cave E, et al. (2009) Limited neutralizing antibody specificities drive neutralization escape in early HIV-1 subtype C infection. PLoS Pathog 5: e1000598.

29. Rong R, Li B, Lynch RM, Haaland RE, Murphy MK, et al. (2009) Escape from autologous neutralizing antibodies in acute/early subtype C HIV-1 infection requires multiple pathways. PLoS Pathog 5: e1000594.

30. Bosch KA, Rainwater S, Jaoko W, Overbaugh J (2009) Temporal analysis of HIV envelope sequence evolution and antibody escape in a subtype A-infected individual with a broad neutralizing antibody response. Virology 398: 115-124.

31. Lynch RM, Rong R, Boliar S, Sethi A, Li B, et al. (2011) The B cell response is redundant and highly focused on V1V2 during early subtype C infection in a Zambian seroconverter. J Virol 85: 905-915.

32. Volpe JM, Cowell LG, Kepler TB (2006) SoDA: implementation of a 3D alignment algorithm for inference of antigen receptor recombinations. Bioinformatics 22: 438-444.

33. Kabat EA, Wu TT (1991) Identical V region amino acid sequences and segments of sequences in antibodies of different specificities. Relative contributions of VH and VL genes, minigenes, and complementarity-determining regions to binding of antibody-combining sites. J Immunol 147: 1709-1719.

34. Sanders RW, Venturi M, Schiffner L, Kalyanaraman R, Katinger H, et al. (2002) The mannose-dependent epitope for neutralizing antibody 2G12 on human immunodeficiency virus type 1 glycoprotein gp120. J Virol 76: 7293-7305.

35. Scanlan CN, Pantophlet R, Wormald MR, Ollmann Saphire E, Stanfield R, et al. (2002) The broadly neutralizing anti-human immunodeficiency virus type 1 antibody 2G12 recognizes a cluster of alpha1-->2 mannose residues on the outer face of gp120. J Virol 76: 7306-7321.

36. Moore PL, Gray ES, Choge IA, Ranchobe N, Mlisana K, et al. (2007) The C3-V4 Region Is a Major Target of Autologous Neutralizing Antibodies in Hiv-1 Subtype C Infection. J Virol.

37. Li B, Decker JM, Johnson RW, Bibollet-Ruche F, Wei X, et al. (2006) Evidence for potent autologous neutralizing antibody titers and compact envelopes in early infection with subtype C human immunodeficiency virus type 1. J Virol 80: 5211-5218.

38. Tang H, Robinson JE, Gnanakaran S, Li M, Rosenberg ES, et al. (2011) Epitopes immediately below the base of the V3 loop of gp120 as targets for the initial autologous neutralizing antibody response in two HIV-1 subtype B-infected individuals. J Virol 85: 9286-9299.

39. Zhu Z, Qin HR, Chen W, Zhao Q, Shen X, et al. (2011) Cross-reactive HIV-1-neutralizing human monoclonal antibodies identified from a patient with 2F5-like antibodies. J Virol 85: 11401-11408.

40. Bonsignori M, Hwang KK, Chen X, Tsao CY, Morris L, et al. (2011) Analysis of a clonal lineage of HIV-1 envelope V2/V3 conformational epitope-specific broadly neutralizing antibodies and their inferred unmutated common ancestors. J Virol 85: 9998-10009.

41. Gorny MK, Sampson J, Li H, Jiang X, Totrov M, et al. (2011) Human Anti-V3 HIV-1 Monoclonal Antibodies Encoded by the VH5-51/VL Lambda Genes Define a Conserved Antigenic Structure. PLoS One 6: e27780.

42. Gorny MK, Wang XH, Williams C, Volsky B, Revesz K, et al. (2009) Preferential use of the VH5-51 gene segment by the human immune response to code for antibodies against the V3 domain of HIV-1. Mol Immunol 46: 917-926.

43. Diskin R, Scheid JF, Marcovecchio PM, West AP, Jr., Klein F, et al. (2011) Increasing the potency and breadth of an HIV antibody by using structure-based rational design. Science 334: 1289-1293.

44. Changela A, Wu X, Yang Y, Zhang B, Zhu J, et al. (2011) Crystal structure of human antibody 2909 reveals conserved features of quaternary structure-specific antibodies that potently neutralize HIV-1. J Virol 85: 2524-2535.

45. MacDonald KS, Embree J, Njenga S, Nagelkerke NJ, Ngatia I, et al. (1998) Mother-child class I HLA concordance increases perinatal human immunodeficiency virus type 1 transmission. J Infect Dis 177: 551-556.

46. Malherbe DC, Doria-Rose NA, Misher L, Beckett T, Puryear WB, et al. (2011) Sequential immunization with a subtype B HIV-1 envelope quasispecies partially mimics the in vivo development of neutralizing antibodies. J Virol 85: 5262-5274.

47. Haaland RE, Hawkins PA, Salazar-Gonzalez J, Johnson A, Tichacek A, et al. (2009) Inflammatory genital infections mitigate a severe genetic bottleneck in heterosexual transmission of subtype A and C HIV-1. PLoS Pathog 5: e1000274.

48. Price MA, Wallis CL, Lakhi S, Karita E, Kamali A, et al. (2011) Transmitted HIV type 1 drug resistance among individuals with recent HIV infection in East and Southern Africa. AIDS Res Hum Retroviruses 27: 5-12.

49. Salazar-Gonzalez JF, Bailes E, Pham KT, Salazar MG, Guffey MB, et al. (2008) Deciphering human immunodeficiency virus type 1 transmission and early envelope diversification by single-genome amplification and sequencing. J Virol 82: 3952-3970.

50. Blish CA, Nedellec R, Mandaliya K, Mosier DE, Overbaugh J (2007) HIV-1 subtype A envelope variants from early in infection have variable sensitivity to neutralization and to inhibitors of viral entry. Aids 21: 693-702.

51. Long EM, Rainwater SM, Lavreys L, Mandaliya K, Overbaugh J (2002) HIV type 1 variants transmitted to women in Kenya require the CCR5 coreceptor for entry, regardless of the genetic complexity of the infecting virus. AIDS Res Hum Retroviruses 18: 567-576.

52. Poss M, Overbaugh J (1999) Variants from the diverse virus population identified at seroconversion of a clade A human immunodeficiency virus type 1-infected woman have distinct biological properties. J Virol 73: 5255-5264.

53. Li M, Gao F, Mascola JR, Stamatatos L, Polonis VR, et al. (2005) Human immunodeficiency virus type 1 env clones from acute and early subtype B infections for standardized assessments of vaccine-elicited neutralizing antibodies. J Virol 79: 10108-10125.

54. Kothe DL, Decker JM, Li Y, Weng Z, Bibollet-Ruche F, et al. (2007) Antigenicity and immunogenicity of HIV-1 consensus subtype B envelope glycoproteins. Virology 360: 218-234.

55. Kothe DL, Li Y, Decker JM, Bibollet-Ruche F, Zammit KP, et al. (2006) Ancestral and consensus envelope immunogens for HIV-1 subtype C. Virology 352: 438-449.

56. Li M, Salazar-Gonzalez JF, Derdeyn CA, Morris L, Williamson C, et al. (2006) Genetic and neutralization properties of subtype C human immunodeficiency virus type 1 molecular env clones from acute and early heterosexually acquired infections in Southern Africa. J Virol 80: 11776-11790.

57. Derdeyn CA, Decker JM, Bibollet-Ruche F, Mokili JL, Muldoon M, et al. (2004) Envelope-Constrained Neutralization-Sensitive HIV-1 After Heterosexual Transmission. Science 303: 2019-2022.

58. Rong R, Bibollet-Ruche F, Mulenga J, Allen S, Blackwell JL, et al. (2007) Role of V1V2 and other human immunodeficiency virus type 1 envelope domains in resistance to autologous neutralization during clade C infection. J Virol 81: 1350-1359.

59. Lynch RM, Rong R, Li B, Shen T, Honnen W, et al. (2010) Subtype-specific conservation of isoleucine 309 in the envelope V3 domain is linked to immune evasion in subtype C HIV-1 infection. Virology.

60. Rong R, Gnanakaran S, Decker JM, Bibollet-Ruche F, Taylor J, et al. (2007) Unique Mutational Patterns in the Envelope {alpha}2 Amphipathic Helix and Acquisition of

Length in gp120 Hyper-variable Domains are Associated with Resistance to Autologous Neutralization of Subtype C Human Immunodeficiency Virus type 1. J Virol 81: 5658-5668.

61. Eswar N, Webb B, Marti-Renom MA, Madhusudhan MS, Eramian D, et al. (2006) Comparative protein structure modeling using Modeller. Curr Protoc Bioinformatics Chapter 5: Unit 5 6.

62. Phillips JC, Braun R, Wang W, Gumbart J, Tajkhorshid E, et al. (2005) Scalable molecular dynamics with NAMD. J Comput Chem 26: 1781-1802.

63. Kwong PD, Wyatt R, Majeed S, Robinson J, Sweet RW, et al. (2000) Structures of HIV-1 gp120 envelope glycoproteins from laboratory-adapted and primary isolates. Structure Fold Des 8: 1329-1339.

64. Huang CC, Tang M, Zhang MY, Majeed S, Montabana E, et al. (2005) Structure of a V3-containing HIV-1 gp120 core. Science 310: 1025-1028.

65. Zhou T, Xu L, Dey B, Hessell AJ, Van Ryk D, et al. (2007) Structural definition of a conserved neutralization epitope on HIV-1 gp120. Nature 445: 732-737.

66. Pancera M, Majeed S, Ban YE, Chen L, Huang CC, et al. (2010) Structure of HIV-1 gp120 with gp41-interactive region reveals layered envelope architecture and basis of conformational mobility. Proc Natl Acad Sci U S A 107: 1166-1171.

67. Liu J, Bartesaghi A, Borgnia MJ, Sapiro G, Subramaniam S (2008) Molecular architecture of native HIV-1 gp120 trimers. Nature 455: 109-113.

68. Doores KJ, Bonomelli C, Harvey DJ, Vasiljevic S, Dwek RA, et al. (2010) Envelope glycans of immunodeficiency virions are almost entirely oligomannose antigens. Proc Natl Acad Sci U S A 107: 13800-13805.

69. Hornak V, Abel R, Okur A, Strockbine B, Roitberg A, et al. (2006) Comparison of multiple Amber force fields and development of improved protein backbone parameters. Proteins 65: 712-725.

70. Kirschner KN, Yongye AB, Tschampel SM, Gonzalez-Outeirino J, Daniels CR, et al. (2008) GLYCAM06: a generalizable biomolecular force field. Carbohydrates. J Comput Chem 29: 622-655.

71. Lahm HW, Stein S (1985) Characterization of recombinant human interleukin-2 with micromethods. J Chromatogr 326: 357-361.

72. Liao HX, Levesque MC, Nagel A, Dixon A, Zhang R, et al. (2009) High-throughput isolation of immunoglobulin genes from single human B cells and expression as monoclonal antibodies. J Virol Methods 158: 171-179.

73. Benoit RM, Wilhelm RN, Scherer-Becker D, Ostermeier C (2006) An improved method for fast, robust, and seamless integration of DNA fragments into multiple plasmids. Protein Expr Purif 45: 66-71.

74. Tiller T, Meffre E, Yurasov S, Tsuiji M, Nussenzweig MC, et al. (2008) Efficient generation of monoclonal antibodies from single human B cells by single cell RT-PCR and expression vector cloning. J Immunol Methods 329: 112-124.

75. Smith K, Garman L, Wrammert J, Zheng NY, Capra JD, et al. (2009) Rapid generation of fully human monoclonal antibodies specific to a vaccinating antigen. Nat Protoc 4: 372-384.

76. Walker LM, Phogat SK, Chan-Hui PY, Wagner D, Phung P, et al. (2009) Broad and potent neutralizing antibodies from an African donor reveal a new HIV-1 vaccine target. Science 326: 285-289.

77. Jiang X, Burke V, Totrov M, Williams C, Cardozo T, et al. (2010) Conserved structural elements in the V3 crown of HIV-1 gp120. Nat Struct Mol Biol 17: 955-961.

78. Spurrier B, Sampson JM, Totrov M, Li H, O'Neal T, et al. (2011) Structural analysis of human and macaque mAbs 2909 and 2.5B: implications for the configuration of the quaternary neutralizing epitope of HIV-1 gp120. Structure 19: 691-699.

79. Burke V, Williams C, Sukumaran M, Kim SS, Li H, et al. (2009) Structural basis of the cross-reactivity of genetically related human anti-HIV-1 mAbs: implications for design of V3-based immunogens. Structure 17: 1538-1546.

80. Otwinowski Z, Minor W (1997) Processing of X-Ray Diffraction Data Collected in Oscillation Mode. In: Carter CW, editor. Methods in Enzymology. Salt Lake City, UT: Academic Press, Inc. pp. 307-326.

81. Vagin A, Teplyakov A (2010) Molecular replacement with MOLREP. Acta Crystallogr D Biol Crystallogr 66: 22-25.

82. Winn MD, Ballard CC, Cowtan KD, Dodson EJ, Emsley P, et al. (2011) Overview of the CCP4 suite and current developments. Acta Crystallogr D Biol Crystallogr 67: 235-242.

83. Emsley P, Cowtan K (2004) Coot: model-building tools for molecular graphics. Acta Crystallogr D Biol Crystallogr 60: 2126-2132.

84. Adams PD, Grosse-Kunstleve RW, Hung LW, Ioerger TR, McCoy AJ, et al. (2002) PHENIX: building new software for automated crystallographic structure determination. Acta Crystallogr D Biol Crystallogr 58: 1948-1954.

85. Abagyan R, Totrov M, Kuznetsov D (1994) ICM—A new method for protein modeling and design: Applications to docking and structure prediction from the distorted native conformation. J Comput Chem 15: 488-506.

Tables

Table 1. Chronology of R880F envelope/monoclonal antibody isolation.

Sample Date	*Time Point*	*HIV-1 Envelopes*	*Monoclonal Antibodies*
12Jan07	0-month[a]	A6, B24	
16Mar07	2-month	A9, A13, B31, A23, A24, B18, A3, B1, B4, B12	
8Jun07	5-month	A5, B52, B53	
31Aug07	7-month	B1, B19, B27, B61, B45	
21Nov07	10-month	B39, C1	
19May08	16-month		19.3H-L1, 19.3H-L3

[a]Viral load at this time point was ~580,422 copies/ml in plasma.

Table 2. IC_{50} values for autologous plasma/mAbs with R880F wild-type and mutant Envs.

Envelope[a]	*Contemp.*[b] *plasma*	*16m plasma*	*19.3H -L1*[d]	*19.3H -L3*[d]	*Description*	*295*[f]	*335*[f]	*338*[f]	*341*[f]
0-A6	<100	5157	1.794	0.095	Founder	I	S	E	D
0-B24	<100	5763	1.519	0.094	Founder	I	S	E	D
0-A6 I295N	nd[c]	nd	>25	>25	Mutant	N*	S	E	D
0-B24 I295R	nd	nd	>25	>25[e]	Mutant	R	S	E	D
0-B24 I295T	nd	nd	>25	0.515	Mutant	T	S	E	D
0-A6 S335N	nd	nd	>25	>25	Mutant	I	N**	E	D
0-B24 D341N	nd	nd	0.095	0.092	Mutant	I	S	E	N
2-A3	<100	1447	>25	>25	2m Escape	I	S	K	D
2-A3 K338D	nd	nd	>25	>25	Mutant	I	S	D	D
2-A3 K338G	nd	nd	>25	>25	Mutant	I	S	G	D
2-A3 K338I	nd	nd	>25	>25	Mutant	I	S	I	D
2-A3 K338Q	nd	nd	>25	>25	Mutant	I	S	Q	D
2-A3 K338R	nd	nd	>25	>25	Mutant	I	S	R	D
2-A3 K338G D341N	nd	nd	>25	0.207	Mutant	I	S	G	N
2-A9	<100	4459	>25	>25[e]	2m Escape	R	S	E	D
2-A13	<100	3221	>25	>25[e]	2m Escape	R	S	E	D
2-A23	<100	4779	>25	>25	2m Escape	I	S	D	D
2-A24	<100	5279	>25	>25	2m Escape	I	S	D	D
2-B1	<100	2491	>25	>25	2m Escape	I	S	K	D
2-B4	<100	2387	>25	>25	2m Escape	I	S	K	D
2-B12	126	3516	0.092	0.092	2m Escape	I	S	E	N
2-B12 I295N	nd	nd	>25	>25	Mutant	N*	S	E	N
2-B12 S335N	nd	nd	>25	>25	Mutant	I	N**	E	N
2-B12 S335Q	nd	nd	1.981	0.113	Mutant	I	Q	E	N
2-B18	<100	3336	>25	>25	2m Escape	I	S	G	D
2-B31	<100	4594	>25	0.512	2m Escape	T	S	E	D
5-A5	<100	1891	>25	>25	5m Escape	I	S	D	D
5-B52	<100	1184	>25	0.152	5m Escape	I	S	G	N
5-B52 S335N	nd	nd	>25	>25	Mutant	I	N**	G	N
5-B53	<100	468	>25	>25	5m Escape	I	N**	K	D
7-B1	<100	558	>25	>25	7m Escape	I	N**	K	N
7-B19	<100	106	>25	>25	7m Escape	I	N**	E	D
7-B27	<100	462	>25	>25	7m Escape	I	N**	E	N
7-B45	<100	539	>25	>25	7m Escape	N*	S	K	N
7-B61	<100	539	>25	>25	7m Escape	I	N**	E	N
10-B39	<100	990	>25	>25	10m Escape	N*	S	Q	N
10-C1	<100	998	>25	>25	10m Escape	N*	N**	E	N

[a]Longitudinal wild-type and mutant Envs were assayed for neutralization sensitivity to autologous plasma and mAbs 19.3H-L1 and 19.3H-L3 in Tzm-bl cells. Average IC_{50} values

for two independent experiments using duplicate wells are given in the second through fifth columns.

[b]Autologous plasma samples assayed in the second column were contemporaneous with envelope isolation dates (e.g. 0-month plasma with 0-month Envs, 2-month plasma with 2-month Envs, etc.).

[c]nd, not done.

[d]19.3H-L1 and 19.3H-L3 were isolated from a 16-month cryopreserved R880F PBMC sample.

[e]These envelopes, though technically demonstrating IC_{50} values greater than 25μg/ml, saw slight neutralization at the highest concentration of antibody tested.

[f]The four right-most columns detail which amino acids appear at the specified Env residues (295, 335, 338, and 341). N* denotes the introduction of a potential N-linked glycosylation site, while N** marks where such a site has been shifted downstream from a previously existing site in the Env sequence.

Table S1. Fab crystal structure data collection and refinement statistics.

		19.3H-L1	*19.3H-L3*
Data Collection[a]			
Space group		C2	$P2_1$
Cell dimensions	a, b, c (Å)	152.10, 57.46, 60.04	73.40, 126.41, 120.08
	α, β, γ (°)	90.00, 112.78, 90.00	90.00, 90.08, 90.00
Resolution (Å)		1.70 (1.73-1.70)	2.70 (2.85-2.70)
R_{merge} (%)		4.2 (35.5)	14.8 (49.7)
$I / \sigma I$		31.9 (2.92)	11.2 (2.5)
Completeness (%)		95.8 (81.8)	99.8 (99.0)
Redundancy		3.8 (3.1)	3.4 (3.1)
Refinement[b]			
Resolution (Å)		41.5-1.70	46.5-2.5
Number of reflections		50,557	75,512
R_{work} / R_{free}		18.65/20.91	20.80/25.64
Number of atoms	Protein	3,296	13,078
	Solvent	532	682
B-factors	Protein	24.3	34.2
	Solvent	34.4	34.2
R.m.s. deviations	Bond lengths (Å)	0.0066	0.0075
	Bond angles (°)	1.114	1.165

[a]Fab fragments of R880F mAbs 19.3H-L1 (PDB code 4F57) and 19.3H-L3 (PDB code 4F58) were crystallized with the hanging drop method after papain digestion, affinity and size exclusion chromatography purification, and concentration. X-ray diffraction data were collected and processed using HKL2000.

[b]Statistics in parentheses in the 19.3H-L1 and 19.3H-L3 columns refer to outer shell resolutions. The structures were refined using COOT and PHENIX and analyzed using ICM.

Figures

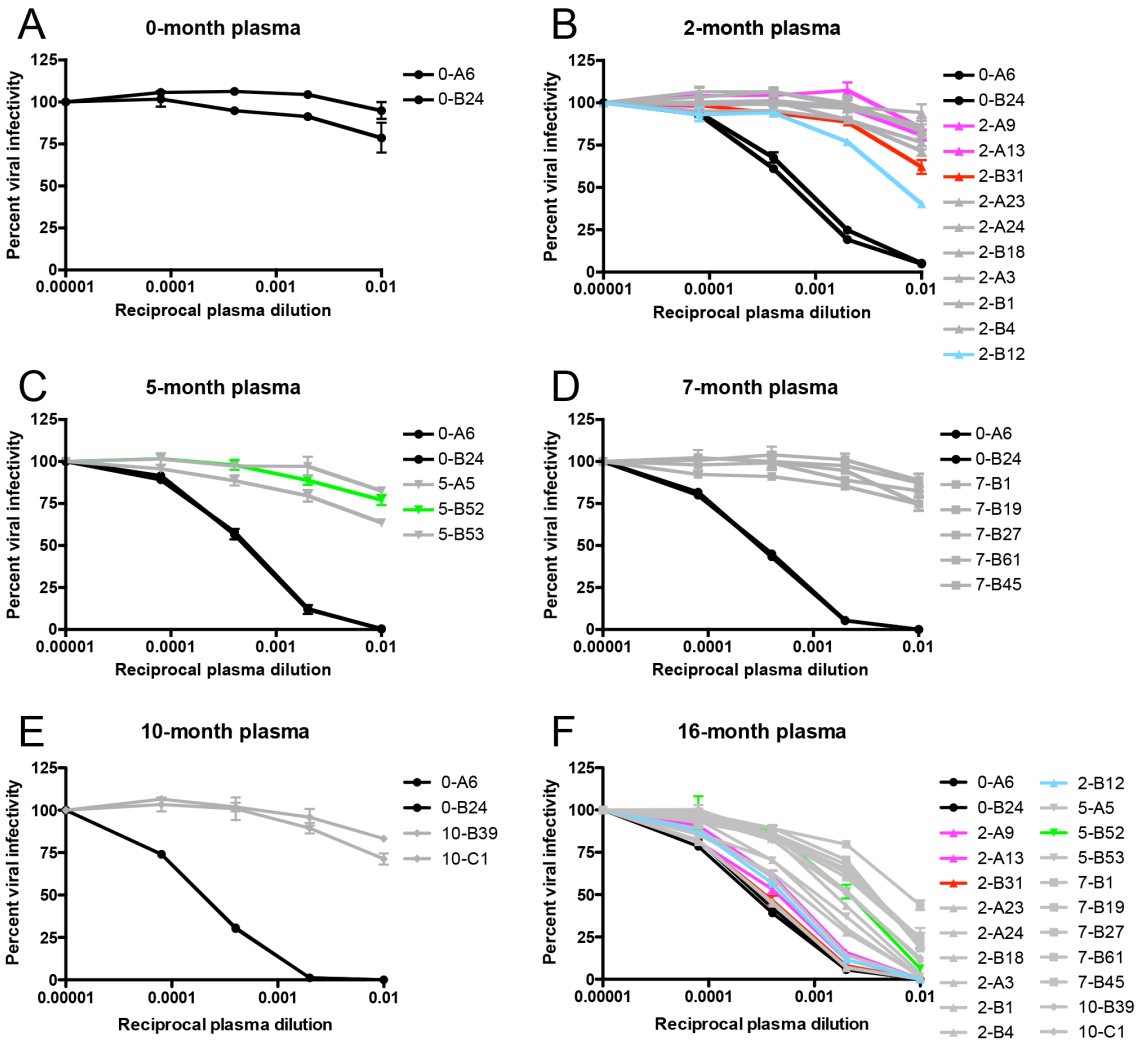

Figure 1. Identification of R880F nAb escape variants. Twenty-two single-genome amplified subtype A HIV-1 Envs were cloned out of R880F plasma collected at 0-months **(A)**, 2-months **(B)**, 5-months **(C)**, 7-months **(D)**, and 10-months **(E)** post-seroconversion, pseudotyped, and assayed against autologous plasma contemporaneous to their respective dates of isolation. Two 0-month Envs (0-A6/B24) representative of the transmitted/founder sequence are included in each panel. To demonstrate that humoral escape variants were neutralized during the course of infection, all 22 longitudinal Envs

were assayed for neutralization with 16-month plasma **(F)**; it was from PBMC collected at this time point that the two autologous R880F mAbs, 19.3H-L1 and 19.3H-L3, were derived. Percent viral infectivity, as adjusted against wells containing no test plasma, is depicted on the vertical axis; reciprocal plasma dilutions are plotted along the horizontal axis in a logarithmic fashion. Each curve represents a single Env-plasma combination, and error bars demonstrate the standard error of the mean of two independent experiments using duplicate wells (0-month Envs = circles, 2-month Envs = triangles, 5-month Envs = inverted triangles, 7-month Envs = squares, 10-month Envs = diamonds). Colored lines (2-A9/2-A13 in magenta, 2-B31 in red, 2-B12 in cyan, and 5-B52 in green) indicate Envs that succumbed to neutralization, in varying combinations, by the isolated R880F mAbs.

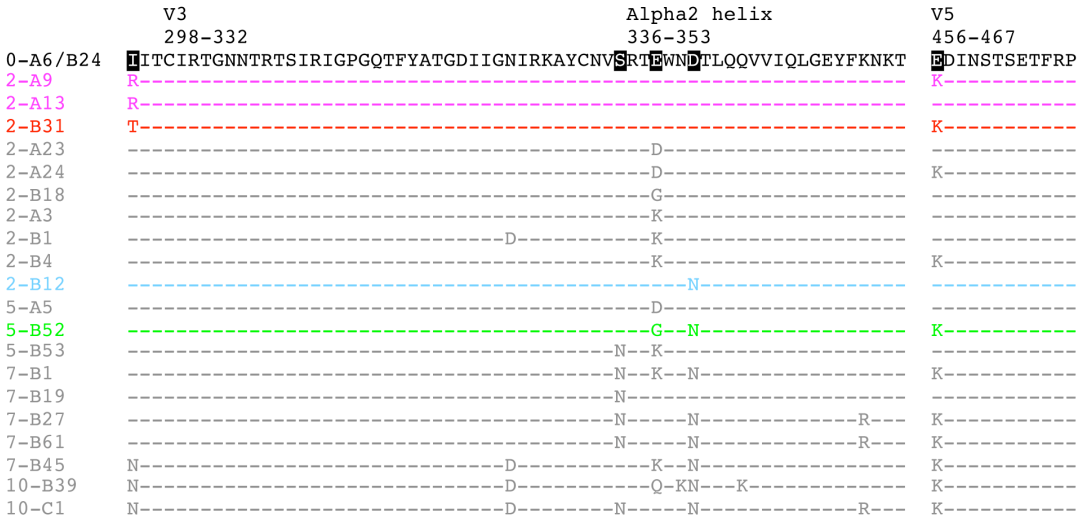

Figure 2. Amino acid alignment of longitudinal R880F Envs. Longitudinal Env amino acid sequences from 20 R880F contemporaneous plasma escape variants were aligned and examined using Sequencher v5.0 and Geneious v5.0.3 software, with particular emphasis on the three mutational hot spots--C2, the alpha2 helix in C3, and V5--that developed during early infection, as compared to the transmitted/founder Env (0-A6/B24). Dashes represent conserved positions. Subject-specific amino acid numbering labels the demarcated regions at their points of origination. Five residues including 295, 335, 338, 341, and 456 (HXB2 residues 293, 334, 337, 340, and 460) were specifically interrogated to define their contributions to nAb evasion and have been highlighted in black in 0-A6/B24 for easy identification. Colored sequences (2-A9/2-A13 in magenta, 2-B31 in red, 2-B12 in cyan, and 5-B52 in green) indicate Envs that succumbed to neutralization, in varying combinations, by the isolated R880F mAbs. Note that additional differences from the transmitted/founder Env, which occurred over time in these sequences but are not diagrammed here, may be viewed in Figure S1.

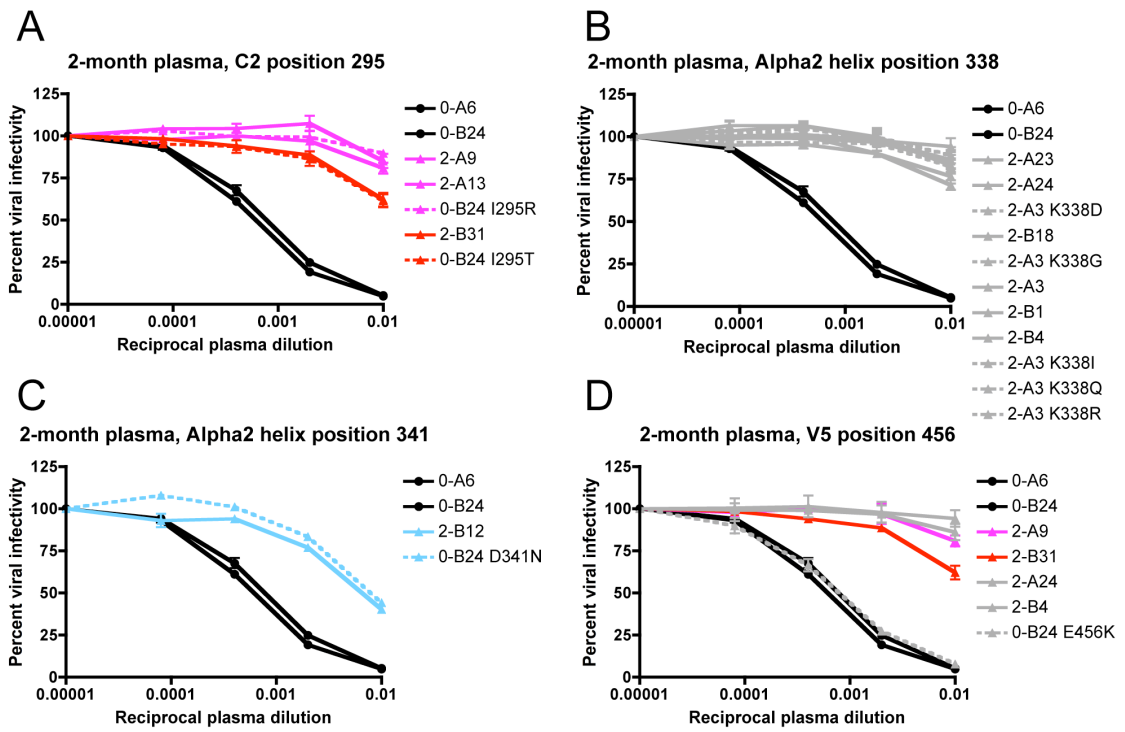

Figure 3. Determination of the earliest R880F nAb escape signatures in Env. Suspected 2-month nAb escape mutations from four different amino acid positions were introduced by site-directed mutagenesis into the transmitted/founder Env 0-B24 or escape Env 2-A3, which differed from the founder only at the site of mutation introduction. The transmitted/founder and wild-type 2-month Envs (solid lines) along with site-directed mutant Envs (dashed lines) were pseudotyped and assayed with 2-month plasma to determine if substitutions at C2 295 **(A)**, alpha2 helix 338 **(B)**, alpha2 helix 341 **(C)**, or V5 456 **(D)** (HXB2 residues 293, 337, 340, or 460) could individually confer resistance. Percent viral infectivity, as adjusted against wells containing no test plasma, is depicted on the vertical axis; reciprocal plasma dilutions are plotted along the horizontal axis in a logarithmic fashion. Each curve represents a single Env-plasma combination, and error bars demonstrate the standard error of the mean of two independent experiments using duplicate wells (0-month Envs = circles, 2-month Envs and representative point mutants =

triangles). Colored lines (2-A9/2-A13/0-B24 I295R in magenta, 2-B31/0-B24 I295T in red, and 2-B12/0-B24 D341N in cyan) indicate Envs that succumbed to neutralization, in varying combinations, by the isolated R880F mAbs.

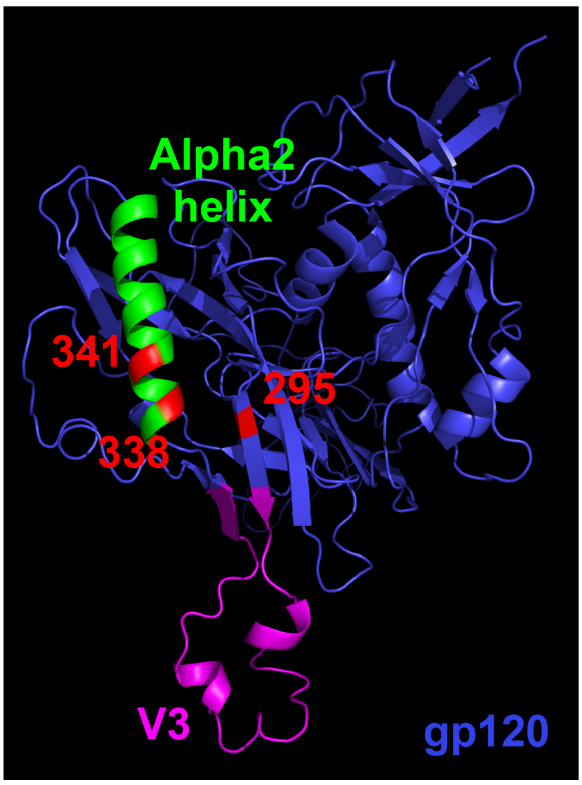

Figure 4. Homology model of R880F gp120. A 3-dimensional gp120 monomer (blue) based on the R880F transmitted/founder Env 0-A6/B24 sequence was homology modeled from existing gp120 structures (see Materials and Methods) and spatially oriented using MacPyMOL software to illuminate the region targeted by the earliest nAbs in this subject. Functional domains such as the alpha2 helix (green) and V3 (magenta) are delineated, and subject-specific amino acid numbering indicates positions that mutated at 2-months post-seroconversion to confer nAb escape. These residues (295, 338, and 341 in red) nest together in a putative epitope.

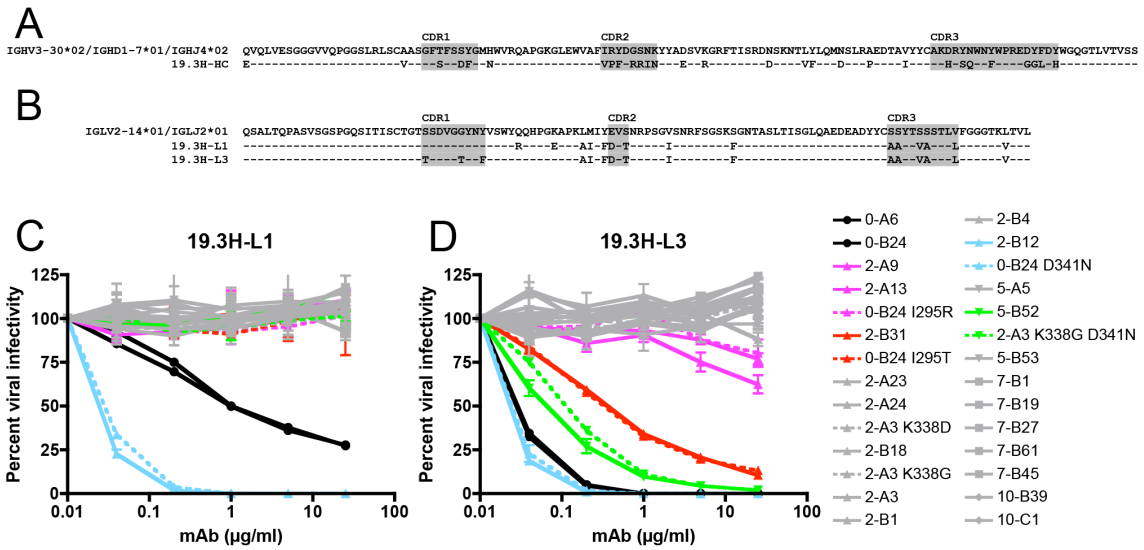

Figure 5. Amino acid alignment of R880F immunoglobulin heavy and light chain variable domains and neutralization by R880F mAbs 19.3H-L1 and 19.3H-L3. Germline heavy and light chain gene segment utilization was determined by SoDA, a somatic diversification analysis program [32], and amino acid sequences were aligned and examined using Sequencher v5.0 and Geneious v5.0.3 software. Dashes represent conserved positions. Complementarity-determining regions (CDRs) are highlighted in gray. The two R880F mAbs share a common heavy chain, 19.3H-HC **(A)**, which utilizes V3-30*02, D1-7*01, and J4*02 gene families, while the somatically related light chains 19.3H-L1 and 19.3H-L3 **(B)** employ V2-14*01 and J2*01 gene families and differ from each other at five positions in and just downstream of CDR1. Heavy chain 19.3H-HC, when paired with either 19.3H-L1 **(C)** or 19.3H-L3 **(D)**, was evaluated for neutralization against pseudotyped R880F wild-type (solid lines) and site-directed mutant Envs (dashed lines). Percent viral infectivity, as adjusted against wells containing no mAb, is depicted on the vertical axis; mAb concentrations (in µg/ml) are plotted along the horizontal axis in a logarithmic fashion. Each curve represents a single Env-mAb combination, and error bars demonstrate the standard error of the mean

of two independent experiments using duplicate wells (0-month Envs = circles, 2-month Envs and representative point mutants = triangles, 5-month Envs and a representative point mutant = inverted triangles, 7-month Envs = squares, 10-month Envs = diamonds). Colored lines (2-A9/2-A13/0-B24 I295R in magenta, 2-B31/0-B24 I295T in red, 2-B12/0-B24 D341N in cyan, and 5-B52/2-A3 K338G D341N in green) indicate Envs that succumbed to neutralization, in varying combinations, by the isolated R880F mAbs.

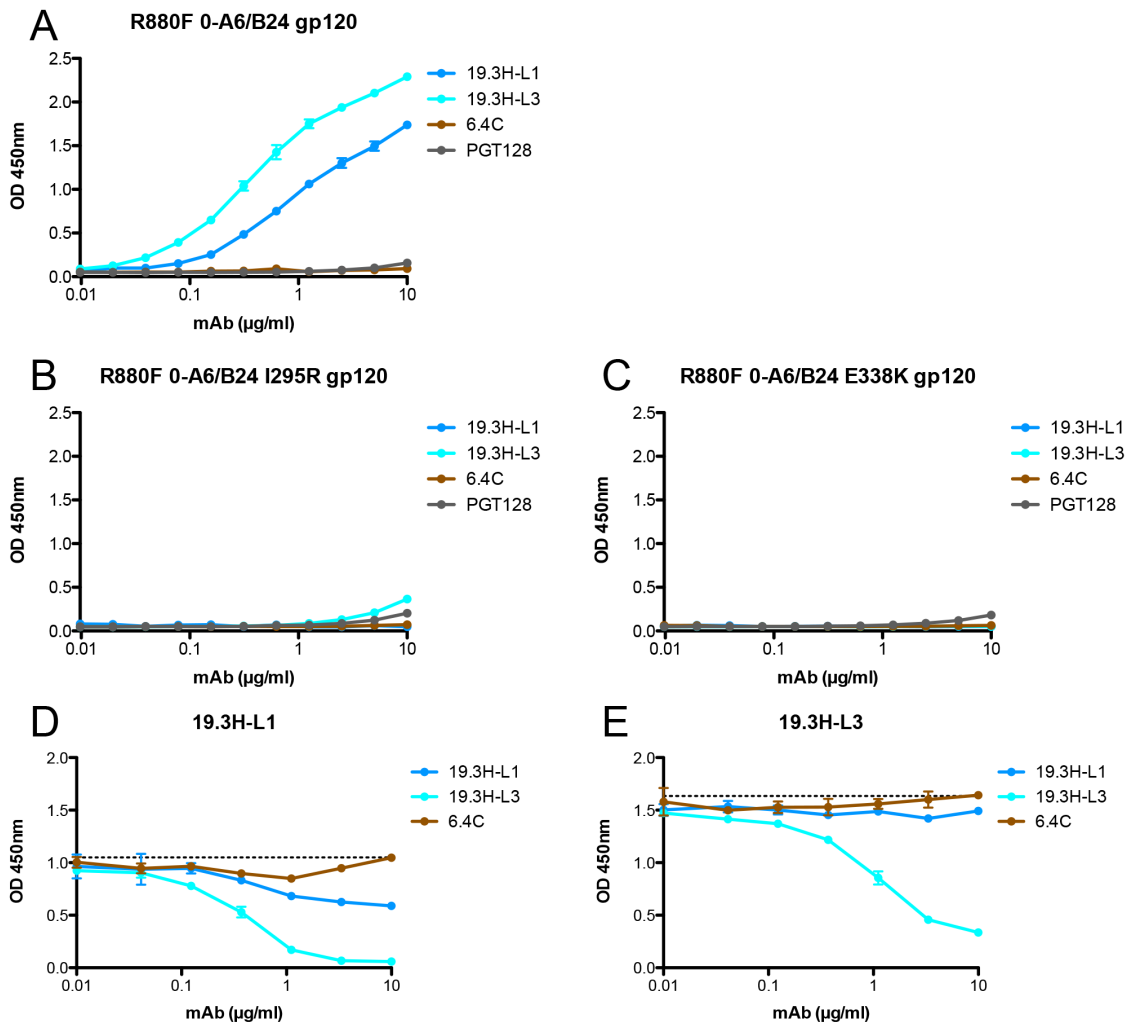

Figure 6. gp120 binding by and competition of R880F mAbs 19.3H-L1 and 19.3H-L3. The baseline binding of four biotinylated mAbs, 19.3H-L1, 19.3H-L3, 6.4C, or PGT128, was evaluated by ELISA with three R880F gp120 proteins: **(A)** wild-type 0-A6/B24, **(B)** point mutant 0-A6/B24 I295R, and **(C)** point mutant 0-A6/B24 E338K. R880F mAbs 19.3H-L1 and 19.3H-L3 were then competed with themselves, each other, and the negative control antibody, 6.4C. For the competition ELISAs, plates were coated with wild-type R880F 0-A6/B24 gp120 protein, pre-incubated with serially-diluted 19.3H-L1, 19.3H-L3, or 6.4C, washed, and then incubated with 1 µg/ml biotinylated 19.3H-L1 **(D)** or 19.3H-L3 **(E)**. From data in **(A)**, 1 µg/ml was selected as a point of non-saturated binding. The horizontal

dashed lines in **(D)** and **(E)** represent 100% binding of biotinylated 19.3H-L1 or 19.3H-L3, at 1 μg/ml in the absence of competitor, respectively. Optical density values at 450 nm are depicted on the vertical axis; mAb concentrations (in μg/ml) are plotted along the horizontal axis in a logarithmic fashion. Error bars demonstrate the standard error of the mean of two independent experiments.

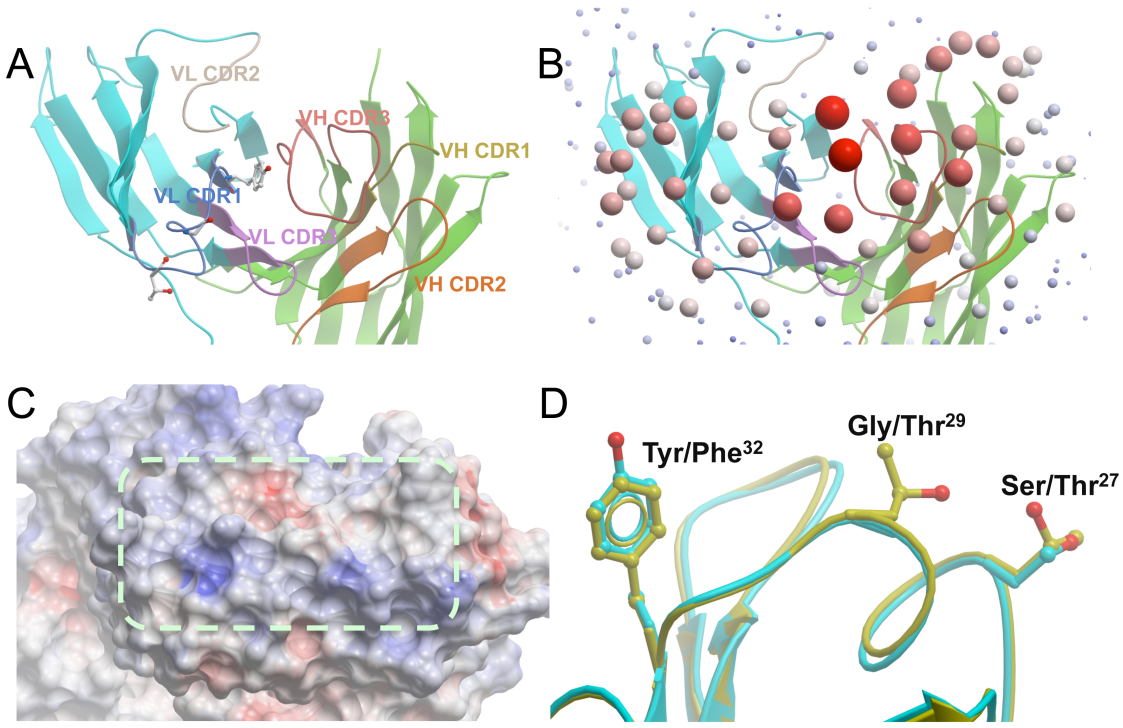

Figure 7. Crystal structures of R880F mAbs 19.3H-L1 and 19.3H-L3. **(A)** CDR loops. A top view looking down at the antigen-binding site of 19.3H-L1 represented by ribbons. The framework regions of the light chain and heavy chain are colored cyan and green, respectively, while each CDR loop is colored separately. The side chains of the three VL CDR1 residues different between 19.3H-L1 and 19.3H-L3 are displayed. **(B)** ODA analysis of the Fab 19.3H-L1. The size/redness of each sphere is proportional to the binding strength of the region indicated. Note that the antigen-binding site is centered at VL CDR1 and VH CDR3. **(C)** The electrostatic surface potentials of the antigen-binding site of 19.3H-L1. Red and blue coloration represents the negatively and positively charged regions, respectively, while a dashed line encircles the flat surface of the antigen-binding site. **(D)** The three VL CDR1 amino acid differences, S27T, G29T, and Y32F, between 19.3H-L1 (cyan) and 19.3H-L3 (yellow).

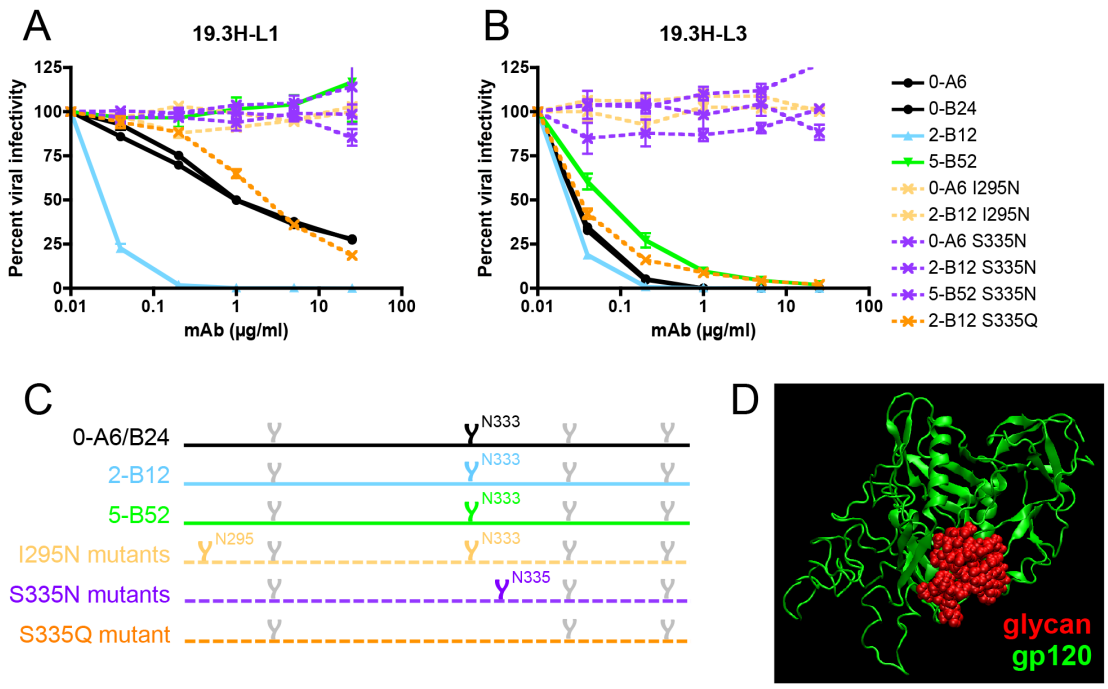

Figure 8. Escape from mAbs 19.3H-L1 and 19.3H-L3 by glycan addition and/or shifting. To investigate how longitudinal viruses, namely 7- and 10-month Envs, could harbor the humoral vulnerability associated with mutation D341N whilst maintaining neutralization-resistant phenotypes, two potential compensatory mutations were investigated. I295N, which inserts a PNGS near the N-terminus of V3, was introduced by site-directed mutagenesis into two mAb-sensitive Envs, 0-A6 and 2-B12 (light orange). S335N, which shifts a PNGS closer to the N-terminus of the alpha2 helix, was similarly created in 0-A6, 2-B12, and 5-B52 (purple). Wild-type (solid lines) and site-directed mutant Envs (dashed lines) were pseudotyped and assayed with mAbs 19.3H-L1 **(A)** and 19.3H-L3 **(B)**. To determine if mAb resistance was glycan-dependent, an S335Q substitution that destroyed the N333 PNGS was also created in Env 2-B12 (dark orange). Percent viral infectivity, as adjusted against wells containing no mAb, is depicted on the vertical axis; mAb concentrations (in µg/ml) are plotted along the horizontal axis in a logarithmic fashion. Each curve represents a single Env-mAb combination, and error bars demonstrate the standard

error of the mean of two independent experiments using duplicate wells. In **(C)**, the V3/alpha2 helix portion of the labeled Envs has been conceptualized with glycan forks, each of which represents a PNGS in the corresponding amino acid sequences. Glycans of particular interest (N295, N333, and N335) are designated using R880F-specific numbering. In **(D)**, the proposed escape glycans N295 and N335 (red) have been modeled onto the R880F 0-B24 Env gp120 monomer (green) to illustrate how such masking could obscure underlying epitopes and prevent recognition by mAbs 19.3H-L1 and 19.3H-L3.

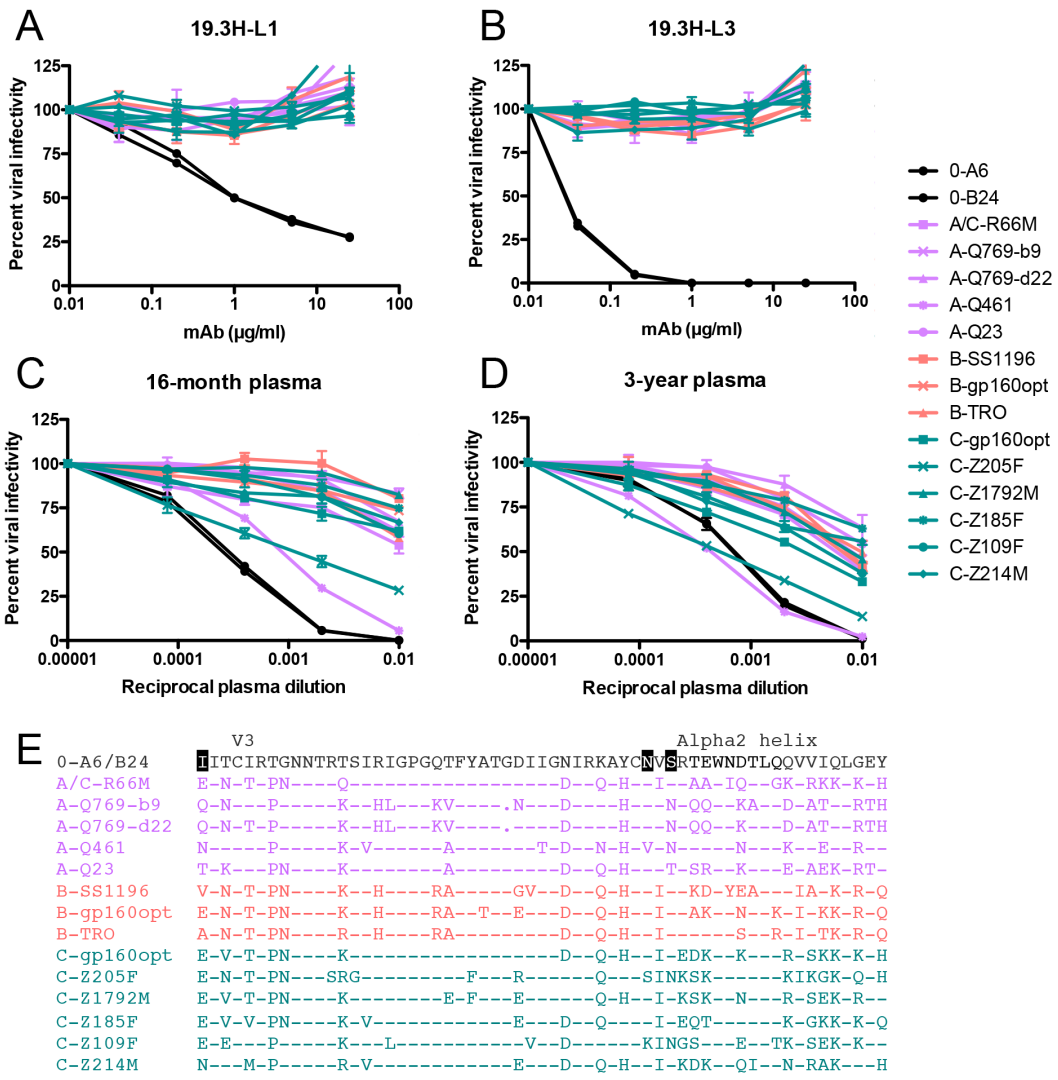

Figure 9. Heterologous neutralization breadth in R880F. The two R880F mAbs, 19.3H-L1 **(A)** and 19.3H-L3 **(B)**, in conjunction with 16-month **(C)** and 3-year **(D)** autologous plasma were evaluated for cross-neutralizing capacity against virions pseudotyped with fourteen heterologous HIV-1 Envs from three clades (A/C recombinant and subtype A Envs = lavender, subtype B Envs = coral, subtype C Envs = teal). Two 0-month Envs (0-A6/B24) representative of the transmitted/founder sequence are included in each of these panels. Percent viral infectivity, as adjusted against wells containing no mAb or test plasma, is depicted on the vertical axis; mAb concentrations (in µg/ml) or reciprocal plasma dilutions

are plotted along the horizontal axis in a logarithmic fashion. Each curve represents a single Env-mAb or Env-plasma combination, and error bars demonstrate the standard error of the mean of two independent experiments using duplicate wells. V3/alpha2 helix amino acid sequences were aligned and examined using Sequencher v5.0 and Geneious v5.0.3 software **(E)**. Dashes represent conserved positions; dots represent gaps. Significant PNGS sequons (N295, N333, N335) are highlighted in black at their points of origin.

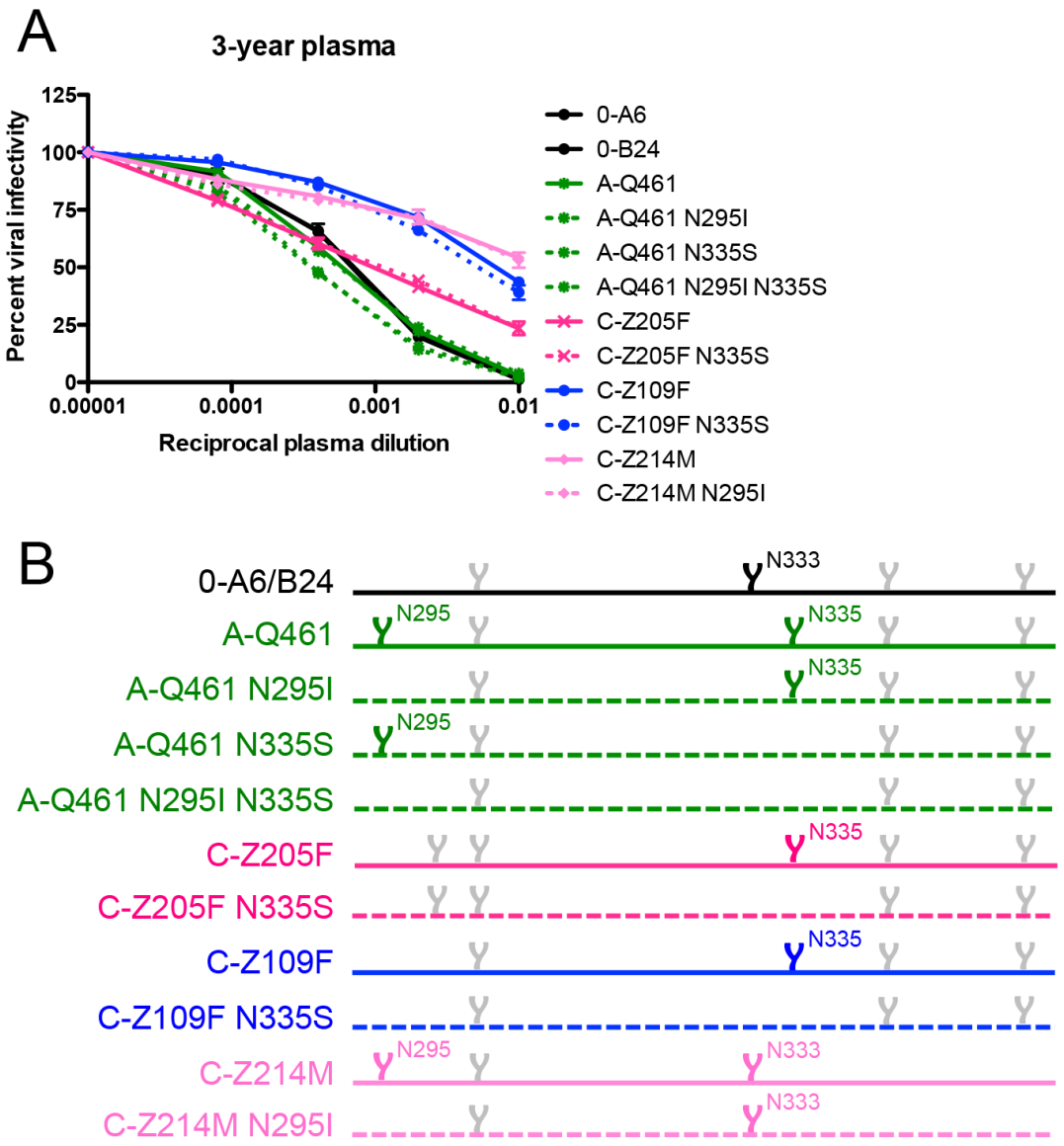

Figure 10. Contribution of specific glycans to heterologous neutralization breadth in R880F.

To gauge if nAb responses continued to exert pressure, specifically against escape glycans, on the N- and C-terminal V3 flanks of envelope during long-term HIV-1 infection, wild-type (solid lines) and site-directed mutant (dashed lines) heterologous Envs were pseudotyped and assayed for neutralization with 3-year R880F autologous plasma **(A)**. Percent viral infectivity, as adjusted against wells containing no test plasma, is depicted on the vertical axis; reciprocal plasma dilutions are plotted along the horizontal axis in a

logarithmic fashion. Each curve represents a single Env-plasma combination, and error bars demonstrate the standard error of the mean of two independent experiments using duplicate wells. In **(B)**, the V3/alpha2 helix portion of the labeled Envs has been conceptualized with glycan forks, each of which represents a PNGS in the corresponding amino acid sequences. Glycans of particular interest (N295, N333, and N335) are designated using R880F-specific numbering.


V1
V2
V3
Alpha2 helix
V4

Figure S1. Full-length R880F Env gp160 alignment. The complete Env gp160 amino acid sequences of twenty longitudinal R880F humoral escape variants have been aligned in comparison to the founder Envs 0-A6/B24 and examined using Sequencher v5.0 and

Geneious v5.0.3 software. Dashes represent conserved positions; dots represent gaps. Significant structural domains are highlighted for simple visual discernment (V1 = red, V2 = blue, V3 = magenta, alpha2 helix = green, V4 = orange, V5 = purple).

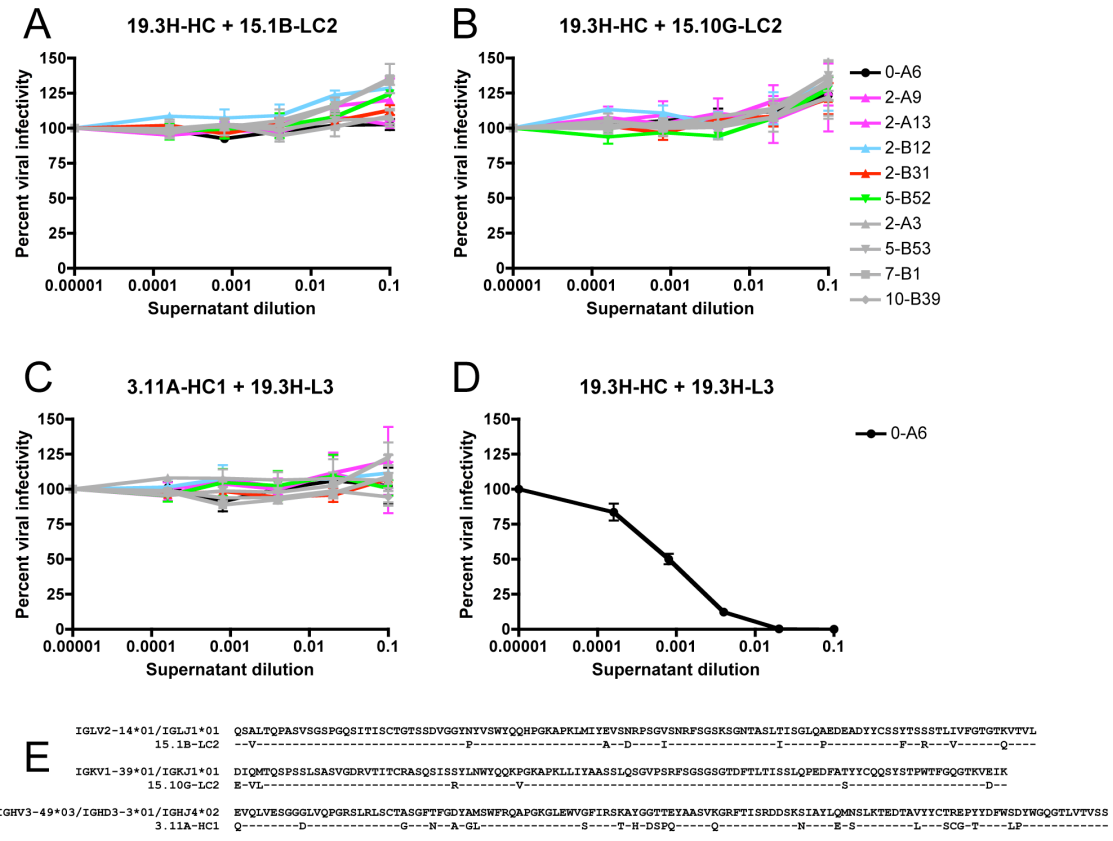

Figure S2. Specificity of R880F VH and VL pairing. 19.3H-HC, a common R880F heavy chain shared by the two R880F mAbs, was stochastically paired and co-transfected with two unrelated R880F light chains, 15.1B-LC2 **(A)** and 15.10G-LC2 **(B)**. Similarly, the wild-type 19.3H-L3 light chain was matched with a random R880F heavy chain, 3.11A-HC1 **(C)**. All chimeric mAbs were examined for neutralization capacity against a panel of ten R880F longitudinal Envs (0-month Env = circle, 2-month Envs = triangles, 5-month Envs = inverted triangles, 7-month Env = square, 10-month Env = diamond). Percent viral infectivity, as adjusted against wells containing no supernatant, is depicted on the vertical axis; supernatant dilutions are plotted along the horizontal axis in a logarithmic fashion. Each curve represents a single Env-supernatant combination, and error bars demonstrate the standard error of the mean of two independent experiments using duplicate wells.

Supernatant from the co-transfection of 19.3H-HC with wild-type light chain 19.3H-L3 was used as a positive control in these experiments **(D)**. Germline heavy and light chain gene segment utilization was determined by SoDA, a somatic diversification analysis program [32], and amino acid sequences were aligned and examined using Sequencher v5.0 and Geneious v5.0.3 software **(E)**. Dashes represent conserved positions.

Chapter 2

B-lymphocyte Dysfunction in Chronic HIV-1 Infection Does Not Prevent Cross-clade Neutralization Breadth

Published in *Journal of Virology*, 86(15):8031-40, 2012

Megan K. Murphy performed the neutralization experiments in this study (Figures 6 and S1), while Saikat Boliar characterized B-lymphocyte dysfunction (Figures 1-5).

Saikat Boliar, Megan K. Murphy, and Cynthia A. Derdeyn wrote the manuscript.

Abstract

Aberrant expression of regulatory receptors PD-1 and BTLA are linked with dysregulation and exhaustion of T-lymphocytes during chronic HIV-1 infection; however, less is known about whether a similar process impacts B-lymphocyte function during HIV-1 infection. We reasoned that disruption of the peripheral B cell compartment might be associated with decreased neutralizing antibody activity. Expression of markers that indicate dysregulation (BTLA and PD-1), immune activation (CD95), and proliferation (Ki-67) were evaluated in B cells from HIV-1 infected viremic and aviremic subjects and healthy subjects, in conjunction with immunoglobulin production and CD4 T cell count. Viral load and cross-clade neutralizing activity in plasma from viremic subjects was also assessed. Dysregulation of B-lymphocytes was indicated by a marked disruption of peripheral B cell subsets, increased levels of PD-1 expression, and decreased levels of BTLA expression in viremic subjects, compared to aviremic subjects and healthy controls. PD-1 and BTLA were correlated in a divergent fashion with immune activation, CD4 T cell count, and the total plasma IgG level, a functional correlate of B cell dysfunction. Within viremic subjects, the total IgG level correlated directly with cross-clade neutralizing activity in plasma. The findings demonstrate that even in chronically infected subjects where B-lymphocytes display multiple indications of dysfunction, antibodies that mediate cross-clade neutralization breadth continue to circulate in plasma.

Introduction

Infection with human immunodeficiency virus type-1 (HIV-1) leads to widespread dysfunction of the immune system, including B-lymphocytes. One sign of B cell dysfunction in HIV-1 infection is an increase in the production of IgG, or hypergammaglobulinemia [1-3]. B-lymphocytes of HIV-1 infected persons also exhibit signs of polyclonal activation and auto-reactivity [4] and impaired responses to both T-dependent and -independent antigenic stimuli or immunization [5-8]. These dysfunctions have been attributed, in part, to an imbalance of four major subsets within the B cell compartment [9,10]. Combination antiretroviral therapy (cART) only partially restores the balance, even after 12 months of treatment [9].

Since first introduced by Ascher and Sheppard in the late 1980s, the concept of immune activation as a causative mechanism of HIV-1 pathogenesis/AIDS has garnered immense consideration and experimental evaluation [11]. The degree of immune activation has been implicated in disease progression pace [12]. Normally, delicate interplay among several regulatory receptors tightly governs activation of the immune system. Recently, the importance of programmed death-1 (PD-1, CD279) has been emphasized in the development of hyper immune activation and exhaustion within T-lymphocytes during chronic viral infections, including HIV-1 [13-18]. Less is known about the role of PD-1 in the maintenance of B cell function, but a recent study demonstrated that PD-1 expression on activated memory B cells in SIV infection was associated with rapid disease progression [19]. Similar to PD-1, B and T lymphocyte attenuator (BTLA, CD272) is another member of the B7/CD28 superfamily [20]. This regulatory receptor is decreased on CD4 and CD8 T cells during chronic HIV-1 infection, and its expression is inversely correlated with disease

progression [21]. Thus, aberrant expression of PD-1 and BTLA on T cells in HIV-1 infection has been associated with disease progression.

Antibodies that can mediate neutralization of heterologous HIV-1 viruses are desirable from a vaccine perspective, but it is unclear how they arise or if they provide any benefit to the patient. Furthermore, these types of neutralizing antibodies (nAbs) are detected only after several years of infection, and in only a subset of infected individuals [22-30]. Factors that have been suggested to promote the development of neutralization breadth include prolonged exposure to antigen, higher envelope diversity, and plasma viral load [22,26,31-34]. Nevertheless, neutralization breadth does not delay disease progression [22,30,32]. Others have demonstrated that peripheral B cell decline and other perturbations do not necessarily impede nAb activity as measured in vitro [28,35], but to date no one has measured neutralization breadth in a cohort of HIV-1 infected subjects where multiple aspects of B cell dysfunction have been evaluated in parallel.

Here we evaluated the state of the peripheral B cell compartment in chronically HIV-1 infected individuals, infected but aviremic subjects treated with cART, and healthy controls by evaluating levels of PD-1 and BTLA expression on total B cells, and within peripheral B cell subsets. Aberrant expression of these receptors was observed in viremic individuals and was correlated with increased levels of immune activation, proliferation, IgG production, and CD4 T cell decline. We also investigated whether individuals experiencing these signs of B cell dysfunction possessed antibody-mediated neutralization capacity against pseudotyped heterologous HIV-1 envelope (Env) glycoproteins. Strong cross-clade neutralizing antibody activity was detected in the plasma of a subset of these infected individuals, even though the B cell compartment was perturbed.

Materials and Methods

Study subjects

In compliance with procedures approved by the Emory University Institutional Review Board (IRB), 41 individuals were enrolled with informed consent for this study. Participants were categorized into three groups: healthy controls (HC, n=12) included persons without HIV-1 infection or any clinical symptoms at the time of enrollment; viremic subjects (VI, n=16) had clinical records of HIV-1 infection, but were cART naïve and had plasma viral loads greater than 1000 copies/ml; and aviremic subjects (AV, n=13) were HIV-1 infected and currently on cART with a plasma viral load of fewer than 100 copies/ml. Median age, CD4 T cell count, and viral load, as well as the gender and ethnicity of the study participants, are listed in Table 1.

PBMC isolation

Approximately 50 ml blood were collected from each participant in ACD containing BD-vacutainer® blood collection tubes with informed consent from the donor. Peripheral blood mononuclear cells (PBMCs) were isolated from fresh blood by standard Ficoll-Paque density gradient centrifugation (Ficoll-Paque Plus, GE Healthcare). PBMCs were then aliquoted and cryopreserved in liquid nitrogen (-160℃) until needed for flow cytometry.

Flow cytometric analysis of peripheral B cells

PBMCs were thawed and washed twice with PBS and then re-suspended in FACS buffer (PBS with 1% BSA and 0.1% sodium azide). Two million cells were used for surface staining with the following antibodies: yellow fluorescent reactive dye (live/dead stain), anti-CD3 V500 (SP34-2), anti-CD14 V500 (M5E2), anti-PD-1 APC (EH12.2H7), anti-BTLA PE

(J168-540), anti-CD19 Qdot655 (SJ25C1), anti-CD10 APC-Cy7 (HI10a), anti-CD21 PE-Cy5 (B-ly4), anti-CD27 PE-Cy7 (1A4CD27), and anti-CD95 FITC (DX2). Following live/dead cell staining, PBMCs were incubated with antibodies at 4°C for 30 min; cells were fixed, and any contamination of RBC was removed by incubation in 1X lysing solution (BD Bioscience) for 10 min at room temperature. For intracellular staining, PBMCs were further washed twice with FACS buffer and permeabilized with 1X permeabilizing solution (BD Bioscience) for 30 min at room temperature. Anti-Ki-67 Alexa Fluor 700 (B56) antibody was used for the intracellular staining at room temperature for 30 min. After washing twice, cells were re-suspended in 400 µl FACS buffer containing 1% paraformaldehyde. Fluorescence minus one (FMO) negative controls were included for staining. An LSR-II cell analyzer (BD Bioscience) was used to acquire data. Lymphocytes were gated based on forward vs. side scatter profile, and B-lymphocytes were gated as $CD19^+$ cells after exclusion of dead, $CD3^+$, and $CD14^+$ cells. Data was analyzed using FlowJo software (version 9.3.1, TreeStar Inc., USA).

ELISA assay for plasma IgG

Total IgG concentration in plasma was measured by using a human IgG ELISA quantitation set (Bethyl Laboratories Inc.) following the manufacturer's directions. Plasma was heat inactivated (56°C for 60 min) and then diluted to 1:100,000 for the experiments. Endpoint absorbance was measured at 450nm with a BioTek Synergy multi-detection microplate reader, and data was analyzed with KC4 v3.4 software. A human reference serum was used to normalize total IgG concentrations in plasma.

ELISA assay for binding to monomeric gp120

Immulon microtiter 96 well plates were coated with 100 μl of HIV-1 BaL gp120 diluted to 5 μg/ml in coating buffer (Institute of Human Virology, μQuant Facility). Plates were washed 3 times and then blocked for 30 min at 37°C. Following washing, 100 μl of heat-inactivated plasma was added to each well and incubated for 1 hour. Plates were washed 3 times and 100 μl of HRP-conjugated goat anti-human IgG was added to each well. After a 1 hour incubation at 37°C, plates were washed, and TMB substrate was added. After 10 min, reactions were stopped with 4N H_2SO_4, endpoint absorbance was measured at 450nm with a BioTek Synergy multi-detection microplate reader, and data was analyzed with KC4 v3.4 software.

Neutralization assay

The ability of plasma from 16 viremic individuals to neutralize a cross-clade panel of 13 HIV-1 envelope (Env) pseudotyped virions was measured using the Tzm-bl luciferase assay as described previously [36-39]. Each plasma-Env combination was analyzed independently at least two times with duplicate wells. The neutralization IC_{50} for each plasma-Env combination was calculated using linear regression analysis in GraphPad Prism version 5.0. IC_{50} values that were less than the highest dilution of plasma tested (1:100) were assigned a score of 1:50. Neutralization breadth was calculated as the number of pseudoviruses neutralized with an IC_{50} of greater than 1:100, and potency was defined by (i) dividing the IC_{50} value for each given plasma-Env combination by the median IC_{50} value for that pseudovirus against all plasma samples and (ii) adding the scores for each plasma sample, as described by [40]. Higher scores indicate greater breadth and potency. All Env clones were obtained from the AIDS Research and Reference Reagent Program, Division of AIDS,

NIAID, NIH: 6535.3, TRO.11, AC10.0.29, and PVO.4 are from the Standard Reference Panel for Subtype B HIV-1 Env Clones [41]; ZM197M.PB7, Du172.17, Du156.12, ZM109F.PB4, CAP45.2.00.G3, and ZM214M.PL15 are from the Subtype C HIV-1 Reference Panel of Env Clones [42]; subtype A Env clones Q23ENV17 [43] and Q769ENVd22 [44] were contributed by Dr. Julie Overbaugh.

Blood CD4 T cell count and plasma HIV-1 viral load

Blood CD4 T cell count was measured by the Emory University CFAR Immunology core, and plasma viral load was quantified by the Virology core. Briefly, absolute number of peripheral blood lymphocytes was calculated from the total white blood cell (WBC) count determined with an automated hematology analyzer, and the percentage of CD4 T-lymphocyte population was determined by flow cytometry. Plasma HIV-1 RNA level was measured using the Cobas® Amplicor HIV Monitor test (version 1.5, Roche) or the Abbott Real Time HIV-1 Assay on an automated m2000 system, according to the manufacturer's directions.

Statistical analysis

Non-parametric one-way analysis of variance (1-way ANOVA, Kruskal-Wallis with Dunn's post-test) and Spearman rank correlation tests were performed with GraphPad Prism version 5.0 to evaluate the data. A p-value of less than 0.05 (95% confidence level) was considered significant.

Results

Regulatory receptors PD-1 and BTLA are aberrantly expressed on B-lymphocytes during chronic HIV-1 infection.

To investigate dysregulation within the B cell compartment during chronic HIV-1 infection, expression of the inhibitory receptors PD-1 and BTLA was assessed by flow cytometry and compared among healthy controls (HC), aviremic subjects (AV), and viremic subjects (VI) (Figure 1). In HC, only a minor proportion of B cells expressed PD-1 (Figure 1A), consistent with what is observed in T-lymphocytes [14,15]. In VI, expression of PD-1 was significantly increased (Figure 1A, $p<0.001$). AV subjects had PD-1 expression levels that were significantly lower than VI (Figure 1A, $p<0.001$), but were not significantly different from HC. Thus, active viral replication in VI is associated with a significant increase in PD-1 expression on B cells that is alleviated by cART. Despite a greater percentage of B cells expressing PD-1 in VI, the level of receptor expression per $CD19^+$ $PD\text{-}1^+$ cell was not different from HC or AV (Figure 1B). Instead, comparable mean fluorescence intensity (MFI) values were observed across the three groups.

The majority of B cells in HC expressed BTLA on their surface (Figure 1C). However, VI showed a significant decline in BTLA expression compared to HC (Figure 1C, $p<0.001$). AV individuals had intermediate levels of BTLA expression that were significantly different than both HC and VI (Figure 1C, $p<0.05$) representing only partial restoration of normal BTLA levels. In addition to the decrease in percentage of BTLA-expressing B cells in VI and AV, the MFIs of individual $CD19^+$ $BTLA^+$ cells were significantly lower in VI and AV compared to HC (Figure 1D, $p<0.001$ and $p<0.05$, respectively). Thus, modulation of BTLA expression by HIV-1 infection occurred at both the population and single cell level and remained depressed even when viral replication was suppressed by cART. HIV-1 infection

exerts a differential effect on B cell expression of PD-1 and BTLA, as evidenced by the strong inverse correlation between the two receptors (Figure 1E, $p<0.0001$). The aberrant expression of these receptors in VI indicates that homeostasis within the B cell compartment is significantly disrupted.

Peripheral B cell subsets are dysregulated during chronic HIV-1 infection.

We next examined whether altered PD-1 and BTLA expression in the total B cells of VI were reflected in specific B-lymphocyte subsets. Figure 2A displays the strategy used for separating total B cells ($CD19^+$) into 4 phenotypic subsets: immature ($CD10^+CD27^-$), mature ($CD10^-CD21^{lo}$), naïve ($CD10^-CD21^{hi}CD27^-$), and classical memory ($CD10^-CD21^{hi}CD27^+$), as described previously [9]. Similar to a published study by Moir *et al*. [9], a decrease in the proportion of naïve and memory B cells and an increase in the immature and mature populations were observed in VI compared to HC (Figure 2B). The change in the proportion of mature B cells was dramatic, increasing from 8% in HC to 43% in VI. Likewise, a substantial decline in the memory B cell subset, from 36% in HC to 8% in VI, was observed. Thus, mature B cells came to dominate the peripheral B cell compartment in VI. The balance within B cell subsets in AV was partially restored, falling somewhere in between HC and VI.

The B cell subsets differed in their respective PD-1 and BTLA expression patterns (Figure 2C and D, respectively). In HC, low PD-1 expression was observed in all subsets, but particularly within naive and memory B cells (Figure 2C). In VI, PD-1 expression was significantly increased in the naive and immature subpopulations of B cells compared to HC (Figure 2C, $p<0.01$ and $p<0.001$, respectively). However, PD-1 expression on naive and immature B cells in AV was not different from HC, indicating some partial restoration

(Figure 2C). BTLA expression in VI was significantly decreased in the naive, immature, and memory B cell subsets compared to HC and AV (Figure 2D, $p<0.001$ and at least $p<0.05$, respectively). BTLA expression in AV was not different from HC except for in immature B cells, where it remained significantly lower than HC (Figure 2D, $p<0.05$). In the mature B cell subset, significant differences in the expression of PD-1 and BTLA were not detected among HC, AV, and VI. However, because the mature B cell subset is expanded in VI (Figure 2B), these B cells may contribute disproportionately to the overall increase in PD-1 and decrease in BTLA expression.

PD-1 and BTLA expression on B-lymphocytes are correlated with markers of immune activation, proliferation, and disease progression.

Because generalized immune activation is an important factor in determining the course of HIV-1 infection, we also investigated whether PD-1 and BTLA expression were associated with Ki-67 or CD95 on total B cells. A strong positive correlation was found between PD-1 expression and Ki-67 ($p<0.0001$) and CD95 ($p=0.0004$) (Figure 3A and B, respectively), whereas BTLA exhibited an inverse correlation with these markers (Figure 3C and D, $p<0.0001$ and $p=0.006$, respectively). These results suggest a direct link between dysregulation and immune activation in the B cell compartment.

The relationship between PD-1 and BTLA expression on total B cells and two indicators of disease progression, plasma viral load and blood CD4 T cell count, was also assessed. PD-1 or BTLA expression on B-lymphocytes was not significantly associated with plasma viral load in VI (Figure 4A and B, respectively). However, a significant correlation was observed between CD4 T cell count and PD-1 or BTLA expression, including data from the three subject groups (Figure 4C and D, respectively, $p<0.0001$).

PD-1 expression on total B cells was inversely correlated with CD4 T cell count, while the correlation for BTLA expression and CD4 T cell count was direct.

PD-1 and BTLA expression on B-lymphocytes are correlated with plasma IgG level.

Hypergammaglobulinemia is a direct manifestation of B cell dysfunction during HIV-1 infection. We therefore examined the relationship between PD-1 and BTLA expression on B cells and plasma total IgG level for each group of subjects. Concurrent with previous reports, a significant increase in the plasma total IgG level was observed in VI compared to both AV and HC (Figure 5A, $p<0.05$ and $p<0.001$, respectively). Viral suppression mediated by cART resulted in lower levels of total IgG production. In addition, highly significant direct and indirect correlations were identified between total IgG level and PD-1 or BTLA expression on B cells (Figure 5B and C, $p=0.0005$ and $p<0.0001$, respectively). Thus, regulatory receptor expression is linked with this functional anomaly of the B cell compartment.

Total IgG level in plasma but not immune dysregulation is associated with HIV-1 neutralization breadth in viremic individuals.

We next investigated if heterologous neutralizing activity was present in VI with established B cell dysfunction and if nAb breadth was dependent upon the level of B cell activation or dysfunction. Plasma samples from VI were tested for their ability to neutralize a panel of 13 HIV-1 envelope (Env) pseudotyped virions from clades A, B, and C, which included three tiers of sensitivity, as determined by Seaman *et al*. [45]. While HIV-1 subtypes were not determined, our cohort of viremic subjects was most likely infected with subtype B, as this viral clade predominates in the southeastern United States. The

neutralization IC_{50} was calculated for each plasma-Env combination, and this data was used to calculate a breadth (how many Envs were neutralized) and potency (the strength of neutralization) score for each plasma sample, as described in [32]. Infectivity curves for each plasma sample are shown in Figure S1. A range of neutralization breadth was observed in these 16 subjects: three plasma samples (19%) demonstrated widespread neutralizing activity against this panel of Envs while five subjects (31%) exhibited a complete lack of detectable neutralization at the lowest dilution of plasma tested (1:100) (Figure 6A). No correlation was observed between neutralization breadth or potency and parameters of B cell dysfunction (PD-1, BTLA), immune activation (Ki-67, CD95), or disease progression (CD4 T cell count, plasma viral load) (data not shown). However, the level of total IgG in each VI plasma sample was significantly correlated with both neutralization breadth and potency (Figure 6B and C, p=0.009 and p=0.02, respectively). We next quantitated the level of antibodies that binds to the monomeric form of a subtype B Env gp120 (HIV-1 BaL) in each VI plasma sample, and determined whether antibodies with this specificity were correlated with nAb breadth or potency. Like total IgG, anti-gp120 antibodies were positively correlated with nAb breadth and potency, but in this case the correlations only trended towards significance (Figure 6D and E, respectively, p=0.09 for both). Anti-gp120 antibodies did not correlate with parameters of B cell dysfunction, immune activation, disease progression, or total IgG level. These findings suggest that gp120 binding as well as other IgG antibody specificities contribute to nAb breadth, but neither is overtly influenced by perturbations in the B cell compartment during chronic HIV-1 infection.

Discussion

An effective humoral immune response, in concert with cell-mediated immunity, may contribute to the control of HIV-1 replication. Several lines of evidence from SIV and SHIV infection of nonhuman primates and from studies of HIV-1 infection support the importance of B-lymphocytes. A suboptimal antibody response can influence disease progression and even lead to fatal outcome during SIV/SHIV infections [19,46-50]. Furthermore, studies of HIV-1 infection have shown that B-lymphocyte dysfunction correlates with markers of disease progression [51-53]. In one HIV-1 infected individual, monoclonal antibody-mediated depletion of B cells resulted in a decrease in neutralizing antibody titer and an increase in plasma viral load, which was reversed when the neutralizing antibody titer recovered to the pre-treatment level [54]. Thus, strategies to reverse or limit B cell dysfunction during HIV-1 infection could potentially limit disease progression.

Here we have demonstrated that PD-1 and BTLA, previously recognized mainly for their effects on T cells, are also aberrantly expressed on B-lymphocytes during chronic HIV-1 infection. Our data demonstrate that expression of PD-1 was increased and BTLA decreased on B-lymphocytes during persistent HIV-1 viremia, and that alteration in PD-1 and BTLA expression on B cells is comparable to the patterns observed in T cells [14,15,21]. Expanded analysis into the four major subsets of B-lymphocytes revealed that PD-1 expression was notably higher in naive and immature B cells, and BTLA was lower in naive, immature, and memory B cells in VI. Interestingly, the mature B cell subset exhibited the least quantifiable differences in expression of these regulatory markers among VI, AV, and HC but was the most affected with respect to the peripheral B cell subset distribution.

Plasma viral load in VI was not significantly correlated with either PD-1 or BTLA expression on B cells. In contrast, other studies have reported correlations between PD-1 or BTLA expression on T cells and plasma viral load [14,21]. These studies also demonstrated that the CD4 T cell count was inversely correlated with PD-1 expression and directly correlated with BTLA expression on T cells [14,21]. Similarly in our study, peripheral blood CD4 T cell count was also indirectly and directly correlated with PD-1 and BTLA expression on B-lymphocytes, respectively. Thus, an imbalance in immune homeostasis, rather than simply the presence of persistent viral antigen, could be reflected in the aberrant expression of these regulatory receptors on B cells. A strong correlation was also observed between PD-1 and BTLA expression on B cells and markers of cell proliferation and activation. These findings suggest a possible role for aberrant PD-1 and BTLA expression in driving increased B cell activation. Finally, this report is among the first to link B cell dysregulation with the extent of hypergammaglobulinemia, a functional measure of B cell dysfunction in HIV-1 infection.

Having established multiple tiers of disruption within the B cell compartment in the VI cohort, we investigated whether plasma from these individuals contained nAbs with cross neutralizing capacity. Broad and potent neutralization was observed in 3 of the 16 subjects analyzed here. This frequency of 19% is consistent with that reported for individuals possessing greater nAb breadth in other cohorts. These three individuals did not systematically differ from the others exhibiting less nAb activity with regard to measures of immune activation, dysregulation, CD4 T cell count, or plasma viral load. Instead, in this cohort of typical progressor patients, nAb breadth and potency were associated directly with the level of hypergammaglobulinemia and gp120 binding antibodies, even though the latter did not reach statistical significance. A recent study from Oballah *et al*. demonstrated

that the absolute B cell count in a subtype A HIV-1 infected cohort in Uganda was inversely correlated with neutralizing activity against heterologous Envs [28]. In our study, we did not find a correlation between total B cell count and nAb breadth or potency (data not shown). However, consistent with their results, we did observe that relatively strong and broad nAbs are present in individuals that exhibit B cell dysregulation and hypergammaglobulinemia. Others have reported that the time since infection [22,26] and plasma viral load or CD4 T cell count were associated with nAb breadth [26,30-32]. It is likely that these associations did not emerge in our study because of the smaller cohort size, which was targeted toward facilitating an extensive flow cytometric analysis of B cells in addition to measuring nAb breadth.

In summary, this paper is among the first to demonstrate aberrant expression profiles of the regulatory receptors PD-1 and BTLA on peripheral B cells, as well as within individual B cell subsets, during HIV-1 infection. These receptors were associated with activation, proliferation, and dysfunction in B cells in viremic subjects. Despite this, broad and potent nAbs were produced in some individuals, and their activity was possibly augmented through increased IgG production. The observations reported here provide new insight into peripheral B cell dysfunction in chronic HIV-1 infection, supporting its impact on immune activation and disease progression but revealing a less dramatic effect on nAb activity and breadth.

Acknowledgements

We thank Dr. Chris Ibegbu, Kiran Gill, and Deborah Abdul-Ali for their technical assistance. We appreciate the cooperation of all healthy, viremic, and aviremic participants of this study. All Env clone plasmids were obtained through the AIDS Research and Reference Reagent Program, Division of AIDS, NIAID, NIH. This work was supported by the National Institutes of Health through grants R01-AI58706 to CAD and P30-AI050409 to the Emory University Center for AIDS Research, supporting the Clinical Research, Immunology, and Virology cores.

References

1. Lane HC, Masur H, Edgar LC, Whalen G, Rook AH, et al. (1983) Abnormalities of B-cell activation and immunoregulation in patients with the acquired immunodeficiency syndrome. N Engl J Med 309: 453-458.

2. Mizuma H, Litwin S, Zolla-Pazner S (1988) B-cell activation in HIV infection: relationship of spontaneous immunoglobulin secretion to various immunological parameters. Clin Exp Immunol 71: 410-416.

3. De Milito A, Nilsson A, Titanji K, Thorstensson R, Reizenstein E, et al. (2004) Mechanisms of hypergammaglobulinemia and impaired antigen-specific humoral immunity in HIV-1 infection. Blood 103: 2180-2186.

4. Shirai A, Cosentino M, Leitman-Klinman SF, Klinman DM (1992) Human immunodeficiency virus infection induces both polyclonal and virus-specific B cell activation. J Clin Invest 89: 561-566.

5. Kroon FP, van Dissel JT, de Jong JC, Zwinderman K, van Furth R (2000) Antibody response after influenza vaccination in HIV-infected individuals: a consecutive 3-year study. Vaccine 18: 3040-3049.

6. Kroon FP, van Dissel JT, de Jong JC, van Furth R (1994) Antibody response to influenza, tetanus and pneumococcal vaccines in HIV-seropositive individuals in relation to the number of CD4+ lymphocytes. AIDS 8: 469-476.

7. Opravil M, Fierz W, Matter L, Blaser J, Luthy R (1991) Poor antibody response after tetanus and pneumococcal vaccination in immunocompromised, HIV-infected patients. Clin Exp Immunol 84: 185-189.

8. Rodriguez-Barradas MC, Musher DM, Lahart C, Lacke C, Groover J, et al. (1992) Antibody to capsular polysaccharides of Streptococcus pneumoniae after

vaccination of human immunodeficiency virus-infected subjects with 23-valent pneumococcal vaccine. J Infect Dis 165: 553-556.

9. Moir S, Malaspina A, Ho J, Wang W, Dipoto AC, et al. (2008) Normalization of B cell counts and subpopulations after antiretroviral therapy in chronic HIV disease. J Infect Dis 197: 572-579.

10. Moir S, Malaspina A, Ogwaro KM, Donoghue ET, Hallahan CW, et al. (2001) HIV-1 induces phenotypic and functional perturbations of B cells in chronically infected individuals. Proc Natl Acad Sci U S A 98: 10362-10367.

11. Ascher MS, Sheppard HW (1988) AIDS as immune system activation: a model for pathogenesis. Clin Exp Immunol 73: 165-167.

12. Hazenberg MD, Otto SA, van Benthem BH, Roos MT, Coutinho RA, et al. (2003) Persistent immune activation in HIV-1 infection is associated with progression to AIDS. AIDS 17: 1881-1888.

13. Barber DL, Wherry EJ, Masopust D, Zhu B, Allison JP, et al. (2006) Restoring function in exhausted CD8 T cells during chronic viral infection. Nature 439: 682-687.

14. Day CL, Kaufmann DE, Kiepiela P, Brown JA, Moodley ES, et al. (2006) PD-1 expression on HIV-specific T cells is associated with T-cell exhaustion and disease progression. Nature 443: 350-354.

15. Zhang JY, Zhang Z, Wang X, Fu JL, Yao J, et al. (2007) PD-1 up-regulation is correlated with HIV-specific memory CD8+ T-cell exhaustion in typical progressors but not in long-term nonprogressors. Blood 109: 4671-4678.

16. Kaufmann DE, Kavanagh DG, Pereyra F, Zaunders JJ, Mackey EW, et al. (2007) Upregulation of CTLA-4 by HIV-specific CD4+ T cells correlates with disease

progression and defines a reversible immune dysfunction. Nat Immunol 8: 1246-1254.

17. Kaufmann DE, Walker BD (2009) PD-1 and CTLA-4 inhibitory cosignaling pathways in HIV infection and the potential for therapeutic intervention. J Immunol 182: 5891-5897.
18. Blackburn SD, Shin H, Haining WN, Zou T, Workman CJ, et al. (2009) Coregulation of CD8+ T cell exhaustion by multiple inhibitory receptors during chronic viral infection. Nat Immunol 10: 29-37.
19. Titanji K, Velu V, Chennareddi L, Vijay-Kumar M, Gewirtz AT, et al. (2010) Acute depletion of activated memory B cells involves the PD-1 pathway in rapidly progressing SIV-infected macaques. The Journal of clinical investigation 120: 3878-3890.
20. Watanabe N, Gavrieli M, Sedy JR, Yang J, Fallarino F, et al. (2003) BTLA is a lymphocyte inhibitory receptor with similarities to CTLA-4 and PD-1. Nat Immunol 4: 670-679.
21. Zhang Z, Xu X, Lu J, Zhang S, Gu L, et al. (2011) B and T lymphocyte attenuator down-regulation by HIV-1 depends on type I interferon and contributes to T-cell hyperactivation. The Journal of infectious diseases 203: 1668-1678.
22. Gray ES, Madiga MC, Hermanus T, Moore PL, Wibmer CK, et al. (2011) The neutralization breadth of HIV-1 develops incrementally over four years and is associated with CD4+ T cell decline and high viral load during acute infection. J Virol 85: 4828-4840.
23. Beirnaert E, Nyambi P, Willems B, Heyndrickx L, Colebunders R, et al. (2000) Identification and characterization of sera from HIV-infected individuals with broad

cross-neutralizing activity against group M (env clade A-H) and group O primary HIV-1 isolates. J Med Virol 62: 14-24.

24. Binley JM, Lybarger EA, Crooks ET, Seaman MS, Gray E, et al. (2008) Profiling the specificity of neutralizing antibodies in a large panel of plasmas from patients chronically infected with human immunodeficiency virus type 1 subtypes B and C. J Virol 82: 11651-11668.
25. Doria-Rose NA, Klein RM, Manion MM, O'Dell S, Phogat A, et al. (2009) Frequency and phenotype of human immunodeficiency virus envelope-specific B cells from patients with broadly cross-neutralizing antibodies. J Virol 83: 188-199.
26. Sather DN, Armann J, Ching LK, Mavrantoni A, Sellhorn G, et al. (2009) Factors associated with the development of cross-reactive neutralizing antibodies during human immunodeficiency virus type 1 infection. J Virol 83: 757-769.
27. Simek MD, Rida W, Priddy FH, Pung P, Carrow E, et al. (2009) Human immunodeficiency virus type 1 elite neutralizers: individuals with broad and potent neutralizing activity identified by using a high-throughput neutralization assay together with an analytical selection algorithm. J Virol 83: 7337-7348.
28. Oballah P, Flach B, Eller LA, Eller MA, Ouma B, et al. (2011) B cell depletion in HIV-1 subtype A infected Ugandan adults: relationship to CD4 T cell count, viral load and humoral immune responses. PLoS One 6: e22653.
29. van Gils MJ, Euler Z, Schweighardt B, Wrin T, Schuitemaker H (2009) Prevalence of cross-reactive HIV-1-neutralizing activity in HIV-1-infected patients with rapid or slow disease progression. AIDS 23: 2405-2414.

30. Euler Z, van Gils MJ, Bunnik EM, Phung P, Schweighardt B, et al. (2010) Cross-reactive neutralizing humoral immunity does not protect from HIV type 1 disease progression. J Infect Dis 201: 1045-1053.

31. Doria-Rose NA, Klein RM, Daniels MG, O'Dell S, Nason M, et al. (2010) Breadth of human immunodeficiency virus-specific neutralizing activity in sera: clustering analysis and association with clinical variables. J Virol 84: 1631-1636.

32. Piantadosi A, Panteleeff D, Blish CA, Baeten JM, Jaoko W, et al. (2009) Breadth of neutralizing antibody response to human immunodeficiency virus type 1 is affected by factors early in infection but does not influence disease progression. J Virol 83: 10269-10274.

33. Moore JP, Cao Y, Leu J, Qin L, Korber B, et al. (1996) Inter- and intraclade neutralization of human immunodeficiency virus type 1: genetic clades do not correspond to neutralization serotypes but partially correspond to gp120 antigenic serotypes. J Virol 70: 427-444.

34. Euler Z, van den Kerkhof TL, van Gils MJ, Burger JA, Edo-Matas D, et al. (2012) Longitudinal analysis of early HIV-1-specific neutralizing activity in an elite neutralizer and in five patients who developed cross-reactive neutralizing activity. J Virol 86: 2045-2055.

35. Beniguel L, Begaud E, Cognasse F, Gabrie P, Mbolidi CD, et al. (2004) Specific antibody production by blood B cells is retained in late stage drug-naive HIV-infected Africans. Clin Dev Immunol 11: 121-127.

36. Li B, Decker JM, Johnson RW, Bibollet-Ruche F, Wei X, et al. (2006) Evidence for potent autologous neutralizing antibody titers and compact envelopes in early

infection with subtype C human immunodeficiency virus type 1. J Virol 80: 5211-5218.

37. Rong R, Bibollet-Ruche F, Mulenga J, Allen S, Blackwell JL, et al. (2007) Role of V1V2 and other human immunodeficiency virus type 1 envelope domains in resistance to autologous neutralization during clade C infection. J Virol 81: 1350-1359.

38. Rong R, Li B, Lynch RM, Haaland RE, Murphy MK, et al. (2009) Escape from autologous neutralizing antibodies in acute/early subtype C HIV-1 infection requires multiple pathways. PLoS pathogens 5: e1000594.

39. Lynch RM, Rong R, Boliar S, Sethi A, Li B, et al. (2011) The B cell response is redundant and highly focused on V1V2 during early subtype C infection in a Zambian seroconverter. Journal of virology 85: 905-915.

40. Lynch JB, Nduati R, Blish CA, Richardson BA, Mabuka JM, et al. (2011) The breadth and potency of passively acquired human immunodeficiency virus type 1-specific neutralizing antibodies do not correlate with the risk of infant infection. J Virol 85: 5252-5261.

41. Li M, Gao F, Mascola JR, Stamatatos L, Polonis VR, et al. (2005) Human immunodeficiency virus type 1 env clones from acute and early subtype B infections for standardized assessments of vaccine-elicited neutralizing antibodies. J Virol 79: 10108-10125.

42. Li M, Salazar-Gonzalez JF, Derdeyn CA, Morris L, Williamson C, et al. (2006) Genetic and neutralization properties of subtype C human immunodeficiency virus type 1 molecular env clones from acute and early heterosexually acquired infections in Southern Africa. J Virol 80: 11776-11790.

43. Rainwater SM, Wu X, Nduati R, Nedellec R, Mosier D, et al. (2007) Cloning and characterization of functional subtype A HIV-1 envelope variants transmitted through breastfeeding. Current HIV research 5: 189-197.

44. Long EM, Rainwater SM, Lavreys L, Mandaliya K, Overbaugh J (2002) HIV type 1 variants transmitted to women in Kenya require the CCR5 coreceptor for entry, regardless of the genetic complexity of the infecting virus. AIDS Res Hum Retroviruses 18: 567-576.

45. Seaman MS, Janes H, Hawkins N, Grandpre LE, Devoy C, et al. (2010) Tiered categorization of a diverse panel of HIV-1 Env pseudoviruses for assessment of neutralizing antibodies. J Virol 84: 1439-1452.

46. Dykhuizen M, Mitchen JL, Montefiori DC, Thomson J, Acker L, et al. (1998) Determinants of disease in the simian immunodeficiency virus-infected rhesus macaque: characterizing animals with low antibody responses and rapid progression. The Journal of general virology 79 (Pt 10): 2461-2467.

47. Schmitz JE, Kuroda MJ, Santra S, Simon MA, Lifton MA, et al. (2003) Effect of humoral immune responses on controlling viremia during primary infection of rhesus monkeys with simian immunodeficiency virus. Journal of virology 77: 2165-2173.

48. Schmitz JE, Zahn RC, Brown CR, Rett MD, Li M, et al. (2009) Inhibition of adaptive immune responses leads to a fatal clinical outcome in SIV-infected pigtailed macaques but not vervet African green monkeys. PLoS pathogens 5: e1000691.

49. Tasca S, Zhuang K, Gettie A, Knight H, Blanchard J, et al. (2011) Effect of B-cell depletion on coreceptor switching in R5 simian-human immunodeficiency virus infection of rhesus macaques. Journal of virology 85: 3086-3094.

50. Zhang ZQ, Casimiro DR, Schleif WA, Chen M, Citron M, et al. (2007) Early depletion of proliferating B cells of germinal center in rapidly progressive simian immunodeficiency virus infection. Virology 361: 455-464.

51. Moir S, Ho J, Malaspina A, Wang W, DiPoto AC, et al. (2008) Evidence for HIV-associated B cell exhaustion in a dysfunctional memory B cell compartment in HIV-infected viremic individuals. J Exp Med 205: 1797-1805.

52. Malaspina A, Moir S, Ho J, Wang W, Howell ML, et al. (2006) Appearance of immature/transitional B cells in HIV-infected individuals with advanced disease: correlation with increased IL-7. Proceedings of the National Academy of Sciences of the United States of America 103: 2262-2267.

53. Moir S, Malaspina A, Pickeral OK, Donoghue ET, Vasquez J, et al. (2004) Decreased survival of B cells of HIV-viremic patients mediated by altered expression of receptors of the TNF superfamily. The Journal of experimental medicine 200: 587-599.

54. Huang KH, Bonsall D, Katzourakis A, Thomson EC, Fidler SJ, et al. (2010) B-cell depletion reveals a role for antibodies in the control of chronic HIV-1 infection. Nature communications 1: 102.

Tables

Table 1. Characteristics of the study participants.

		Healthy Control (HC)	*Aviremic (AV)*[a,b]	*Viremic (VI)*[b]
Number of subjects		12	13	16
Gender	Male	8	9	14
	Female	4	4	2
Ethnicity	Caucasian	5	0	2
	African American	3	13	14
	Asian	2	0	0
	Mixed	2	0	0
Age, years		32 (20-56)	46 (33-65)	37 (22-50)
[c]CD4 count, cells/µl		632 (375-1,094)	329 (31-988)	104 (4-465)
Viral load, copies/ml		NA[d]	<100	129,092 (4,189-676,811)

[a]The duration of the cART regimen was greater than 6 months for all aviremic subjects.

[b]All HIV-1-infected subjects (aviremic and viremic) were classified as CDC Stage C3.

[c]$P < 0.05$ for HC versus VI and AV versus VI.

[d]NA, not applicable.

Figures

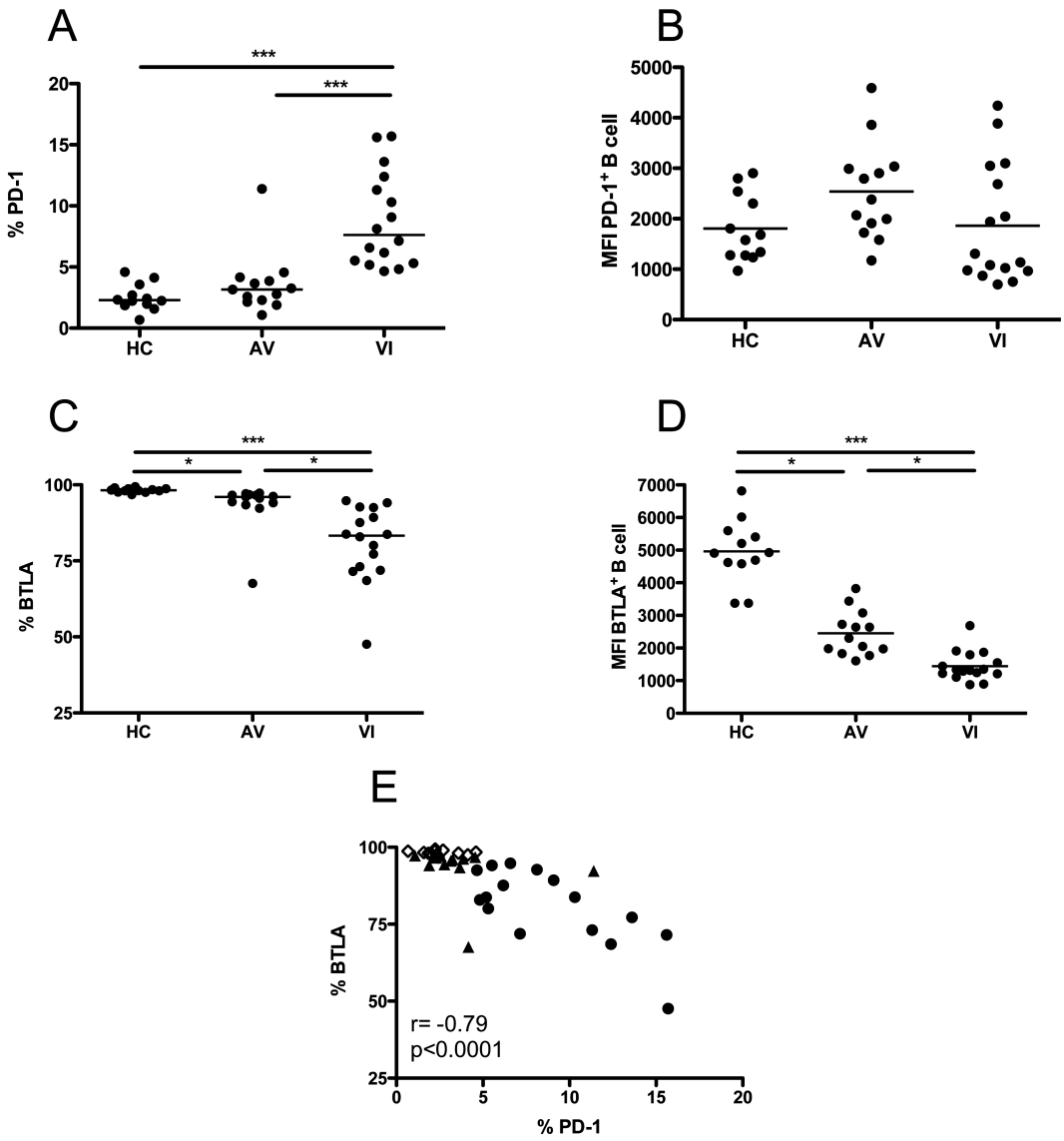

Figure 1. Expression of PD-1 and BTLA by B-lymphocytes. The percentage of total B cells ($CD19^+$) that express PD-1 and BTLA in HC, AV, and VI subjects is shown in panels **(A)** and **(C)**, respectively. The mean fluorescence intensity (MFI) for PD-1 and BTLA expression by individual $PD\text{-}1^+$ or $BTLA^+$ $CD19^+$ B cells is shown in panels **(B)** and **(D)**, respectively. Each point represents data from a single subject. Horizontal bars within the point plots indicate the median percentage for each group. Significance between groups determined by 1-way

ANOVA is indicated above the groups, depicted as * = $p<0.05$, ** = $p<0.01$, and *** = $p<0.001$. The correlation between percentage of total B cells that express PD-1 and BTLA is presented in the graph in panel **(E)**. Spearman correlation coefficient (r) and level of significance (p) are indicated within the graph (open diamonds = HC; closed triangles = AV; closed circles = VI).

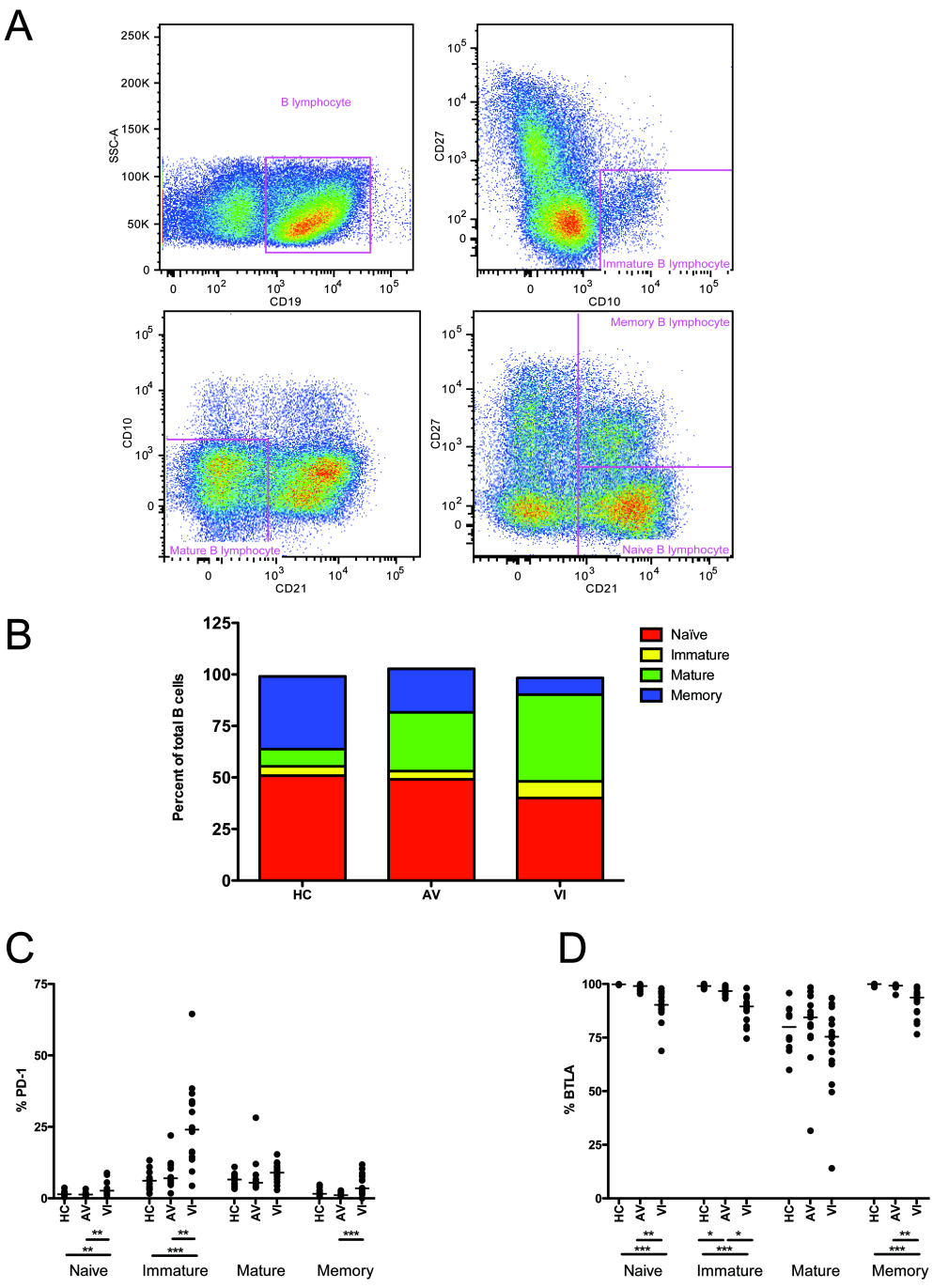

Figure 2. Distribution of B-lymphocyte subsets and expression of PD-1 and BTLA. The flow cytometry gating strategy for separating B cell subsets is shown in panel **(A)**. Within the B-lymphocytes ($CD19^{+}$), cells were further gated into four subsets, defined as: immature ($CD10^{+}CD27^{-}$), mature ($CD10^{-}CD21^{lo}$), naive ($CD10^{-}CD21^{hi}CD27^{-}$), and memory ($CD10^{-}$

$CD21^{hi}CD27^{+}$). The mean proportions of naive, immature, mature, and memory subsets within the total B cell population in HC, AV, and VI subjects are shown in panel **(B)**. The percentage of naive, immature, mature, and memory B cells that express PD-1 **(C)** and BTLA **(D)** in HC, AV, and VI is presented in each graph. Each point represents data from a single subject. Horizontal bars within the point plots indicate median percentage for each group. Significance between groups determined by 1-way ANOVA is indicated below the groups, depicted as * = $p<0.05$, ** = $p<0.01$ and *** = $p<0.001$.

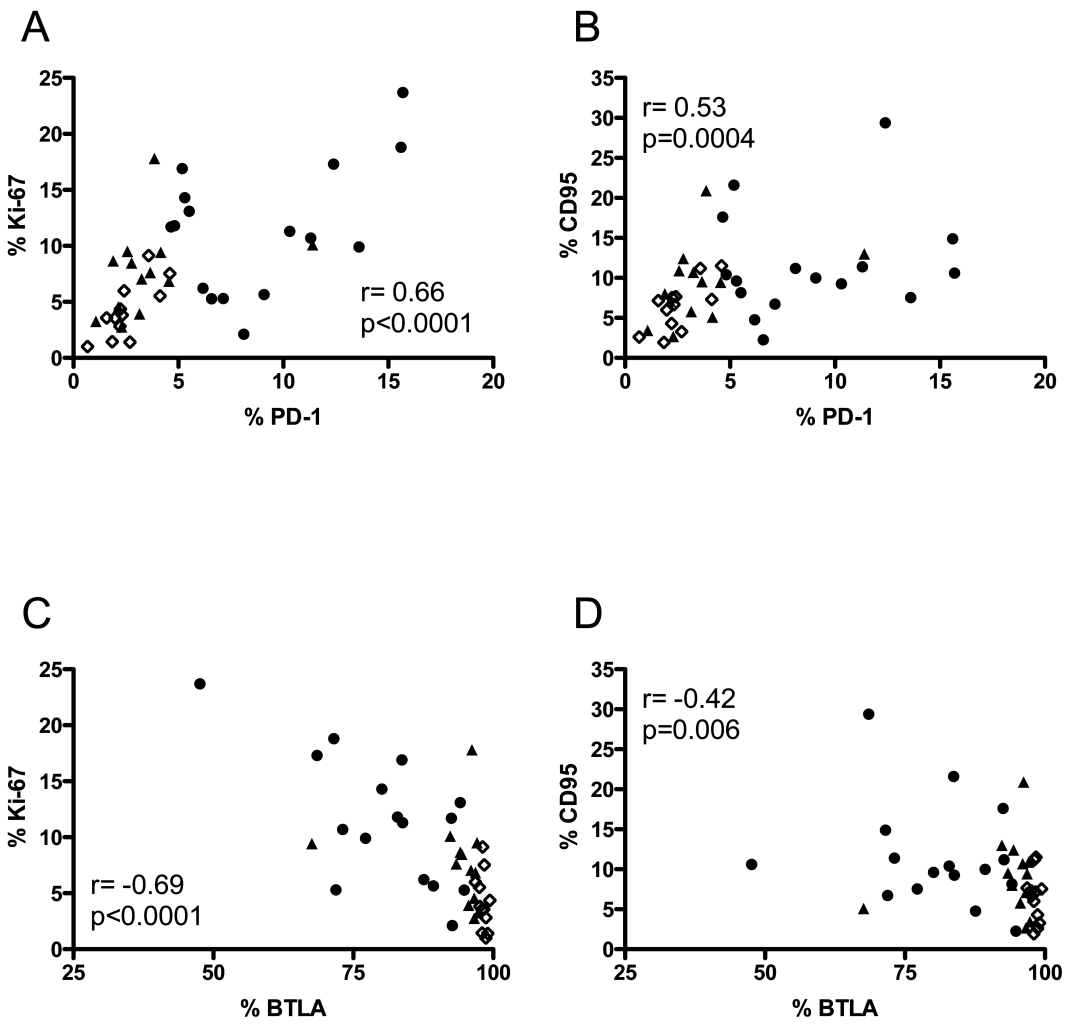

Figure 3. Correlation of PD-1 and BTLA expression on B-lymphocytes with Ki-67 and CD95. The correlations between percentage of total B cells ($CD19^{+}$) that express PD-1 and percentage expressing Ki-67 or CD95 are shown in panels **(A)** and **(B)**, respectively. The correlations between BTLA and Ki-67 or CD95 expression are shown in panels **(C)** and **(D)**, respectively. Spearman correlation coefficient (r) and level of significance (p) are indicated within each graph. Each point represents data from a single subject (open diamonds = HC; closed triangles = AV; closed circles = VI).

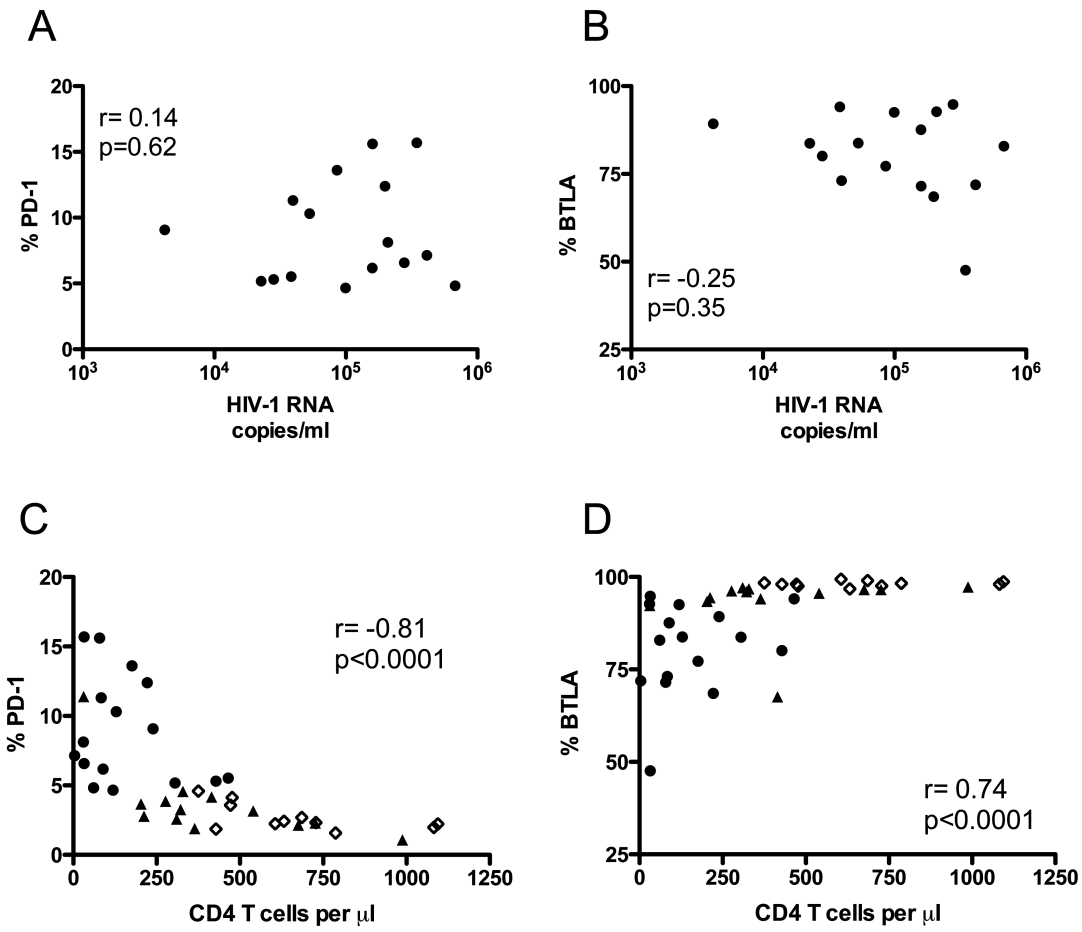

Figure 4. Correlation of PD-1 and BTLA expression on B-lymphocytes with markers of HIV-1 disease progression. The correlations between plasma viral load (HIV-1 RNA copies/ml) and percentage of total B cells ($CD19^+$) that express PD-1 or BTLA are shown in panels **(A)** and **(B)**, respectively. The correlations between blood CD4 count (CD4 T cells/μl) and percentage of total B cells ($CD19^+$) that express PD-1 or BTLA are shown in panels **(C)** and **(D)**, respectively. Spearman correlation coefficient (r) and level of significance (p) are indicated in each graph. Each point represents data from a single subject (open diamonds = HC; closed triangles = AV; closed circles = VI).

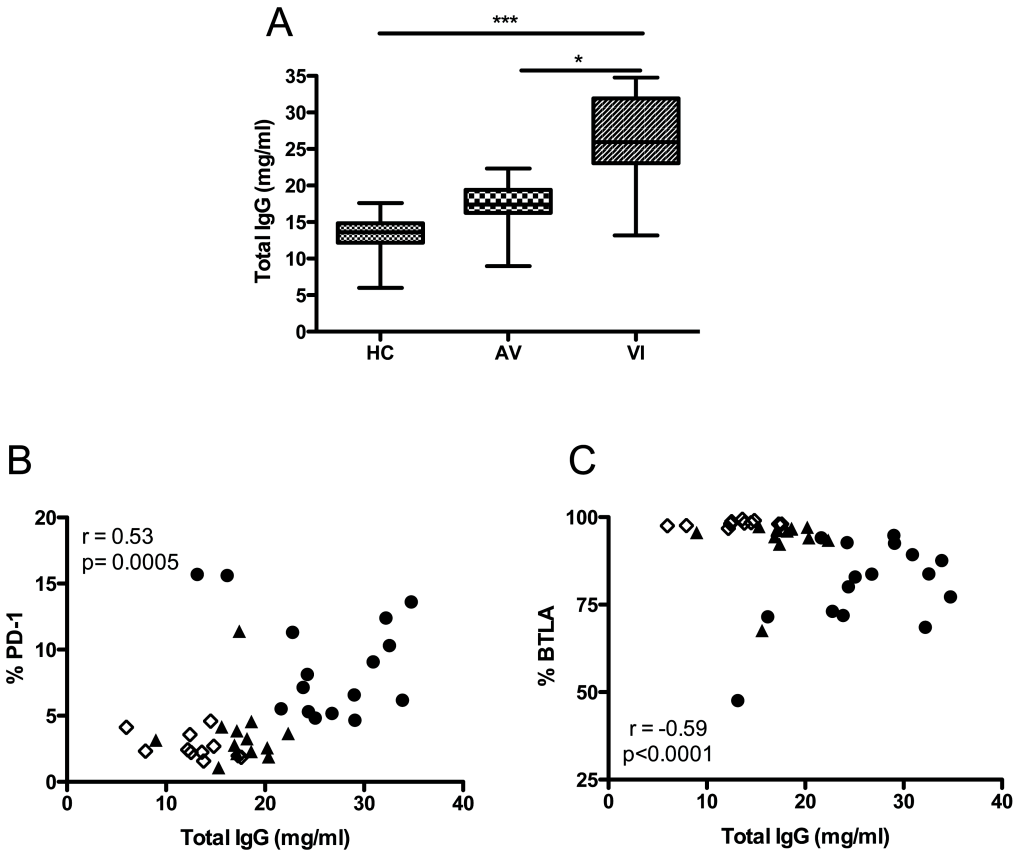

Figure 5. Correlation of PD-1 and BTLA expression on B-lymphocytes with total plasma IgG levels. The concentrations of total IgG (mg/ml) in the plasma of HC, AV, and VI subjects are presented in panel **(A)**. Horizontal lines within the boxes indicate the median value for each group. Boxes represent the 25th to 75th percentile, and brackets represent the minimum to maximum values in each group. Significance between groups by 1-way ANOVA is indicated above the groups, depicted as * = $p<0.05$ and *** = $p<0.001$. The correlations between total IgG concentration (mg/ml) in plasma and percentage of total B cells ($CD19^+$) that express PD-1 or BTLA are presented in panels **(B)** and **(C)**, respectively. Spearman correlation coefficient (r) and level of significance (p) are indicated within each graph. Each point represents data from a single subject (open diamonds = HC; closed triangles = AV; closed circles = VI).

A

	Subtype B					Subtype C						Subtype A			
	1B	1B	2	2	3	1B	1B	2	2	2	2	1B	2		
VI Plasma	6535.3	SS1196.1	TRO.11	AC10.0.29	PVO.4	ZM197M.PB7	ZM109F.PB4	Du156.12	Du172.17	CAP45.2.00.G3	ZM214M.PL15	Q23ENV17	Q769ENVd22	Potency	Breadth
1	213	309	436	180	453	282	131	256	199	160	200	204	260	60	13
2	206	198	153	158	50	211	137	227	216	159	129	251	169	41	12
3	190	178	162	138	152	188	108	266	167	112	141	150	50	36	12
4	261	153	50	159	50	50	50	229	112	50	50	323	50	28	6
5	118	164	179	50	50	50	104	103	50	50	50	50	129	20	6
6	123	153	50	50	50	50	50	125	116	50	50	105	50	18	5
7	50	50	50	119	50	50	50	50	50	308	112	181	50	22	4
8	102	199	50	50	50	132	50	114	50	50	50	50	50	17	4
9	136	208	191	50	50	50	50	50	50	50	50	50	50	17	3
10	50	50	50	50	50	104	50	50	50	50	50	50	50	13	1
11	100	50	50	50	50	50	50	50	50	50	50	50	50	12	1
12	50	50	50	50	50	50	50	50	50	50	50	50	50	12	0
13	50	50	50	50	50	50	50	50	50	50	50	50	50	12	0
14	50	50	50	50	50	50	50	50	50	50	50	50	50	12	0
15	50	50	50	50	50	50	50	50	50	50	50	50	50	12	0
16	50	50	50	50	50	50	50	50	50	50	50	50	50	12	0

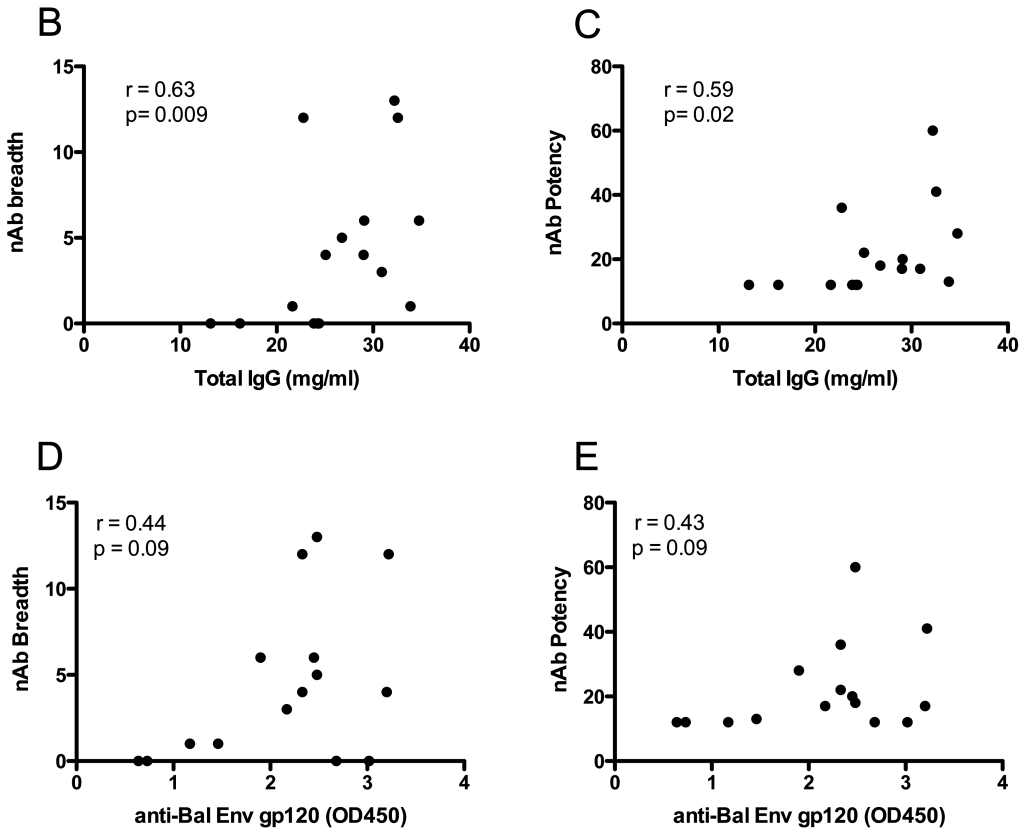

Figure 6. Correlation of neutralization breadth and potency with total IgG levels. Sixteen plasma samples from VI were evaluated for their neutralization breadth and potency against a cross-clade panel of 13 HIV-1 Env pseudotypes. The neutralization IC_{50} was calculated for each plasma-Env combination using linear regression, and these values are shown in panel **(A)**. IC_{50} values of less than 1:100 were assigned a value of 1:50. Color shading indicates the potency of neutralization: red > dark orange > light orange > green. HIV-1

Envs are listed along the top and are grouped by subtype. The tier designation for each Env (1B, 2, or 3) is shown and represents overall neutralization phenotype, as described by (45). Tier 1B viruses are 'easy' to neutralize; tier 2 are representative of most patient viruses; tier 3 are 'difficult' to neutralize. Higher breadth and potency scores shown in panel (A) indicate greater neutralization capacity. Panels **(B)** and **(C)** show the correlations between neutralization breadth (the number of Env pseudotypes neutralized) or potency (the sum of IC_{50} values for each plasma-Env combination divided by the median IC_{50} value for that virus against all plasma samples) and total IgG level for each plasma sample. Panels **(D)** and **(E)** show the correlations between nAb breadth and potency and the level of anti-gp120 binding antibodies in plasma, detected by ELISA (plotted as the optical density reading at 450 nm). The Spearman correlation coefficient (r) and level of significance (p) are indicated within each graph. Panels **(D)** and **(E)** showed positive r values and trended toward significance, but did not reach a level of $p<0.05$.

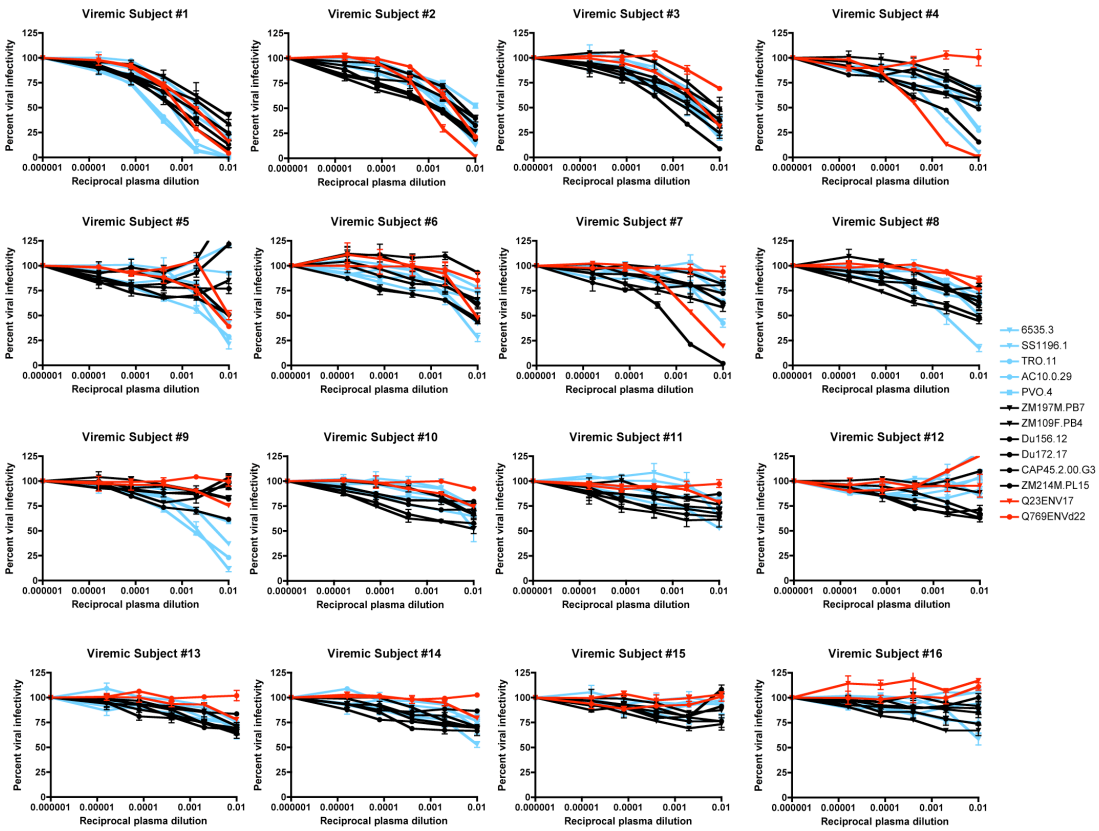

Figure S1. Heterologous neutralization capacity of plasma from 16 viremic HIV-1 subjects. Plasma from 16 viremic subjects was evaluated for cross-neutralizing capacity against virions pseudotyped with 13 heterologous HIV-1 envelopes (Envs) from three clades (subtype B Envs = light blue, subtype C Envs = black, subtype A Envs = red). Pseudoviruses were produced through co-transfection of each heterologous Env with the subtype B HIV-1 *env*-deficient backbone, pSG3Δ*env*. Subsequent viral infectivity, measured by production of luciferase, was assayed in Tzm-bl cells in the presence or absence of serially-diluted plasma. Percent viral infectivity, as adjusted against wells containing no test plasma, is depicted on the vertical axis; reciprocal plasma dilutions are plotted along the horizontal axis in a logarithmic fashion. Each graph illustrates the heterologous neutralization breadth of one viremic subject, where every curve represents a single Env-plasma combination, and error bars demonstrate the standard error of the mean

of two independent experiments using duplicate wells: closed inverted triangles = tier 1B Envs, closed circles = tier 2 Envs, closed squares = tier 3 Envs, as defined by [45].

Discussion

The End of AIDS

What primarily drives progress in the field of HIV-1 research is the need for a cure. If thirty years of ardent laboratory effort has offered any resounding hint at how to end the pandemic, it is that a multifaceted plan of action appears inevitable. Just as the virus employs manifold strategies to escape, so must scientists apply myriad counteroffensives that irrevocably cripple the virus and any foothold for the disease that it causes. Subsequently, as laborers participatory in an infectious disease program that may lead to viral eradication, we meet the peculiar paradox that realizing our end goal inadvertently puts us out of business.

During the interim period where no vaccine exists, prevention/intervention methods are currently and valuably exercised including, but not limited to, couples' voluntary counseling and testing, antiretroviral microbicides, group motivational interviewing to improve medication adherence behavior, reduction of gender-based violence, and integrative care for HIV/AIDS patients with mental disorder and substance abuse co-morbidities [102-108]. One might argue that the synergism of these and other methodologies could outcompete the efficacy of a vaccine, but non-vaccine headway still meets barriers--even in developed countries. For instance, ART administered in the United States over the last ten to fifteen years was projected to reduce the aggregate rate of new infections; instead, over 500,000 Americans became infected, at a near constant rate of ~50,000 cases per year [109]. Furthermore, economists project that the barriers to realization of a successful HIV-1 vaccine are relative, not absolute and that our financial commitment to research and development will ultimately determine at what pace we achieve disease eradication [110]. Studies of the HIV-1 envelope much like the ones

described in this body of work will be required to advance the field toward such a realization.

A logical but complex question that follows acknowledgement of the need for an HIV-1 vaccine, then, is what multiple hits to the virus will be required? Completed vaccine trials offer some indication as to what immunogenic components might be imperative and render support for the concept that overcoming HIV-1's genetic diversity could necessitate intersection of the adaptive immune system's dichotomous protective forces: neutralizing antibodies and cytotoxic T lymphocytes (CTLs). Vaccine constituents that elicit both of these immune mediators and qualitatively enhance their protection over what occurs naturally *in vivo* may be optimal.

VaxGen piloted two trials, VAX004 in 1998 and VAX003 in 1999, which solely aimed to trigger the production of neutralizing antibodies by vaccine inclusion of *env*; bivalent, recombinant gp120 (named AIDSVAX B/B for its subtype composition) was ineffective in the US men who have sex with men (MSM) population, just as AIDSVAX B/E failed to protect intravenous drug users (IDU) in Thailand [111]. Similarly one-dimensional, the Merck STEP trial of 2004, which aimed to induce sole CTL protection by injection of *gag/pol/nef* vectors, was stopped early when researchers discovered that vaccine recipients were acquiring HIV infection at an increased rate as compared to the placebo control group of participants [112].

The only potentially efficacious HIV-1 vaccine to date in humans possessed viral products capable of stimulating both neutralizing antibodies and CTLs. Sanofi-Pasteur's RV144 Thai trial of 2003 married the previously unsuccessful AIDSVAX B/E with ALVAC (a recombinant canarypox vector engineered to express a subtype E envelope, *gag*, and protease), and vaccine recipients experienced ~30% protection [113]. Although RV144

elicited neither neutralizing antibodies nor CTLs, ancillary studies identified the binding of IgG antibodies to V1V2 as a correlate of reduced infection rate. Binding titers inversely correlated with risk, as vaccinees were as much as 50% less likely to acquire HIV-1 than those who received placebo alone; interestingly, envelope-specific IgA antibodies directly correlated with infection rate but did not seem to enhance infection [114]. V2-specific antibodies in vaccinee plasma recognized both conformational and linear epitopes and demonstrated reactivity against multiple HIV-1 clades [115].

Improving Epitopic Coverage

Autologous neutralizing antibody titers that arise naturally during HIV-1 infection are often robust and emerge in repeated waves that directly address the concomitant viral population [42-44,55]. These responses, however, typically recognize strain-specific epitopes and fail to contain widespread infection, even over time as more envelope sites are ostensibly recognized. Because vaccines beneficial to human health have historically prompted neutralizing antibody production, we and others conjecture that an HIV-1 vaccine will require no less [116-120]. The fundamental objective, then, is to find a suitable neutralizing antibody combination to induce prophylactically.

The register of known envelope vulnerabilities and/or immunogenic localities (V1V2, the CD4bs, the alpha2 helix, MPER, particular glycan positions) provides a potential list from which to choose combinatorial targets. This dissertation highlights a novel epitope at the base of the V3 loop in subtype A HIV-1 as one such option; previous reports have identified other positions in this immediate vicinity as humoral targets in viral clades B and C, suggesting an exposed and common envelope target [121,122]. V1V2 responses, though potentially preventative in certain confines, afforded only limited protection in

Thailand during RV144. In concert with effectors aimed at distant sites, however, these binding titers could push vaccine efficacy above ~30%. Indeed, we witness in the work described here that subject R880F developed moderate heterologous neutralization breadth only after autologous responses re-focused away from the single, consistently targeted V3-proximal space.

A recent publication functionally supports the idea that distinct envelope targets, when recognized together, can lead to improved neutralization capacity [123]. Two CD4bs monoclonal antibodies (VRC01 and VRC-PG04) and two glycan-dependent, quaternary V1V2 monoclonal antibodies (PG9 and PG16) were first assayed independently against a panel of ~200 pseudotyped viruses, the envelopes of which were chosen from a pool largely composed of primary isolates; these isolates encompassed all nine classic HIV-1 subtypes and the major CRFs. VRC-PG04 or PG9 alone neutralized 78% of isolates at an IC50 less than 50 μg/ml, but when the two effectors were partnered, neutralization surged to 94% [123]. This trend held constant for any combination of CD4bs and V1V2 antibody tested. Cross-competition ELISAs additionally suggested that binding of either distinct epitope did not interfere with recognition of the other. Such steric considerations would certainly need to be included in the design of an ideal immunogen. Precedent also exists for the synergistic, and not merely additive, benefit of multi-antibody binding to HIV-1 envelope [124-126].

One significant caveat of this two-pronged approach is that five of the viral isolates tested proved completely resistant to neutralization by VRC01, VRC-PG04, PG9, and PG16. These viruses were not found to be inherently neutralization-resistant, but this occurrence points to the idea that two simultaneous targets may not be enough in every case of infection.

A transmission bottleneck, whereby a single viral variant passes from donor to recipient, describes most heterosexual HIV-1 transmission events; mitigating factors such as inflammatory genital infections and transmission routes in populations such as IDU and MSM increase the number of transferred variants significantly [127-131]. Having a failsafe neutralizing antibody network in place during an influx of one or multiple variants is key to HIV-1 prevention. The passive transfer of neutralizing antibodies preceding viral challenge in nonhuman primate and mouse models supports this concept [132-144]. Furthermore, understanding what threshold is sufficient but not excessive is critical for resource and manpower conservation. At this juncture, knowing which iteration of envelope targets is best remains difficult, but evidence advocates for the selection of at least three separately recognizable and stimulatory envelope sites.

Establishing Routes to Breadth

Heterologous neutralizing antibody formation is currently constricted to a finite subset of HIV-1 patients and appears only after years for unresolved reasons. In our cohort of 16 subtype B-infected viremic individuals, we discovered that cross-clade neutralization could occur even when canonical B cell subsets were disrupted and that expansion of such a response correlated with the total level of IgG in plasma. The creation of a model flush with the intricacies of how that neutralization breadth might emerge was, however, attempted only for subtype A-infected subject R880F.

Neutralization scope from more than one HIV-1 patient has now been attributed to a glycosylation motif resident at N332 in the gp120 subunit of envelope. Broadly neutralizing antibodies such as 2G12 and PGT128 target this glycan [87,145]. Our Rwandan findings in subtype A, contrasted with a South African study of subtype C,

emphasize how the ordering of antibody elicitation can influence eventual neutralization prospects. In this instance, N332 and N334 glycans, surfacing in opposite successions may participate in the triggering of different immune outcomes.

The transmitted/founder virus that established infection in R880F contained an NVS sequon beginning at HXB2 residue 332 [44]. This PNGS persisted in all of the 2-month envelopes. Not until 5-months did this glycosylation motif change to NRT at 334 in one envelope. Point mutational studies suggest that this shift likely arose in response to immune pressure from autologous monoclonal antibodies 19.3H-L1 and 19.3H-L3 and persisted as late as 10-months, the last time point of envelope sampling. Three-year autologous plasma from chronic infection confirmed that the V3-proximal glycans that developed as an escape route in R880F did not mediate the observed cross-clade neutralization breadth. In this patient, then, the N332 glycan was not recognized, the N332 to N334 glycan shift conferred one early pathway of escape, and chronic neutralizing effectors recognized envelope regions separate from these epitopes.

In contrast, Moore *et al*. examined viral variants from two subjects who *did* develop N332-dependent broadly neutralizing antibodies [23]. The transmitted/founder virus in CAP117 possessed an NGS motif at 334 that switched to NIS at 332 at 25-weeks and persisted as far as 30-months after infection. Similarly in CAP314, NST occupied residue 334 in the initiating virus and mutated to NIS at 332 by 19-weeks. Evidence suggests that these 334 to 332 glycan shifts, opposite in order from the switch observed in R880F, simultaneously conferred early escape and formed the epitopes that would eventually afford heterologous neutralization breadth. Two- and three-year autologous plasma samples from CAP117 and CAP314 failed to neutralize viruses lacking the N332 glycan, making their activities similar to 2G12 and PGT128.

If CAP117 and CAP314 were examined in isolation, or even in the light of antibodies such as 2G12 and PGT128, one might put forth N332 as a prime vaccination target. (And this still might be a valuable hypothesis.) R880F reinforces, however, that the mere presence of a PNGS does not automatically force development of heterologous neutralization breadth. The N332 glycosylation motif was present at infection in R880F and endured for at least five months before mutation to N334. This indicates that timing and context, not inclusion alone, might facilitate neutralization outcomes. What currently exists in the HIV-1 literature regarding tracks to breadth is but the beginning of what will be required. Just two studies juxtaposed tell us that the same mutations, when elicited in different orders--or perhaps even autonomously appearing at different points during infection--can oppositely calibrate an immune response. Resources should be devoted to determining the antibody trajectories that lead to heterologous neutralization capacity in multiple hetero-subtypic patients. After thirty years, we know now with some confidence the applicable destinations of recognition in envelope and must rewind to their origins. From there, we can trace forward the applicable B cell lineages.

Summary

American children of the early 1960s received vaccinations for diphtheria, pertussis, poliomyelitis, smallpox, and tetanus; the contemporary tally for vaccine preventable diseases appends another twelve recommendations: *Haemophilus influenza* type b, hepatitis A, hepatitis B, human papillomavirus, influenza, measles, meningococcal disease, mumps, pneumococcal disease, rotavirus, rubella, and varicella [146]. Under ideal circumstances, a single HIV-1 vaccine added to this list and administered globally would preempt the millions of annual infections. We as researchers (and vaccinologists) must,

however, keep in mind the real possibility that the most transformative vaccination protocols might engage communities with protection fashioned for that population's HIV-1 subtype(s). This specialization could require several formulations, but the stimulated routes of immunity among them should share features.

A common theme in HIV-1 infection is that desirable outcomes appear, but often at the wrong time, accumulated to insufficient levels, or within an imperfect set of circumstances. Autologous neutralizing antibodies form robustly, but they are outstripped by a breakneck viral mutation rate. Heterologous neutralizing antibodies accrue in a limited number of subjects but tardily when immune dysfunction may already be operative and disease course set. Traceable routes of virus/immune system interplay, such as the one detailed for R880F, should educate the future selection of immunization regimens. The considerations for immunogen creation proposed and defended herein include: (i) equipping the dual branches of human adaptive immunity to respond, (ii) eliciting neutralizing antibodies against at least three loci on the native HIV-1 envelope trimer, and (iii) elucidating (and then applying) mechanisms for the evocation and acceleration of breadth. Chosen envelope targets should be well exposed, immunogenic, and conserved across viral genetic diversity where possible; they should also adopt stable conformations during natural infection. The combinatorial efficacy of these strategies, applied through framing of geographical subtype distribution, could orchestrate a breed of protection that curtails the HIV-1 pandemic.

Literature Cited in the Introduction and Discussion

1. Barre-Sinoussi F, Chermann JC, Rey F, Nugeyre MT, Chamaret S, et al. (1983) Isolation of a T-lymphotropic retrovirus from a patient at risk for acquired immune deficiency syndrome (AIDS). Science 220: 868-871.

2. Temin HM, Mizutani S (1970) RNA-dependent DNA polymerase in virions of Rous sarcoma virus. Nature 226: 1211-1213.

3. Baltimore D (1970) RNA-dependent DNA polymerase in virions of RNA tumour viruses. Nature 226: 1209-1211.

4. Maddon PJ, Dalgleish AG, McDougal JS, Clapham PR, Weiss RA, et al. (1986) The T4 gene encodes the AIDS virus receptor and is expressed in the immune system and the brain. Cell 47: 333-348.

5. Deng H, Liu R, Ellmeier W, Choe S, Unutmaz D, et al. (1996) Identification of a major co-receptor for primary isolates of HIV-1. Nature 381: 661-666.

6. Dragic T, Litwin V, Allaway GP, Martin SR, Huang Y, et al. (1996) HIV-1 entry into CD4+ cells is mediated by the chemokine receptor CC- CKR-5. Nature 381: 667-673.

7. Ho DD, Neumann AU, Perelson AS, Chen W, Leonard JM, et al. (1995) Rapid turnover of plasma virions and CD4 lymphocytes in HIV-1 infection. Nature 373: 123-126.

8. Hemelaar J (2012) The origin and diversity of the HIV-1 pandemic. Trends Mol Med 18: 182-192.

9. Gao F, Bailes E, Robertson DL, Chen Y, Rodenburg CM, et al. (1999) Origin of HIV-1 in the chimpanzee Pan troglodytes troglodytes. Nature 397: 436-441.

10. Korber B, Muldoon M, Theiler J, Gao F, Gupta R, et al. (2000) Timing the ancestor of the HIV-1 pandemic strains. Science 288: 1789-1796.

11. Wertheim JO, Worobey M (2009) Dating the age of the SIV lineages that gave rise to HIV-1 and HIV-2. PLoS Comput Biol 5: e1000377.

12. Worobey M, Gemmel M, Teuwen DE, Haselkorn T, Kunstman K, et al. (2008) Direct evidence of extensive diversity of HIV-1 in Kinshasa by 1960. Nature 455: 661-664.

13. Taylor BS, Sobieszczyk ME, McCutchan FE, Hammer SM (2008) The challenge of HIV-1 subtype diversity. N Engl J Med 358: 1590-1602.

14. Hemelaar J, Gouws E, Ghys PD, Osmanov S (2011) Global trends in molecular epidemiology of HIV-1 during 2000-2007. Aids 25: 679-689.

15. (UNAIDS) JUNPoHA (2012) Global report: UNAIDS report on the global AIDS epidemic 2012.

16. Korber B, Gaschen B, Yusim K, Thakallapally R, Kesmir C, et al. (2001) Evolutionary and immunological implications of contemporary HIV-1 variation. Br Med Bull 58: 19-42.

17. Hemelaar J, Gouws E, Ghys PD, Osmanov S (2006) Global and regional distribution of HIV-1 genetic subtypes and recombinants in 2004. AIDS 20: W13-23.

18. Robertson DL, Sharp PM, McCutchan FE, Hahn BH (1995) Recombination in HIV-1. Nature 374: 124-126.

19. Perelson AS, Neumann AU, Markowitz M, Leonard JM, Ho DD (1996) HIV-1 dynamics in vivo: virion clearance rate, infected cell life-span, and viral generation time. Science 271: 1582-1586.

20. Coffin JM (1992) Genetic diversity and evolution of retroviruses. Curr Top Microbiol Immunol 176: 143-164.

21. Wei X, Ghosh SK, Taylor ME, Johnson VA, Emini EA, et al. (1995) Viral dynamics in human immunodeficiency virus type 1 infection. Nature 373: 117-122.

22. Ramirez BC, Simon-Loriere E, Galetto R, Negroni M (2008) Implications of recombination for HIV diversity. Virus Res 134: 64-73.

23. Zhang M, Foley B, Schultz AK, Macke JP, Bulla I, et al. (2010) The role of recombination in the emergence of a complex and dynamic HIV epidemic. Retrovirology 7: 25.

24. Leitner T, Korber BT, Daniels M, Calef C, Foley B (2005) HIV-1 Subtype and Circulating Recombinant Form (CRF) Reference Sequences, 2005. In: Leitner T FB, Hahn B, Marx P, McCutchan F, Mellors J, Wolinksy S, and Korber B, editor. HIV Sequence Compendium. Los Alamos, NM: Theoretical Biology and Biophysics Group, Los Alamos National Laboratory.

25. Roux KH, Taylor KA (2007) AIDS virus envelope spike structure. Curr Opin Struct Biol 17: 244-252.

26. Willey RL, Rutledge RA, Dias S, Folks T, Theodore T, et al. (1986) Identification of conserved and divergent domains within the envelope gene of the acquired immunodeficiency syndrome retrovirus. Proc Natl Acad Sci U S A 83: 5038-5042.

27. Chen B, Vogan EM, Gong H, Skehel JJ, Wiley DC, et al. (2005) Structure of an unliganded simian immunodeficiency virus gp120 core. Nature 433: 834-841.

28. Kwong PD, Wyatt R, Majeed S, Robinson J, Sweet RW, et al. (2000) Structures of HIV-1 gp120 envelope glycoproteins from laboratory-adapted and primary isolates. Structure Fold Des 8: 1329-1339.

29. Kwong PD, Wyatt R, Robinson J, Sweet RW, Sodroski J, et al. (1998) Structure of an HIV gp120 envelope glycoprotein in complex with the CD4 receptor and a neutralizing human antibody. Nature 393: 648-659.

30. Huang CC, Stricher F, Martin L, Decker JM, Majeed S, et al. (2005) Scorpion-toxin mimics of CD4 in complex with human immunodeficiency virus gp120 crystal structures, molecular mimicry, and neutralization breadth. Structure 13: 755-768.

31. Huang CC, Tang M, Zhang MY, Majeed S, Montabana E, et al. (2005) Structure of a V3-containing HIV-1 gp120 core. Science 310: 1025-1028.

32. Kwon YD, Finzi A, Wu X, Dogo-Isonagie C, Lee LK, et al. (2012) Unliganded HIV-1 gp120 core structures assume the CD4-bound conformation with regulation by quaternary interactions and variable loops. Proc Natl Acad Sci U S A 109: 5663-5668.

33. Mao Y, Wang L, Gu C, Herschhorn A, Xiang SH, et al. (2012) Subunit organization of the membrane-bound HIV-1 envelope glycoprotein trimer. Nat Struct Mol Biol 19: 893-899.

34. Liu J, Bartesaghi A, Borgnia MJ, Sapiro G, Subramaniam S (2008) Molecular architecture of native HIV-1 gp120 trimers. Nature 455: 109-113.

35. Pantophlet R, Burton DR (2006) GP120: target for neutralizing HIV-1 antibodies. Annu Rev Immunol 24: 739-769.

36. Huang W, Eshleman SH, Toma J, Fransen S, Stawiski E, et al. (2007) Coreceptor tropism in human immunodeficiency virus type 1 subtype D: high prevalence of CXCR4 tropism and heterogeneous composition of viral populations. J Virol 81: 7885-7893.

37. Huang CC, Lam SN, Acharya P, Tang M, Xiang SH, et al. (2007) Structures of the CCR5 N terminus and of a tyrosine-sulfated antibody with HIV-1 gp120 and CD4. Science 317: 1930-1934.

38. Choe H, Farzan M, Sun Y, Sullivan N, Rollins B, et al. (1996) The beta-chemokine receptors CCR3 and CCR5 facilitate infection by primary HIV-1 isolates. Cell 85: 1135-1148.

39. Speck RF, Wehrly K, Platt EJ, Atchison RE, Charo IF, et al. (1997) Selective employment of chemokine receptors as human immunodeficiency virus type 1 coreceptors determined by individual amino acids within the envelope V3 loop. J Virol 71: 7136-7139.

40. Xiao L, Owen SM, Goldman I, Lal AA, deJong JJ, et al. (1998) CCR5 coreceptor usage of non-syncytium-inducing primary HIV-1 is independent of phylogenetically distinct global HIV-1 isolates: delineation of consensus motif in the V3 domain that predicts CCR-5 usage. Virology 240: 83-92.

41. Frost SD, Wrin T, Smith DM, Kosakovsky Pond SL, Liu Y, et al. (2005) Neutralizing antibody responses drive the evolution of human immunodeficiency virus type 1 envelope during recent HIV infection. Proc Natl Acad Sci U S A 102: 18514-18519.

42. Rong R, Li B, Lynch RM, Haaland RE, Murphy MK, et al. (2009) Escape from autologous neutralizing antibodies in acute/early subtype C HIV-1 infection requires multiple pathways. PLoS Pathog 5: e1000594.

43. Moore PL, Ranchobe N, Lambson BE, Gray ES, Cave E, et al. (2009) Limited neutralizing antibody specificities drive neutralization escape in early HIV-1 subtype C infection. PLoS Pathog 5: e1000598.

44. Murphy MK, Yue L, Pan R, Boliar S, Sethi A, et al. (2013) Viral Escape from Neutralizing Antibodies in Early Subtype A HIV-1 Infection Drives an Increase in Autologous Neutralization Breadth. PLoS Pathog 9: e1003173.

45. Lynch RM, Rong R, Boliar S, Sethi A, Li B, et al. (2011) The B cell response is redundant and highly focused on V1V2 during early subtype C infection in a Zambian seroconverter. J Virol 85: 905-915.

46. Sagar M, Wu X, Lee S, Overbaugh J (2006) Human immunodeficiency virus type 1 V1-V2 envelope loop sequences expand and add glycosylation sites over the course of infection, and these modifications affect antibody neutralization sensitivity. J Virol 80: 9586-9598.

47. Rong R, Gnanakaran S, Decker JM, Bibollet-Ruche F, Taylor J, et al. (2007) Unique Mutational Patterns in the Envelope {alpha}2 Amphipathic Helix and Acquisition of Length in gp120 Hyper-variable Domains are Associated with Resistance to Autologous Neutralization of Subtype C Human Immunodeficiency Virus type 1. J Virol 81: 5658-5668.

48. Wei X, J.M. Decker, S. Wang, H. Hui, J.C. Kappes, X. Wu, J.F. Salazar, M.G. Salazar, J.M. Kilby, M.S. Saag, N.L. Komarova, M.A. Nowak, B.H. Hahn, P.D. Kwong, G.M. Shaw (2003) Antibody Neutralization and Escape by HIV-1. Nature 422: 307-312.

49. Kwong PD, Doyle ML, Casper DJ, Cicala C, Leavitt SA, et al. (2002) HIV-1 evades antibody-mediated neutralization through conformational masking of receptor-binding sites. Nature 420: 678-682.

50. Aasa-Chapman MM, Hayman A, Newton P, Cornforth D, Williams I, et al. (2004) Development of the antibody response in acute HIV-1 infection. AIDS 18: 371-381.

51. Arendrup M, Nielsen C, Hansen JE, Pedersen C, Mathiesen L, et al. (1992) Autologous HIV-1 neutralizing antibodies: emergence of neutralization-resistant escape virus and subsequent development of escape virus neutralizing antibodies. J Acquir Immune Defic Syndr 5: 303-307.

52. Bunnik EM, Pisas L, van Nuenen AC, Schuitemaker H (2008) Autologous Neutralizing Humoral Immunity and Evolution of the Viral Envelope in the Course of Subtype B Human Immunodeficiency Virus Type 1 Infection. J Virol.

53. Richman DD, Wrin T, Little SJ, Petropoulos CJ (2003) Rapid evolution of the neutralizing antibody response to HIV type 1 infection. Proc Natl Acad Sci U S A 100: 4144-4149.

54. Gray ES, Moore PL, Choge IA, Decker JM, Bibollet-Ruche F, et al. (2007) Neutralizing antibody responses in acute human immunodeficiency virus type 1 subtype C infection. J Virol 81: 6187-6196.

55. Li B, Decker JM, Johnson RW, Bibollet-Ruche F, Wei X, et al. (2006) Evidence for potent autologous neutralizing antibody titers and compact envelopes in early infection with subtype C human immunodeficiency virus type 1. J Virol 80: 5211-5218.

56. Pinter A, Honnen WJ, He Y, Gorny MK, Zolla-Pazner S, et al. (2004) The V1/V2 domain of gp120 is a global regulator of the sensitivity of primary human immunodeficiency virus type 1 isolates to neutralization by antibodies commonly induced upon infection. J Virol 78: 5205-5215.

57. Wyatt R, Moore J, Accola M, Desjardin E, Robinson J, et al. (1995) Involvement of the V1/V2 variable loop structure in the exposure of human immunodeficiency virus type 1 gp120 epitopes induced by receptor binding. J Virol 69: 5723-5733.

58. Chackerian B, Rudensey LM, Overbaugh J (1997) Specific N-linked and O-linked glycosylation modifications in the envelope V1 domain of simian immunodeficiency virus variants that evolve in the host alter recognition by neutralizing antibodies. J Virol 71: 7719-7727.

59. Rong R, Bibollet-Ruche F, Mulenga J, Allen S, Blackwell JL, et al. (2007) Role of V1V2 and other human immunodeficiency virus type 1 envelope domains in resistance to autologous neutralization during clade C infection. J Virol 81: 1350-1359.

60. Cormier EG, Dragic T (2002) The crown and stem of the V3 loop play distinct roles in human immunodeficiency virus type 1 envelope glycoprotein interactions with the CCR5 coreceptor. J Virol 76: 8953-8957.

61. Suphaphiphat P, Thitithanyanont A, Paca-Uccaralertkun S, Essex M, Lee TH (2003) Effect of amino acid substitution of the V3 and bridging sheet residues in human immunodeficiency virus type 1 subtype C gp120 on CCR5 utilization. J Virol 77: 3832-3837.

62. Kwong PD, Wyatt R, Sattentau QJ, Sodroski J, Hendrickson WA (2000) Oligomeric modeling and electrostatic analysis of the gp120 envelope glycoprotein of human immunodeficiency virus. J Virol 74: 1961-1972.

63. Davis KL, Gray ES, Moore PL, Decker JM, Salomon A, et al. (2009) High titer HIV-1 V3-specific antibodies with broad reactivity but low neutralizing potency in acute infection and following vaccination. Virology 387: 414-426.

64. Moore PL, Gray ES, Choge IA, Ranchobe N, Mlisana K, et al. (2007) The C3-V4 Region Is a Major Target of Autologous Neutralizing Antibodies in Hiv-1 Subtype C Infection. J Virol.

65. Davis KL, Bibollet-Ruche F, Li H, Decker JM, Kutsch O, et al. (2009) Human immunodeficiency virus type 2 (HIV-2)/HIV-1 envelope chimeras detect high titers of broadly reactive HIV-1 V3-specific antibodies in human plasma. J Virol 83: 1240-1259.

66. Pauling L, Corey RB, Branson HR (1951) The structure of proteins; two hydrogen-bonded helical configurations of the polypeptide chain. Proc Natl Acad Sci U S A 37: 205-211.

67. Gnanakaran S, Lang D, Daniels M, Bhattacharya T, Derdeyn CA, et al. (2007) Clade Specific Differences in HIV-1: Diversity and Correlations in C3-V4 Regions of gp120. J Virol 81: 4886-4891.

68. Tan H, Rader AJ (2009) Identification of putative, stable binding regions through flexibility analysis of HIV-1 gp120. Proteins 74: 881-894.

69. Gaschen B, Taylor J, Yusim K, Foley B, Gao F, et al. (2002) Diversity considerations in HIV-1 vaccine selection. Science 296: 2354-2360.

70. Gray ES, Moody MA, Wibmer CK, Chen X, Marshall D, et al. (2011) Isolation of a monoclonal antibody that targets the alpha-2 helix of gp120 and represents the initial autologous neutralizing-antibody response in an HIV-1 subtype C-infected individual. J Virol 85: 7719-7729.

71. Marshall RD (1972) Glycoproteins. Annu Rev Biochem 41: 673-702.

72. Marshall RD (1974) The nature and metabolism of the carbohydrate-peptide linkages of glycoproteins. Biochem Soc Symp: 17-26.

73. Gavel Y, von Heijne G (1990) Sequence differences between glycosylated and non-glycosylated Asn-X-Thr/Ser acceptor sites: implications for protein engineering. Protein Eng 3: 433-442.

74. Kasturi L, Eshleman JR, Wunner WH, Shakin-Eshleman SH (1995) The hydroxy amino acid in an Asn-X-Ser/Thr sequon can influence N-linked core glycosylation efficiency and the level of expression of a cell surface glycoprotein. J Biol Chem 270: 14756-14761.

75. Mellquist JL, Kasturi L, Spitalnik SL, Shakin-Eshleman SH (1998) The amino acid following an asn-X-Ser/Thr sequon is an important determinant of N-linked core glycosylation efficiency. Biochemistry 37: 6833-6837.

76. Shakin-Eshleman SH, Spitalnik SL, Kasturi L (1996) The amino acid at the X position of an Asn-X-Ser sequon is an important determinant of N-linked core-glycosylation efficiency. J Biol Chem 271: 6363-6366.

77. Myers G, Lenroot R (1992) HIV glycosylation: what does it portend? AIDS Res Hum Retroviruses 8: 1459-1460.

78. Muster T, Guinea R, Trkola A, Purtscher M, Klima A, et al. (1994) Cross-neutralizing activity against divergent human immunodeficiency virus type 1 isolates induced by the gp41 sequence ELDKWAS. J Virol 68: 4031-4034.

79. Eckhart L, Raffelsberger W, Ferko B, Klima A, Purtscher M, et al. (1996) Immunogenic presentation of a conserved gp41 epitope of human immunodeficiency virus type 1 on recombinant surface antigen of hepatitis B virus. J Gen Virol 77 (Pt 9): 2001-2008.

80. Coeffier E, Clement JM, Cussac V, Khodaei-Boorane N, Jehanno M, et al. (2000) Antigenicity and immunogenicity of the HIV-1 gp41 epitope ELDKWA inserted into permissive sites of the MalE protein. Vaccine 19: 684-693.

81. Simek MD, Rida W, Priddy FH, Pung P, Carrow E, et al. (2009) Human immunodeficiency virus type 1 elite neutralizers: individuals with broad and potent neutralizing activity identified by using a high-throughput neutralization assay together with an analytical selection algorithm. J Virol 83: 7337-7348.

82. Kessler JA, 2nd, McKenna PM, Emini EA, Chan CP, Patel MD, et al. (1997) Recombinant human monoclonal antibody IgG1b12 neutralizes diverse human

immunodeficiency virus type 1 primary isolates. AIDS Res Hum Retroviruses 13: 575-582.

83. Zhou T, Georgiev I, Wu X, Yang ZY, Dai K, et al. (2010) Structural basis for broad and potent neutralization of HIV-1 by antibody VRC01. Science 329: 811-817.

84. Falkowska E, Ramos A, Feng Y, Zhou T, Moquin S, et al. (2012) PGV04, an HIV-1 gp120 CD4 binding site antibody, is broad and potent in neutralization but does not induce conformational changes characteristic of CD4. J Virol 86: 4394-4403.

85. Wu X, Zhou T, Zhu J, Zhang B, Georgiev I, et al. (2011) Focused evolution of HIV-1 neutralizing antibodies revealed by structures and deep sequencing. Science 333: 1593-1602.

86. Walker LM, Huber M, Doores KJ, Falkowska E, Pejchal R, et al. (2011) Broad neutralization coverage of HIV by multiple highly potent antibodies. Nature 477: 466-470.

87. Pejchal R, Doores KJ, Walker LM, Khayat R, Huang PS, et al. (2011) A potent and broad neutralizing antibody recognizes and penetrates the HIV glycan shield. Science 334: 1097-1103.

88. Zwick MB, Labrijn AF, Wang M, Spenlehauer C, Saphire EO, et al. (2001) Broadly neutralizing antibodies targeted to the membrane-proximal external region of human immunodeficiency virus type 1 glycoprotein gp41. J Virol 75: 10892-10905.

89. Morris L, Chen X, Alam M, Tomaras G, Zhang R, et al. (2011) Isolation of a human anti-HIV gp41 membrane proximal region neutralizing antibody by antigen-specific single B cell sorting. PLoS One 6: e23532.

90. Muster T, Steindl F, Purtscher M, Trkola A, Klima A, et al. (1993) A conserved neutralizing epitope on gp41 of human immunodeficiency virus type 1. J Virol 67: 6642-6647.

91. Scheid JF, Mouquet H, Ueberheide B, Diskin R, Klein F, et al. (2011) Sequence and structural convergence of broad and potent HIV antibodies that mimic CD4 binding. Science 333: 1633-1637.

92. Diskin R, Scheid JF, Marcovecchio PM, West AP, Jr., Klein F, et al. (2011) Increasing the potency and breadth of an HIV antibody by using structure-based rational design. Science 334: 1289-1293.

93. Bonsignori M, Hwang KK, Chen X, Tsao CY, Morris L, et al. (2011) Analysis of a clonal lineage of HIV-1 envelope V2/V3 conformational epitope-specific broadly neutralizing antibodies and their inferred unmutated common ancestors. J Virol 85: 9998-10009.

94. Gray ES, Madiga MC, Hermanus T, Moore PL, Wibmer CK, et al. (2011) The neutralization breadth of HIV-1 develops incrementally over four years and is associated with CD4+ T cell decline and high viral load during acute infection. J Virol 85: 4828-4840.

95. Euler Z, van Gils MJ, Bunnik EM, Phung P, Schweighardt B, et al. (2010) Cross-reactive neutralizing humoral immunity does not protect from HIV type 1 disease progression. J Infect Dis 201: 1045-1053.

96. Mikell I, Sather DN, Kalams SA, Altfeld M, Alter G, et al. (2011) Characteristics of the earliest cross-neutralizing antibody response to HIV-1. PLoS Pathog 7: e1001251.

97. Briney BS, Jr JE (2013) Secondary mechanisms of diversification in the human antibody repertoire. Front Immunol 4: 42.

98. Moody MA, Zhang R, Walter EB, Woods CW, Ginsburg GS, et al. (2011) H3N2 influenza infection elicits more cross-reactive and less clonally expanded anti-hemagglutinin antibodies than influenza vaccination. PLoS One 6: e25797.

99. Wrammert J, Smith K, Miller J, Langley WA, Kokko K, et al. (2008) Rapid cloning of high-affinity human monoclonal antibodies against influenza virus. Nature.

100. Zwick MB, Komori HK, Stanfield RL, Church S, Wang M, et al. (2004) The long third complementarity-determining region of the heavy chain is important in the activity of the broadly neutralizing anti-human immunodeficiency virus type 1 antibody 2F5. J Virol 78: 3155-3161.

101. Zwick MB, Parren PW, Saphire EO, Church S, Wang M, et al. (2003) Molecular features of the broadly neutralizing immunoglobulin G1 b12 required for recognition of human immunodeficiency virus type 1 gp120. J Virol 77: 5863-5876.

102. Allen S, K.E. N'Gandu, and A. Tichacek (1998) The evolution of voluntary testing and counseling as an HIV prevention strategy. Preventing HIV in Developing Countries: Biomedical and Behavioral Approaches. New York: Platinum Press.

103. Allen S, Meinzen-Derr J, Kautzman M, Zulu I, Trask S, et al. (2003) Sexual behavior of HIV discordant couples after HIV counseling and testing. Aids 17: 733-740.

104. Allen S, Karita E, Chomba E, Roth DL, Telfair J, et al. (2007) Promotion of couples' voluntary counselling and testing for HIV through influential networks in two African capital cities. BMC Public Health 7: 349.

105. Holstad MM, Dilorio C, Kelley ME, Resnicow K, Sharma S (2011) Group motivational interviewing to promote adherence to antiretroviral medications and risk reduction behaviors in HIV infected women. AIDS Behav 15: 885-896.

106. Jewkes RK, Dunkle K, Nduna M, Shai N (2010) Intimate partner violence, relationship power inequity, and incidence of HIV infection in young women in South Africa: a cohort study. Lancet 376: 41-48.

107. Klinkenberg WD, Sacks S (2004) Mental disorders and drug abuse in persons living with HIV/AIDS. AIDS Care 16 Suppl 1: S22-42.

108. Wagenaar BH, Christiansen-Lindquist L, Khosropour C, Salazar LF, Benbow N, et al. (2012) Willingness of US men who have sex with men (MSM) to participate in Couples HIV Voluntary Counseling and Testing (CVCT). PLoS One 7: e42953.

109. El-Sadr WM, Mayer KH, Hodder SL (2010) AIDS in America--forgotten but not gone. N Engl J Med 362: 967-970.

110. Harris JE (2009) Why we don't have an HIV vaccine, and how we can develop one. Health Aff (Millwood) 28: 1642-1654.

111. Francis DP, Gregory T, McElrath MJ, Belshe RB, Gorse GJ, et al. (1998) Advancing AIDSVAX to phase 3. Safety, immunogenicity, and plans for phase 3. AIDS Res Hum Retroviruses 14 Suppl 3: S325-331.

112. Buchbinder SP, Mehrotra DV, Duerr A, Fitzgerald DW, Mogg R, et al. (2008) Efficacy assessment of a cell-mediated immunity HIV-1 vaccine (the Step Study): a double-blind, randomised, placebo-controlled, test-of-concept trial. Lancet 372: 1881-1893.

113. Rerks-Ngarm S, Pitisuttithum P, Nitayaphan S, Kaewkungwal J, Chiu J, et al. (2009) Vaccination with ALVAC and AIDSVAX to prevent HIV-1 infection in Thailand. N Engl J Med 361: 2209-2220.

114. Haynes BF, Gilbert PB, McElrath MJ, Zolla-Pazner S, Tomaras GD, et al. (2012) Immune-correlates analysis of an HIV-1 vaccine efficacy trial. N Engl J Med 366: 1275-1286.

115. Zolla-Pazner S, deCamp AC, Cardozo T, Karasavvas N, Gottardo R, et al. (2013) Analysis of V2 antibody responses induced in vaccinees in the ALVAC/AIDSVAX HIV-1 vaccine efficacy trial. PLoS One 8: e53629.

116. Mascola JR, Montefiori DC (2010) The role of antibodies in HIV vaccines. Annu Rev Immunol 28: 413-444.

117. McElrath MJ, Haynes BF (2010) Induction of immunity to human immunodeficiency virus type-1 by vaccination. Immunity 33: 542-554.

118. Plotkin SA (2010) Correlates of protection induced by vaccination. Clin Vaccine Immunol 17: 1055-1065.

119. Burton DR, Desrosiers RC, Doms RW, Koff WC, Kwong PD, et al. (2004) HIV vaccine design and the neutralizing antibody problem. Nat Immunol 5: 233-236.

120. Burton DR, Stanfield RL, Wilson IA (2005) Antibody vs. HIV in a clash of evolutionary titans. Proc Natl Acad Sci U S A 102: 14943-14948.

121. Tang H, Robinson JE, Gnanakaran S, Li M, Rosenberg ES, et al. (2011) Epitopes immediately below the base of the V3 loop of gp120 as targets for the initial autologous neutralizing antibody response in two HIV-1 subtype B-infected individuals. J Virol 85: 9286-9299.

122. Bar KJ, Tsao CY, Iyer SS, Decker JM, Yang Y, et al. (2012) Early Low-Titer Neutralizing Antibodies Impede HIV-1 Replication and Select for Virus Escape. PLoS Pathog 8: e1002721.

123. Doria-Rose NA, Louder MK, Yang Z, O'Dell S, Nason M, et al. (2012) HIV-1 neutralization coverage is improved by combining monoclonal antibodies that target independent epitopes. J Virol 86: 3393-3397.

124. Mascola JR, Louder MK, VanCott TC, Sapan CV, Lambert JS, et al. (1997) Potent and synergistic neutralization of human immunodeficiency virus (HIV) type 1 primary isolates by hyperimmune anti-HIV immunoglobulin combined with monoclonal antibodies 2F5 and 2G12. J Virol 71: 7198-7206.

125. Verrier F, Nadas A, Gorny MK, Zolla-Pazner S (2001) Additive effects characterize the interaction of antibodies involved in neutralization of the primary dualtropic human immunodeficiency virus type 1 isolate 89.6. J Virol 75: 9177-9186.

126. Zwick MB, Wang M, Poignard P, Stiegler G, Katinger H, et al. (2001) Neutralization synergy of human immunodeficiency virus type 1 primary isolates by cocktails of broadly neutralizing antibodies. J Virol 75: 12198-12208.

127. Derdeyn CA, Decker JM, Bibollet-Ruche F, Mokili JL, Muldoon M, et al. (2004) Envelope-Constrained Neutralization-Sensitive HIV-1 After Heterosexual Transmission. Science 303: 2019-2022.

128. Haaland RE, Hawkins PA, Salazar-Gonzalez J, Johnson A, Tichacek A, et al. (2009) Inflammatory genital infections mitigate a severe genetic bottleneck in heterosexual transmission of subtype A and C HIV-1. PLoS Pathog 5: e1000274.

129. Abrahams MR, Anderson JA, Giorgi EE, Seoighe C, Mlisana K, et al. (2009) Quantitating the multiplicity of infection with human immunodeficiency virus type 1 subtype C reveals a non-poisson distribution of transmitted variants. J Virol 83: 3556-3567.

130. Fischer W, Ganusov VV, Giorgi EE, Hraber PT, Keele BF, et al. (2010) Transmission of single HIV-1 genomes and dynamics of early immune escape revealed by ultra-deep sequencing. PLoS One 5: e12303.

131. Keele BF, Giorgi EE, Salazar-Gonzalez JF, Decker JM, Pham KT, et al. (2008) Identification and characterization of transmitted and early founder virus envelopes in primary HIV-1 infection. Proc Natl Acad Sci U S A 105: 7552-7557.

132. Baba TW, Liska V, Hofmann-Lehmann R, Vlasak J, Xu W, et al. (2000) Human neutralizing monoclonal antibodies of the IgG1 subtype protect against mucosal simian-human immunodeficiency virus infection. Nat Med 6: 200-206.

133. Ferrantelli F, Rasmussen RA, Buckley KA, Li PL, Wang T, et al. (2004) Complete protection of neonatal rhesus macaques against oral exposure to pathogenic simian-human immunodeficiency virus by human anti-HIV monoclonal antibodies. J Infect Dis 189: 2167-2173.

134. Mascola JR, Stiegler G, VanCott TC, Katinger H, Carpenter CB, et al. (2000) Protection of macaques against vaginal transmission of a pathogenic HIV-1/SIV chimeric virus by passive infusion of neutralizing antibodies. Nat Med 6: 207-210.

135. Mascola JR, Lewis MG, Stiegler G, Harris D, VanCott TC, et al. (1999) Protection of Macaques against pathogenic simian/human immunodeficiency virus 89.6PD by passive transfer of neutralizing antibodies. J Virol 73: 4009-4018.

136. Ruprecht RM, Hofmann-Lehmann R, Smith-Franklin BA, Rasmussen RA, Liska V, et al. (2001) Protection of neonatal macaques against experimental SHIV infection by human neutralizing monoclonal antibodies. Transfus Clin Biol 8: 350-358.

137. Hofmann-Lehmann R, Vlasak J, Rasmussen RA, Smith BA, Baba TW, et al. (2001) Postnatal passive immunization of neonatal macaques with a triple combination of

human monoclonal antibodies against oral simian-human immunodeficiency virus challenge. J Virol 75: 7470-7480.

138. Parren PW, Ditzel HJ, Gulizia RJ, Binley JM, Barbas CF, 3rd, et al. (1995) Protection against HIV-1 infection in hu-PBL-SCID mice by passive immunization with a neutralizing human monoclonal antibody against the gp120 CD4-binding site. Aids 9: F1-6.

139. Parren PW, Marx PA, Hessell AJ, Luckay A, Harouse J, et al. (2001) Antibody protects macaques against vaginal challenge with a pathogenic R5 simian/human immunodeficiency virus at serum levels giving complete neutralization in vitro. J Virol 75: 8340-8347.

140. Prince AM, Reesink H, Pascual D, Horowitz B, Hewlett I, et al. (1991) Prevention of HIV infection by passive immunization with HIV immunoglobulin. AIDS Res Hum Retroviruses 7: 971-973.

141. Shibata R, Igarashi T, Haigwood N, Buckler-White A, Ogert R, et al. (1999) Neutralizing antibody directed against the HIV-1 envelope glycoprotein can completely block HIV-1/SIV chimeric virus infections of macaque monkeys. Nat Med 5: 204-210.

142. Hessell AJ, Rakasz EG, Poignard P, Hangartner L, Landucci G, et al. (2009) Broadly neutralizing human anti-HIV antibody 2G12 is effective in protection against mucosal SHIV challenge even at low serum neutralizing titers. PLoS Pathog 5: e1000433.

143. Hessell AJ, Rakasz EG, Tehrani DM, Huber M, Weisgrau KL, et al. (2010) Broadly neutralizing monoclonal antibodies 2F5 and 4E10 directed against the human immunodeficiency virus type 1 gp41 membrane-proximal external region protect

against mucosal challenge by simian-human immunodeficiency virus SHIVBa-L. J Virol 84: 1302-1313.

144. Hessell AJ, Poignard P, Hunter M, Hangartner L, Tehrani DM, et al. (2009) Effective, low-titer antibody protection against low-dose repeated mucosal SHIV challenge in macaques. Nat Med 15: 951-954.

145. Scanlan CN, Pantophlet R, Wormald MR, Ollmann Saphire E, Stanfield R, et al. (2002) The broadly neutralizing anti-human immunodeficiency virus type 1 antibody 2G12 recognizes a cluster of alpha1-->2 mannose residues on the outer face of gp120. J Virol 76: 7306-7321.

146. Hinman AR, Orenstein WA, Schuchat A (2011) Vaccine-preventable diseases, immunizations, and MMWR--1961-2011. MMWR Surveill Summ 60 Suppl 4: 49-57.